



universität
wien

MASTERARBEIT

Titel der Masterarbeit

„RNA imaging in living hippocampal neurons -
Mechanisms of dendritic mRNA transport
and translational control“

Verfasser

Georg Ammer, BSc

angestrebter akademischer Grad

Master of Science (MSc)

Wien, 2011

Studienkennzahl lt. Studienblatt:

A 066 834

Studienrichtung lt. Studienblatt:

Masterstudium Molekulare Biologie

Betreuerin / Betreuer:

Dr. Georgia Vendra

CONTENTS

Abstract	5
I. Introduction	7
1. The role of dendritic protein synthesis in memory formation	7
2. Why localize mRNAs to dendrites?.....	8
3. Mechanisms of mRNA localization	9
4. Regulation of local translation	10
5. The role of processing bodies in regulating dendritic protein synthesis.....	11
6. mRNA localization in other systems.....	12
7. Methods to visualize RNA transport in living neurons.....	14
8. The MS2 RNA imaging system	15
II. The logistics of dendritic mRNA transport	19
1. Background	19
2. Aims	20
3. Results	20
3.1 Setting up and adapting the MS2 system for live RNA imaging	20
3.2 Analysis of <i>CaMKIIα</i> mRNA transport kinetics	22
3.3 The ‘Mori’ dendritic targeting element of <i>CaMKIIα</i> is not required for dendritic transport	27
3.4 Visualizing transport and localization of <i>CaMKIIα</i> mRNA to synapses	30
3.5 Transport kinetics of <i>β-actin</i> mRNA.....	30
3.6 Dendritic localization of <i>CaMKIIα</i> and <i>β-actin</i> mRNAs is not affected by overexpression of dynamin/p50	34
4. Discussion	37

III. Dynamics and synaptic regulation of dendritic processing bodies	44
1. Background	44
2. Aims	45
3. Results	45
3.1 Dynamics of dendritic P-bodies with respect to postsynaptic sites	45
3.2 Synaptic activity regulates the assembly of P-body components in dendrites	47
3.3 Dendritic mRNAs can be detected in P-bodies but do not accumulate there upon silencing of neuronal activity	48
3.4 Co-transport of <i>CaMKIIα</i> mRNA and P-bodies in dendrites of living neurons	52
4. Discussion	54
IV. Outlook	57
V. Materials	59
1. Buffers and solutions	59
2. DNA-constructs	62
3. Primers	63
4. Antibodies	63
5. Enzymes	64
6. Kits	64
7. Animals	64
8. Software	64
9. Equipment	65
10. Microscope setup	65
VI. Methods	67
1. Cell biology	67
2. Pharmacological treatments	69
3. Molecular biology	70
4. Biochemistry	71
5. Microscopy	72
6. Data analysis	73

References.....	77
Acknowledgements.....	87
Zusammenfassung.....	89
Curriculum Vitae	91

ABSTRACT

Localization of mRNAs to dendrites and subsequent activity-induced local translation plays an important role in the modification of individual synapses, thereby contributing to the molecular mechanisms of learning and memory. To reach their destination, selected mRNAs are packaged into ribonucleoprotein particles (RNPs) and transported along microtubules by molecular motors.

In this thesis, I aimed to investigate the dynamics underlying dendritic RNP transport in living hippocampal neurons. To achieve this, I employed the MS2 system for real-time imaging of dendritic transcripts, tracked individual RNA particles over time and characterized their motility in detail. Kinetic analysis of the well-characterized mRNAs *CaMKII α* and *β -actin* revealed that a subset of particles show fast bidirectional movements with maximum velocities of 2 μ m/s. These movements occurred with equal probability in both directions. Interestingly, *CaMKII α* particles showed a slightly higher velocity in the anterograde direction, which might facilitate fast dendritic targeting. This difference in velocity was not found for *β -actin*. Deletion of a previously published localization element of *CaMKII α* did not interfere with its dendritic transport, supporting the view that localization signals of *CaMKII α* are more complex than previously anticipated. Furthermore, covisualization of MS2-tagged RNA and the postsynaptic marker PSD95 revealed that stationary RNA particles are frequently found close to postsynaptic sites. Together, my results suggest that mRNAs are delivered to dendrites along which they travel bidirectionally, until they get selectively recruited to postsynaptic sites upon demand.

In a side project, I studied the dynamic properties and synaptic regulation of dendritic processing bodies (P-bodies). P-bodies are cytoplasmic RNA granules which have been functionally implicated in the degradation and transient storage of translationally repressed mRNAs. In this work, I detected *Arc*, *β -actin* and *MAP2* mRNAs in P-bodies. Additionally, P-bodies reside near synapses for long periods of time and respond to synaptic activation or silencing by a reversible change in size. These results are in line with the hypothesis that P-bodies store dendritic mRNAs that can be released for translation in response to synaptic stimulation.

I. INTRODUCTION

It is the task of a neuron to receive signals from thousands of inputs, to integrate this information and to convey it on to hundreds of postsynaptic cells, which in turn perform the same computations again. For this purpose, a single hippocampal pyramidal cell forms around 30,000 synaptic contacts with other neurons (Megias et al, 2001). What is even more remarkable, each of these inputs can be modified so that the strength of a given signal depends on the activation history of the synapse. This process is called synaptic plasticity and is thought to be the cellular correlate of learning and memory (Kandel, 2001; Ho et al, 2011). But how do these modifications come about and how are they sustained to give rise to memories that can last for a whole lifetime?

1. The role of dendritic protein synthesis in memory formation

Experiments performed in the last decades have brought clear evidence that long-term functional changes in synaptic strength go hand in hand with structural alterations of individual synapses (Engert and Bonhoeffer, 1999). The great majority of excitatory synapses are located on dendritic spines - small protrusions that emanate from the dendritic shaft. Upon induction of long-term potentiation (LTP), the volume of a dendritic spine can increase dramatically up to twofold (Matsuzaki et al, 2004). The maintenance of this long-lasting structural and functional change is strictly dependent on the synthesis of new proteins (Frey et al, 1988; Govindarajan et al, 2011). Further evidence for the requirement of protein synthesis in long-term memory formation comes from behavioral studies. Injection of protein synthesis inhibitors into the hippocampus of rats, for example, leads to reduced memory consolidation (Davis and Squire, 1984).

With the discovery of polyribosomes in dendrites close to dendritic spines in 1982 (Steward and Levy, 1982), the interesting hypothesis was put forward that local protein synthesis is essential for the modification of specific synapses. Since then several studies have lend support to this idea. For example, Kang and Schuman have surgically separated dendrites from their somata in hippocampal slices to show that BDNF-induced synaptic potentiation requires dendritic protein synthesis (Kang and Schuman, 1996). In a similar approach, it was shown for DHPG-induced long-term depression (LTD) that local translation in dendrites, but not in the soma, is necessary (Huber et al, 2000). Dendritic protein synthesis, of course,

requires the mRNAs coding for the respective proteins to be present at the sites of translation. Up to now several hundred different dendritically localized transcripts have been identified (Eberwine et al, 2001; Andreassi and Riccio, 2009). Importantly, a mutant mouse where dendritic localization of *CaMKII α* mRNA was disrupted suffers from reduced late-phase LTP and impairments in memory tasks (Miller et al, 2002). This was the first study to directly show that the transport of an mRNA to dendrites is necessary for the regulation of synaptic function and memory formation.

2. Why localize mRNAs to dendrites?

The findings described in the previous paragraph pose the question of why a neuron would employ a special mechanism to target mRNAs to dendrites for their subsequent local translation. One answer to this is time. If a stimulus arrives at a distal synapse, local translation can start immediately. Without dendritic protein synthesis the signal would need to be sent to the soma to initiate translation there and the proteins would have to be transported back to the activated synapse again. Thus, mRNA localization increases the temporal resolution in the regulation of gene expression. Another obvious argument is that of economy. A single mRNA can be translated several times at the site where the protein product is needed. This is much more efficient than to translate the proteins in the cell body and transport them to their destination individually. A further advantage of mRNA localization, and especially relevant for synaptic plasticity, is that it allows a tight spatial control of protein synthesis. By confining mRNAs to distinct subcellular compartments, translation, and thereby newly synthesized proteins, can be spatially restricted. In theory this would allow neighboring synapses to be modified independently of each other – a mechanism that would greatly enhance the computational power of a neuron (Frey, 2001). But although there is some evidence in this direction (Tiruchinapalli et al 2003; Okada et al., 2009) it has not been proven so far. On the contrary, recent reports indicate that nearby dendritic spines can compete for proteins that have been newly synthesized after the induction of LTP (Govindarajan et al, 2006; Govindarajan et al, 2011). But whether synapse-specific or not, mRNA localization is a powerful means to spatially confine the response to a synaptic stimulus and contributes to the way neurons process and store information.

Taken together, there is clear evidence for the functional importance of mRNA localization and local translation in neurons. However, the mechanisms underlying the dendritic transport

of mRNAs and the control of local protein synthesis are only poorly understood (Bramham and Wells, 2007).

3. Mechanisms of mRNA localization

Neurons are highly polarized cells with dendrites up to several hundred micrometers in length that are studded with synapses from the base to the distal tips. This raises the question of how mRNAs get to their destinations that are often far away from the cell body.

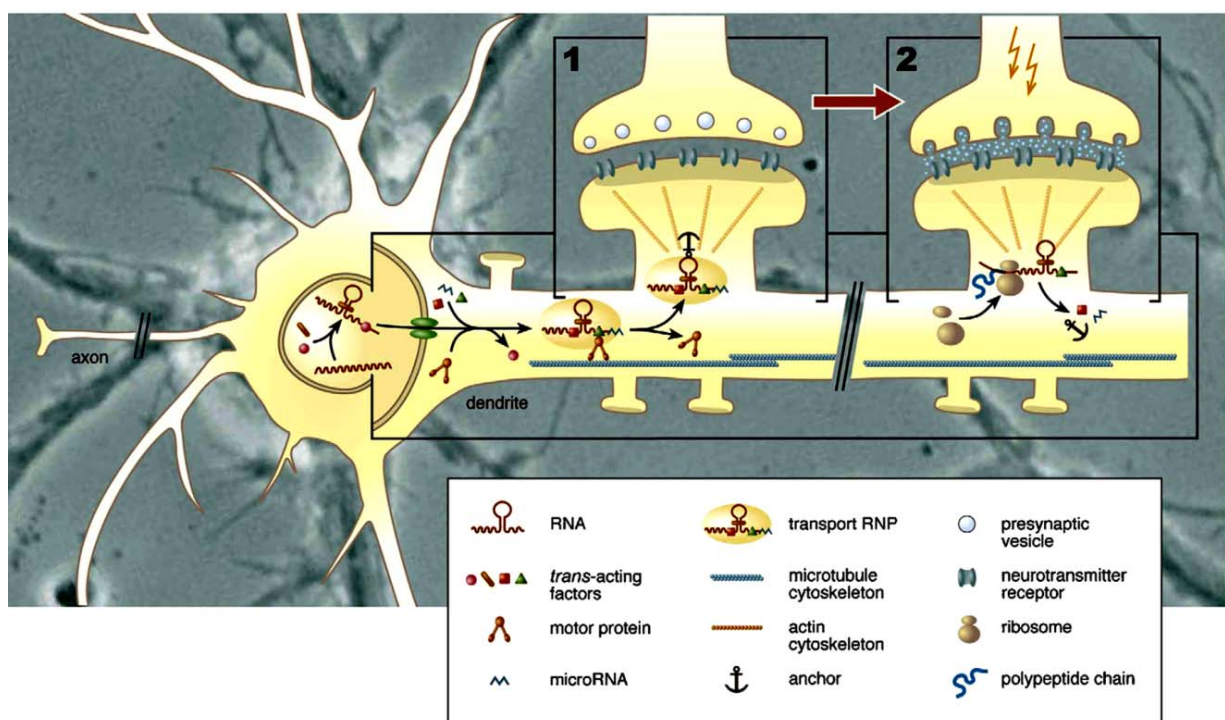


Figure 1. The distinct stages of dendritic mRNA localization

mRNAs are transcribed and processed in the nucleus where they already associate with a first set of trans-acting factors/RNA-binding proteins. After being exported to the cytoplasm through nuclear pores a remodeling of the RNA-protein complex occurs to form transport-competent RNPs. These RNPs are then bound by molecular motors which transport them along the microtubule cytoskeleton to their destination, where they might get anchored (1). During transport, the mRNAs are kept in a translationally silent state. Upon synaptic activation (2), the translational repression is relieved, thereby allowing the synthesis of new proteins. The newly synthesized proteins then contribute to structural and functional modifications of the activated synapse (image taken from Dahm et al, 2007).

mRNA localization begins in the nucleus. Already during transcription, trans-acting factors associate with the nascent mRNA (Farina and Singer, 2002). Most newly transcribed pre-mRNAs are then spliced - a process that has been shown to be important for the correct localization of some mRNAs (Giorgi and Moore, 2007). In *Drosophila* oocytes, for example, the proper localization of *oskar* mRNA is dependent on the removal of the first intron and the deposition of the exon junction complex (EJC) (Hachet and Ephrussi, 2004). Components of the EJC have also been found to associate with dendritic mRNAs and thereby modulate synaptic strength (Giorgi et al, 2007). After nuclear processing the mRNA is exported to the cytoplasm through nuclear pores (Grünwald and Singer, 2010). Here, another set of proteins binds to the mRNA, rendering it competent for transport. The correct localization of an mRNA depends on trans-acting factors that recognize localization elements (LEs) present in the mRNA. These elements are generally located in the 3'-UTR and are often complex structural motifs (Bullock et al, 2010) which makes bioinformatic predictions of LEs difficult. Consequently, few LEs have been thoroughly characterized so far (Andreassi and Riccio, 2009). Upon binding of RNA-binding proteins (RBPs) to their cargo mRNAs, they associate with molecular motors to form so called transport ribonucleoprotein particles (RNPs). These RNPs are then thought to be transported actively along the microtubule cytoskeleton to distal dendritic sites (Knowles et al, 1996; Hirokawa et al, 2010). Evidence for active transport comes on the one hand from live-imaging experiments where mRNAs were observed to move with high speeds along dendrites (Dictenberg et al, 2008; Tübing et al, 2010; Lionnet et al, 2011). On the other hand, motor proteins were identified by biochemical characterization of RNA granules (Kanai et al, 2004). However, it is still unclear which specific motors mediate the targeting and transport of RNPs to dendrites. It has been speculated that upon arrival at their sites of destination, RNPs are anchored to cytoskeletal structures where they await to be translated (Doyle and Kiebler, 2011). Although there is some evidence for anchoring of mRNAs in *Drosophila* oocytes (Forrest and Gavis, 2003; Lopez and Jansen, 2003; Delanoue et al, 2007) and fibroblasts (Liu et al, 2002), this has not been shown in neurons so far (**Fig. 1**).

4. Regulation of local translation

On the way to their destination, mRNAs are transported in a translationally silent manner (Hüttelmaier et al, 2005). This ensures that the protein product is not made at inappropriate locations. For protein synthesis to occur, the translational repression has to be relieved. Considerable evidence suggests that the initiation of dendritic translation can be triggered by

extracellular, and most importantly synaptic, signals (Schuman et al, 2006). It is important to distinguish between mechanisms that lead to a general upregulation of protein synthesis, and others that allow the translational control of specific mRNAs. General mechanisms often involve post-translational modifications of translation initiation or elongation factors. One example is BDNF-induced mTOR signaling, which leads to the phosphorylation of eIF4E-binding protein (eIF4E-BP) and thereby release of eIF4E. This in turn enhances Cap-dependent translation (Bramham and Wells, 2007). Different extracellular signals can lead to distinct synaptic modifications, likely due to the synthesis of different sets of proteins (Pfeiffer and Huber, 2006). This raises the question of how the translation of specific mRNAs is regulated. One mechanism of how this can be achieved is by RBPs that bind only to a subset of dendritic transcripts. A particularly well studied example is that of fragile X mental retardation protein (FMRP), an RBP that acts as a translational repressor. FMRP has been implicated in mGluRI-dependent LTD (Bear et al, 2004). A mutation in its gene causes a severe form of mental retardation (Fragile X Syndrome) that is accompanied by altered dendritic spine morphology (Reiss and Freund, 1990; Hinton et al, 1991; Grossman et al, 2006). An alternative mechanism of mRNA-specific translational control is mediated by micro-RNAs (miRNAs). miRNAs are short (21-23nt) non-coding RNAs that bind to mRNAs and can induce either degradation or translational silencing of their target (Meister and Tuschl, 2004). Interestingly, some miRNAs were found to localize to synapses (Schratt et al, 2006; Siegel et al, 2009). A recent study showed that miR-134 inhibits translation of *Limk1* mRNA at the synapse. Synaptic stimulation with BDNF relieves *Limk1* from translational repression and leads to an increase in the size of dendritic spines (Schratt et al, 2006). It is important to note that in addition to translational control, the degradation of both mRNAs and proteins is another important stage at which fine-tuning of the set and amount of proteins in dendrites can occur (Pak and Sheng, 2003; Banjee et al, 2009; Cajigas et al, 2010).

5. The role of processing bodies in regulating dendritic protein synthesis

Translational control is thought to occur in part in distinct cytoplasmic granules termed processing bodies (P-bodies) (Parker and Sheth, 2007). P-bodies contain factors of the mRNA decapping machinery (e.g. Dcp1, Rck), factors for nonsense-mediated decay (NMD), components of the RNA-induced silencing complex (RISC) (e.g. Ago, Mov10) as well as factors necessary for the general repression of translation (e.g. eIF4E) (Eulalio et al, 2007; Parker and Sheth, 2007). Interestingly, both miRNAs and FMRP were found in P-bodies (Cougot et al, 2008). P-bodies have first been functionally implicated in the degradation of

mRNAs by 5'-3' exonucleolytic decay (Sheth and Parker, 2003). Some years ago, it was shown in yeast that mRNAs can move in and out of P-bodies, implicating that they can act as transient storage sites for translationally repressed mRNAs (Brenques et al, 2005). The discovery of P-bodies in hippocampal and hypothalamic neurons and their dynamic interaction with transport RNPs (Zeitelhofer et al, 2008; Cougot et al, 2008) led to the hypothesis that they play an important role in the regulation of local protein synthesis in dendrites and thus might be involved in neuronal plasticity.

6. mRNA localization in other systems

The employment of mRNA localization to endow distinct subcellular compartments with different functional identities is not restricted to mammalian neurons. The asymmetric localization of mRNAs in the cytoplasm has been extensively studied in many different organisms ranging from bacteria to fruit flies and mammals (St Johnston, 2005; Holt and Bullock, 2009) (**Fig. 2**). Indeed most of the mechanistic insight gained up to date has come from the study of non-neuronal cells. I will therefore briefly review some examples of mRNA localization in systems other than mammalian neurons.

Even in organisms as simple as *E.coli*, certain mRNAs were shown to localize to subcellular domains, for example the poles of the cells, where the proteins they encode are needed (Nevo-Dinur et al, 2011). In yeast, the mRNA for the transcriptional repressor ASH1 localizes to the tip of the bud during cell division (Long et al, 1997). This ensures that mother and daughter cells have different mating types by suppressing mating type switching exclusively in the daughter cell. The localization of *bicoid* mRNA to the anterior pole and *oskar* and *nanos* mRNA to the posterior pole of *Drosophila* oocytes is necessary for the correct formation of the anterior-posterior body axis (St Johnston and Nüsslein-Volhard, 1992; Riechmann and Ephrussi, 2001). In addition to embryonic development, mRNA localization plays a key role in the fate of dividing neuroblasts and in dendritic branching during the development of the *Drosophila* nervous system. During cell division of neuroblasts, *prospero* mRNA acts as a cell fate determinant that localizes selectively to the future ganglion mother cell (Doe et al, 1991). Localization of *nanos* mRNA, mentioned earlier for its role in axis formation, to processes of Class IV da neurons is required for proper dendritic branching (Brechtel and Gavis, 2008). First evidence for mRNA localization in mammals came from the study of fibroblasts. Here, β -actin localizes to the leading edge of lamellipodia where its protein product is needed for the rearrangement of the cytoskeleton that pushes the leading edge forward and thereby

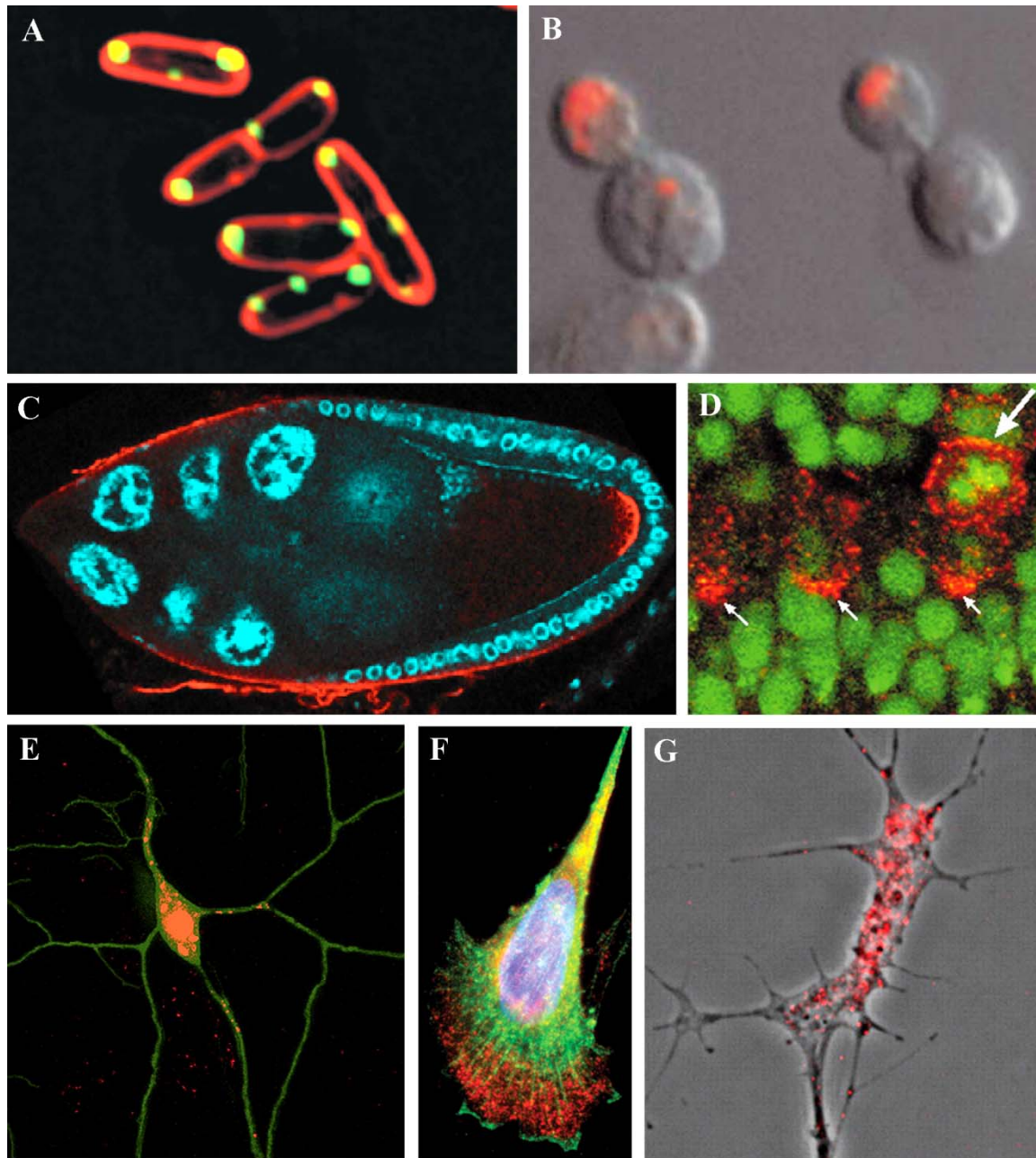


Figure 2. The diversity of asymmetric mRNA localization

(A) *bglG* localizes to the poles of *E.coli* cells. (B) *Ash1* accumulates in the daughter bud of dividing yeast cells. (C) Posterior localization of *oskar* in a *Drosophila* oocyte. (D) Asymmetric localization of *prospero* in *Drosophila* neuroblasts. (E) *nanos* mRNA in dendrites of a *Drosophila* peripheral neuron. (F) β -actin is enriched at the leading edge of a migrating fibroblast. (G) β -actin localizes to the growth cone of *Xenopus* axons. Images are modified from A) Nevo-Dinur et al, 2011; B) Oleynikov and Singer, 1998; C) Jenny et al, 2006; D) Kloc et al, 2002; E) Brechbiel et al, 2008; F) Kiebler and Dahm, 2005 and G) Holt and Bullock, 2009 respectively.

mediates motility of the cell (Shestakova et al, 2001). In oligodendrocytes, the mRNA for myelin basic protein (MBP), which is a protein required for the compaction of the myelin sheath, is transported to the myelinating processes where it is locally translated (Ainger et al, 1993). This prevents the presence of MBP in the cell body, where it would be deleterious for the cell. Long-lasting synaptic modifications are not the only processes in nerve cells that employ mRNA localization. In developing retinal neurons of *Xenopus* embryos, for example, the directed turning of the axonal growth cone to attractants requires local translation of β -actin mRNA (Leung et al, 2006). Taken together, these examples indicate that RNA localization is evolutionarily conserved and therefore very likely to be mediated by similar molecular mechanisms in different organisms (Schnapp, 1999).

7. Methods to visualize RNA transport in living neurons

One reason for the sparseness of mechanistic insight into dendritic mRNA transport has been the lack of tools to visualize RNA in living neurons. In the last years, new techniques have been developed and others that had been used in other model systems were adapted to neurons (**Fig. 3**). These methods have a high potential to play an important role in unraveling the mechanisms of dendritic mRNA transport.

The most straightforward approach to study RNA transport in living neurons is to use fluorescently tagged RBPs as markers for transport RNPs (Köhrmann et al, 1999). A major drawback of this method is that most RBPs bind to a high number of different mRNAs (Maher-Laporte et al, 2010) and thus do not allow the study of specific transcripts. In addition, it is by no means clear whether a given RBP stays associated with its cognate mRNA for the whole lifetime of the transcript. These caveats ask for techniques that allow direct labeling of RNA molecules.

The first attempt to directly visualize RNA in living neurons was by using the membrane-permeable nucleic acid labelling dye SYTO14 (Knowles et al, 1996). This method is, of course, highly unspecific as in addition to all cytoplasmic RNAs also nuclear and mitochondrial DNA is stained. Furthermore, the binding of a chemical dye might significantly alter the structure of the RNA and thereby its properties.

Microinjection of fluorescently labeled RNAs into hippocampal neurons has brought several interesting insights into the dynamics of dendritic RNA transport (Ainger et al 1993; Muslimov et al, 1997; Tübing et al, 2010). However, a major disadvantage of this method is

that the neurons have to be impaled with a sharp electrode – a procedure that very often leads to death of the injected cell. Thus, it is very laborious to obtain high numbers of injected neurons, which prevents a detailed analysis of transport kinetics. Furthermore, the fluorescent RNAs are usually injected directly into the cytoplasm. This circumvents nuclear processing of the RNA, a step which was shown to be important for the correct localization of some mRNAs (Hachet and Ephrussi, 2004; but see discussion in Tübing et al, 2010).

In contrast to the injection of exogenous fluorescent RNA, the use of molecular beacons allows the visualization of endogenous, native transcripts (Bratu et al, 2003). Molecular beacons are stem-loop structured oligonucleotides that generate fluorescence only when bound to their complementary target sequence. In the unbound state, a quencher at one end of the probe is in close proximity to a fluorophore at the other end which causes absorption of the emitted light. Upon binding of the beacon to its target sequence, the quencher and the fluorophore are separated and the fluorescence is restored, thereby allowing detection of the RNA of interest. One problem of this technique is the delivery of molecular beacons into the cell, which is usually done by microinjection. Another important factor to consider is the accessibility of the target sequence. Furthermore, the signal to noise ratio that has been achieved with molecular beacons is quite low. Due to these complications, molecular beacons have not been used in neurons up to now. First insights into the kinetics of neuronal mRNA transport have recently been obtained by the use of the MS2 system (Rook et al, 2000; Dyne and Steward, 2007; Dichtenberg et al, 2008; Kao et al, 2010; Lionnet et al, 2011). As this approach was used throughout this thesis, it will be described in more detail in the next section.

8. The MS2 RNA imaging system

The MS2 system exploits the high-affinity interaction between a fluorescently tagged protein and an RNA aptamer, a 19nt long hairpin structure derived from the MS2 bacteriophage genome (Bertrand et al, 1998). Several tandem repeats of this sequence can be easily attached to any RNA of interest. These MS2 sites are then bound by the MS2 coat protein fused to a fluorescent tag (MCP-FP). Upon simultaneous expression of the MS2-tagged RNA reporter and MCP-FP, the fluorescent proteins are recruited to the MS2 sites and allow visualization of the RNA. Usually, plasmids coding for these two constructs are transiently transfected into cultured neurons (Rook et al, 2000). This system has the advantage over other methods that the RNA is transcribed endogenously and therefore undergoes all nuclear processing events.

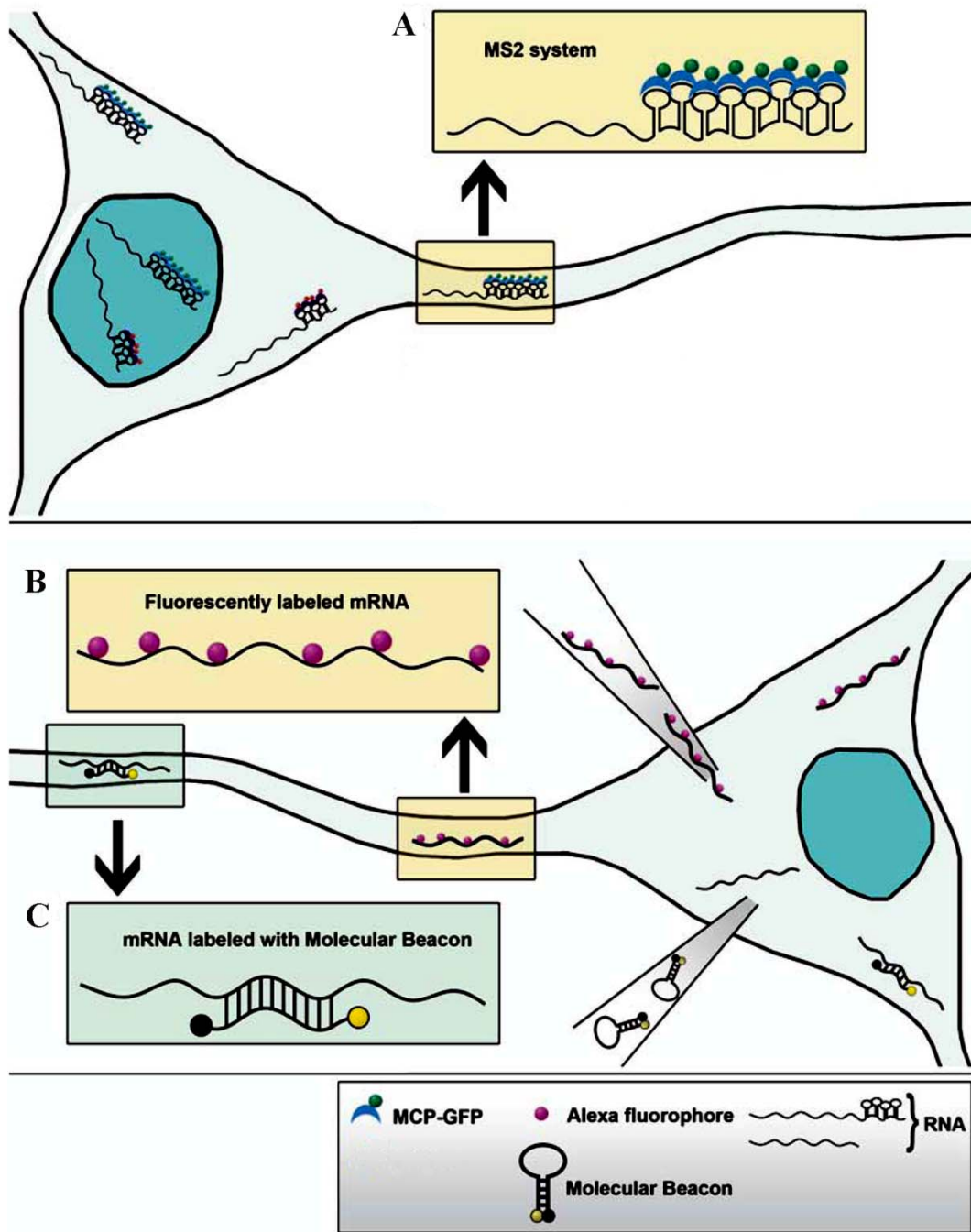


Figure 3. Methods to visualize RNA in living neurons

(A) The MS2 system consists of two-components: an RNA sequence fused to multiple copies of a stemloop structure derived from the MS2 phage (MS2 sites) and a fluorescently tagged MS2 coat protein (MCP) that contains an NLS. Upon simultaneous expression of these two components in a cell, the MCP will bind to the MS2 sites and thereby allow visualization of the RNA. (B) RNA molecules that contain fluorescently labeled NTPs can be delivered into the cell by microinjection. (C) Molecular beacons are stem-loop structured RNA molecules that fluoresce only upon binding to their complementary target sequence. Delivery usually occurs by microinjection (modified from Mikl et al, 2010).

The MS2 system has been used for quite some time to study the transport of mRNAs in the cytoplasm of different cell types (Bertrand et al, 1998; Rook et al, 2000; Fusco et al, 2003). But although this system was first published in 1998 (Bertrand et al, 1998), the number of studies using this approach in neurons is still surprisingly low. One reason for that might be the low signal when compared to background that has been achieved with this method so far. This problem has restricted the analysis to large RNA-containing granules with high fluorescence intensity.

In principle, two adjustments can be made to improve the signal to noise ratio of RNA-reporters visualized with the MS2 method. Logically, one is to increase the signal, the other to suppress the noise. The desired signal comes from the MCP-FP proteins bound to the RNA. More bound fluorescently tagged proteins will yield an enhanced fluorescence intensity and thus increase the signal. This can be achieved by increasing the number of MS2 sites fused to the RNA. The addition of multiple MS2 binding sites, however, may have an effect on the structure of the RNA and thereby influence its transport characteristics. Therefore, it must be confirmed for every reporter construct that it localizes as the endogenous untagged counterpart. The background signal is caused primarily by MCP-FP not bound to MS2 repeats, but freely diffusing in the cytoplasm. The amount of free fluorescent protein is usually restricted by introducing a nuclear localization signal (NLS) (Lionnet et al, 2011). By doing this, free NLS-MCP-FP is transported to the nucleus, which reduces the background fluorescence in dendrites. However, as nuclear transport is not infinitely fast, there will always be a certain amount of background signal in dendrites. Most notably, however, the commonly used NLS does not work well in primary neurons (K.Czaplinski and R. Singer, personal communication). Another important factor is the relative expression level of the MS2-tagged RNA and NLS-MCP-FP. A high excess of NLS-MCP-FP in the cytoplasm would result in high background whereas overexpression of the reporter mRNA, for example by the use of strong viral promoters, might induce artifacts like large RNA aggregates. Recently, a transgenic mouse has been generated where 24xMS2 binding sites were integrated into the genomic locus coding for *β -actin* (Lionnet et al, 2011). This ensures that the reporter RNA is expressed at levels similar to the untagged endogenous mRNA and thus is an important new tool in the study of mRNA transport.

Despite the caveats discussed in the preceding paragraph, the MS2 system is still the best approach to study mRNA transport in living neurons. Thus, setting up this system was the first essential step that allowed the investigation of the mechanisms of dendritic mRNA transport reported in the following sections.

II. THE LOGISTICS OF DENDRITIC mRNA TRANSPORT

1. BACKGROUND

The first study to visualize the transport of RNA in dendrites was already published 15 years ago. Knowles and colleagues used the dye SYTO 14 to label all cytoplasmic RNA. Here, they showed that the motility of RNA granules is bidirectional and depends on an intact microtubule cytoskeleton (Knowles et al, 1996). Some years later, it was again the Kosik group who was the first to use the MS2 system for studying the motility of a single mRNA, *CaMKII α* , in hippocampal neurons. In this important study, they reported that neuronal depolarization by KCl leads to an increased transport of *CaMKII α* granules to dendrites by driving oscillatory granules to move anterogradely (Rook et al, 2000). Another approach to investigate transport of RNA particles in living cells is by microinjecting Alexa-labeled RNA molecules (Wilkie and Davis, 2001). This technique was used in the lab to analyze the transport kinetics of several dendritically localized transcripts. Additionally, by microinjecting two RNAs that were labeled with different fluorophores, Tübing et al. were able to compare the transport characteristics of two RNAs in the same cell. They observed that different RNAs localize preferentially into distinct RNPs, which argues for the existence of multiple dendritic trafficking pathways (Tübing et al, 2010). Nonetheless, it is possible that some RNAs sharing common localization elements coassemble into the same granule. Indeed, this was shown for *CaMKII α* , *Neurogranin* and *Arc* mRNAs (Gao et al, 2008). A recent study using the MS2 system reported an effect of synaptic stimulation on the motility of *CaMKII α* and *Fmr1* mRNAs. Both of these mRNAs were shown to decelerate and move in a more directional manner after application of the mGluRI agonist (S)-3,5-dihydroxyphenylglycine (DHPG) (Kao et al, 2010). It should be noted, however, that although most of the studies dealing with the kinetics of dendritic mRNA transport published so far show qualitative commonalities – active transport of RNPs that can occur in both directions and is regulated by neuronal activity – they differ in the quantitative measurements to a great extent.

2. AIMS

When I joined the lab, my supervisor Georgia Vendra had just achieved to clone the 24xMS2-*CaMKII α* 3'-UTR construct (Mikl et al, 2011) and started to visualize this reporter in neurons. It was my task to further improve the method in order to be able to image a reasonable amount of RNA particles in living neurons. Therefore, my first aim was to optimize transfection as well as imaging parameters that would allow the imaging of an amount of RNA particles sufficient for a detailed kinetic analysis. Once this was achieved, several interesting questions could be addressed. First, I wanted to analyze the transport characteristics of dendritic mRNAs in great detail. This would give a hint to the mechanisms underlying the transport and indicate whether these mechanisms are shared between different mRNAs. Several localization elements have been published in recent years (Andreassi and Riccio, 2009), but it is still unclear how the absence of such an element affects the dynamics of the mRNA in a living neuron (but see Tübing et al, 2010). Would movements of the RNA still be observable but the transport characteristics be affected, as work performed in fibroblasts (Fusco et al, 2003) suggests? Or would the RNA remain completely confined to the cell body and not move at all? Dendritic mRNAs are hypothesized to be transported to dendritic spines where they might get anchored (Steward and Banker, 1992), but experimental evidence for this does not yet exist in living neurons. To investigate this process, I performed live RNA imaging while visualizing a marker for the postsynaptic density at the same time. There is evidence that mRNAs get targeted to dendrites by means of molecular motors, but the identity of these motors is still an unsolved question (Hirokawa et al, 2010). I therefore chose the strategy to selectively disrupt molecular motor components combined with live imaging of RNA transport to address this interesting question.

3. RESULTS

3.1 Setting up and adapting the MS2 system for live RNA imaging

In order to adopt the MS2 method for live cell RNA imaging in primary neurons with high spatiotemporal resolution, several improvements compared to previously published attempts were necessary. Before I joined the lab, some of my colleagues had already put a lot of effort in achieving this goal. First, a NLS-MCP-YFP construct with an improved NLS derived from Cap-binding protein 80 (CBP80) was obtained from K. Czaplinski (now Stony Brook

University, NY) and R. Singer (Albert Einstein College of Medicine, NY). This protein is transported to the nucleus of neurons with high efficiency, thereby keeping the amounts of freely diffusing NLS-MCP-YFP at a minimal extent. Second, the number of MS2 sites was increased to recruit more NLS-MCP-YFP to the MS2-tagged RNA. Most of the studies until recently used a maximum of 8xMS2 repeats (Rook et al, 2000). By a detailed quantification of the amount of light emitted from GFP-labeled particles, people from the Singerlab reported that 24xMS2 sites recruit on average 33 molecules of GFP to the tagged RNA. This was shown to be sufficient to detect single mRNA molecules (Fusco et al, 2003). Based on this study, a reporter construct was created by fusing 24xMS2 sites to the 3'-UTR of *CaMKII α* (Mikl et al, 2011). Upon simultaneous transfection of these two improved constructs, small YFP-labeled RNA particles could be detected in dendrites of hippocampal neurons as far as 200 μ m away from the cell body. To prove that these particles really contain the MS2-tagged RNA, fluorescent *in situ* hybridization (FISH) both against the 3'-UTR of *CaMKII α* and against the MS2 sequence were performed. This resulted in a very high degree of colocalization between the FISH signal and the YFP signal (Mikl et al, 2011). Expression of the NLS-MCP-YFP protein alone or together with the 24xMS2 sites only, resulted exclusively in nuclear YFP-signal with no particles visible in dendrites (data not shown). These controls prove that the dendritic YFP-particles truly represent NLS-MCP-YFP bound to the MS2 tagged RNA-reporter.

With these constructs available, I started to investigate the behavior of the *CaMKII α* 3'-UTR reporter in living neurons. The first experiments were carried out with living neurons grown on 15mm glass coverslips. Due to low transfection efficiency and the inaccessibility of the edge of the coverslip with the microscope objective I could observe only few transfected cells per coverslip and rarely detect any particles in dendrites. This problem could largely be ameliorated by the use of videodishes - culture dishes especially manufactured for live cell imaging - that contain 4-fold more cells than coverslips. A crucial factor for the success of the MS2 imaging approach is a balanced expression level of the NLS-MCP-YFP protein and its RNA target (Schifferer et al., 2009). I obtained good results when using the RNA reporter construct in a 6-fold excess over the NLS-MCP-YFP plasmid. It must nonetheless be noted that even under the best conditions I could never observe RNA particles in all cells with nuclear YFP-signal. This is probably because of a variation in the number of plasmids that different cells take up as well as differences in expression levels. The time of expression also needed to be adjusted accordingly. I found that an expression time between 12 and 16 hours

yielded best results. Another important factor for live RNA imaging was the density of the cell culture. Sparse cultures usually contained neurons that were unhealthy and difficult to transfect. If the culture was too dense, neurons partially overgrew each other, which led to a scattering of the light emitted by the fluorescent proteins. All in all, the MS2 system was adapted sufficiently to allow the visualization of motile dendritic RNA particles in a fair amount of cells per videodish. Setting up this method set the basis for a detailed investigation of the dynamics of mRNA transport in dendrites.

3.2 Analysis of *CaMKII α* mRNA transport kinetics

CaMKII α granule motility was studied and analyzed to some extent before (Rook et al, 2000). An important improvement to this study is that our reporter construct contained 24xMS2 binding sites instead of 8 sites. This significantly increased the signal and allowed me to visualize small, motile RNA particles in the cytoplasm, possibly representing single RNA molecules (Fusco et al, 2003). Furthermore, I increased the temporal resolution of image acquisition from 1 frame every 20 seconds to 1 frame per second. These differences are believed to reveal aspects of RNA motility that have escaped investigations so far. To follow the transport of *CaMKII α* mRNA in living cells, hippocampal neurons were cotransfected with 24xMS2-*CaMKII α* 3'-UTR and NLS-MCP-YFP (**Fig. 4A**). Cells were allowed to express the constructs overnight and were then imaged with a widefield fluorescence microscope. The microscope was equipped with a heating chamber set to 37°C, which allowed to keep the neurons under healthy conditions for up to two hours. A frequently encountered problem was a slight shift of the microscope focus with time. To compensate for this, image acquisition had to be paused and the focus reset manually. Duration of image acquisition was limited by bleaching of the fluorophores and phototoxicity. When a cell was imaged for over 300 time points, a significant decrease in the percentage of motile particles was observed. In most cases, the region of interest was chosen to contain the soma and one primary dendrite. This was important in order to determine the directionality of particle movements when analyzing the movies. Time lapse images were acquired once every second, typically over a time period ranging between 100 and 300 seconds. The kinetics of RNA transport within this time frame was then analyzed in detail.

Live imaging of the *CaMKII α* 3'-UTR reporter allowed the study of RNA particle dynamics in dendrites over time periods of up to 5 minutes. Most of the particles did not move, but fast long-range transport of individual particles was frequently observed. A subset of particles

displayed non-directed, oscillatory movements. In many cases, motile particles traveled tens of micrometers during the imaging period (**Suppl. Movie 1**). Keeping track of motile particles was often limited by the particles going out of focus or moving out of the image frame. RNA particles were observed to move both away (anterograde) and towards (retrograde) the cell body of the neuron. Occasionally, I could observe a particle entering a secondary dendritic branch. YFP-labeled particles had different sizes. Usually fast motile particles were small in size and dim in fluorescence. Larger particles were predominantly stationary and often localized at dendritic branch points. The numbers of RNA particles were very variable from cell to cell. Whereas in some neurons only a few particles could be detected, other cells contained up to hundred clearly definable particles.

To be able to express these observations in numerical terms and to compare them with other RNA-reporters, multiple parameters were defined and analyzed (see Materials and Methods for a detailed description of the particle tracking parameters). In line with previously reported results (Rook et al, 2000) the majority of *CaMKII α* particles was observed to be stationary (52.5%). Another large fraction displayed oscillatory movements (29.2%), which means that the particles changed direction frequently and did not cover long net distances. Apart from that, 18.3% of dendritic RNA particles displayed fast, directed movements along dendrites (**Fig. 4C**). The different categories of motility were not mutually exclusive. Oscillatory particles, for example, often suddenly started to move in a fast and directed manner. Particle runs could be interrupted by periods of pausing or switches in direction (**Fig. 4B,D**). To gain insight into the underlying mechanisms of transport, motile particles were tracked manually with the help of the computer program MetaMorph and then subjected to thorough analysis. In total, 181 particles from 52 different cells were tracked, yielding a total number of 5097 particle displacements (**Table 1**). RNA particles moved with velocities of up to 2 μ m/s and covered distances of more than 100 μ m without pausing (**Fig. 4D**). This clearly argues for active transport along the cytoskeleton that is mediated by molecular motors. A special focus was set on the directionality of moving particles. The whole particle population spent equal amounts of time moving in one or the other direction (**Fig. 4F**). Interestingly, the average velocity of anterogradely directed particle displacements (0.63 μ m/s) was slightly, but significantly, higher than that of retrograde movements (0.54 μ m/s) (**Fig. 4E**). When looking at the velocity histograms, it becomes apparent that this is due to a larger fraction of anterograde particle displacements with very high velocities (>1 μ m/s) when compared to retrograde movements (**Fig. 4G**). With this difference in velocity also the total distance that

all particles covered was higher in the anterograde direction (**Fig. 4F**). Thus, when considering the whole population of *CaMKII α* mRNA particles, a net anterograde displacement was observed. This small net anterograde displacement might account for a fast and efficient targeting of *CaMKII α* mRNA to distal dendritic sites.

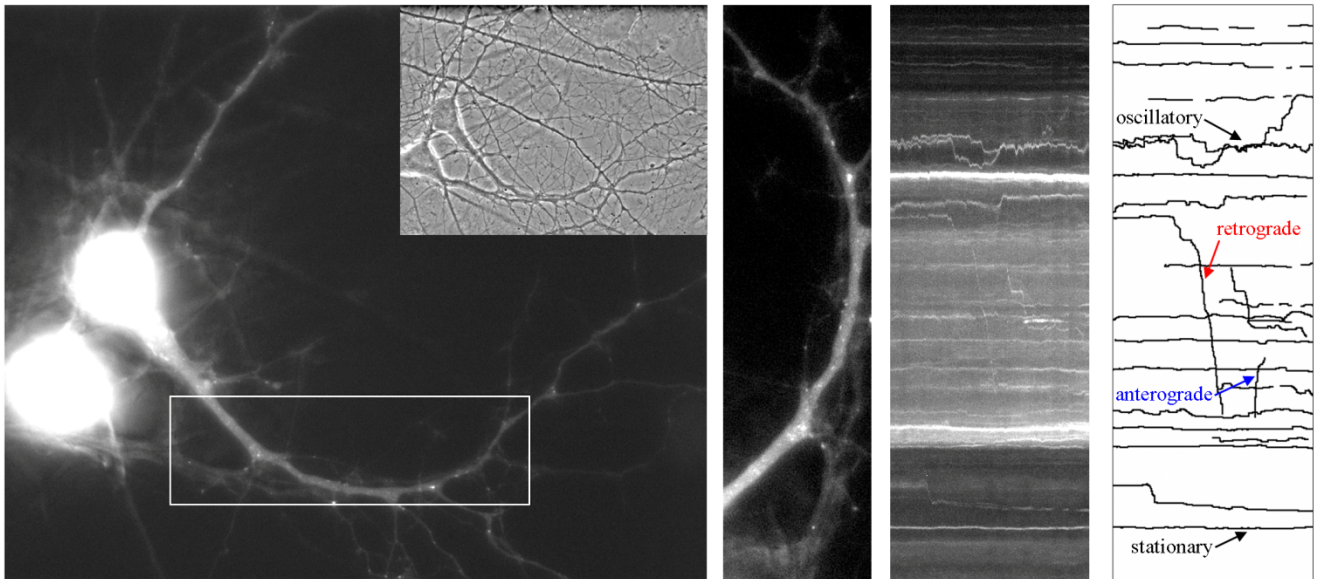
Figure 4 (right side). Kinetics of *CaMKII α* mRNA transport

(**A**) Constructs used for live imaging of *CaMKII α* mRNA in primary neurons. The 3'-UTR of *CaMKII α* was fused to 24xMS2 sites (left). The NLS-MCP-YFP construct contains a nuclear localization signal to reduce the amount of free cytoplasmic protein. (**B**) Left panel: Fluorescence and phase contrast images of a living hippocampal neuron transfected with the two MS2 constructs depicted in (A). Middle panels: Zoom-in (left) and kymograph (right) generated from the boxed region in the left panel. Right panel: Traces of individual particles generated from the kymograph. Examples of stationary, oscillatory, anterograde and retrograde particles are highlighted (**Suppl. Movie 1**). (**C**) Percentage of *CaMKII α* particles that fall into the different categories of motility. (**D**) Diagram depicting traces of all tracked particles. Time is plotted on the x-axis while the y-axis represents the additive distance relative to the first tracking point. (**E**) Median velocity of particle displacements in the anterograde and retrograde direction, respectively. (**F**) Percentage of the number of displacements and total distance that all particles travelled in anterograde or retrograde direction. (**G**) Velocity histogram of anterograde and retrograde particle displacements. Interquartile ranges were 0.81 μ m/s for anterograde and 0.66 μ m/s for retrograde displacements. Statistical significance was assessed with a two-tailed Mann-Whitney test.

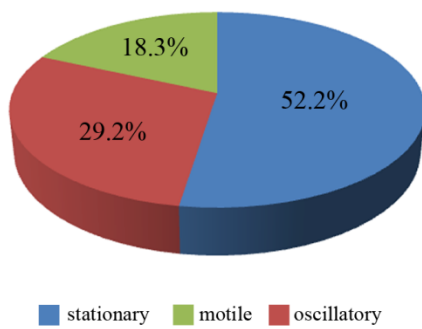
A



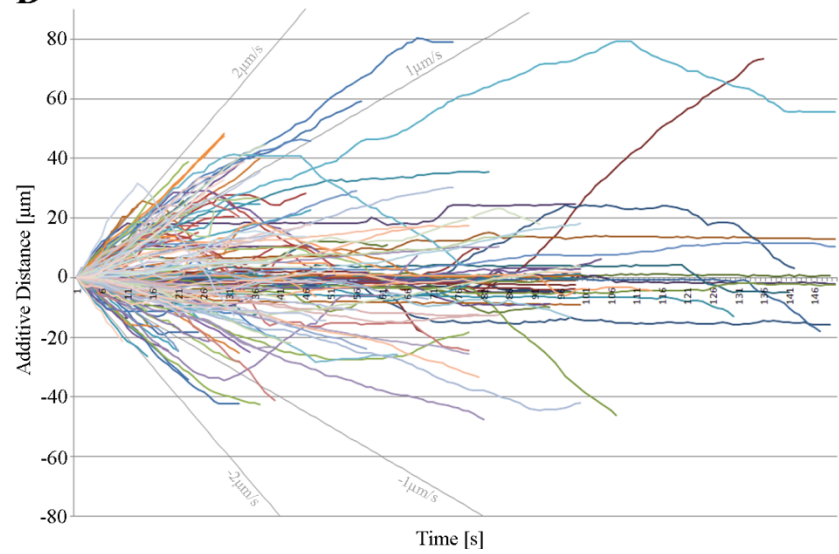
B



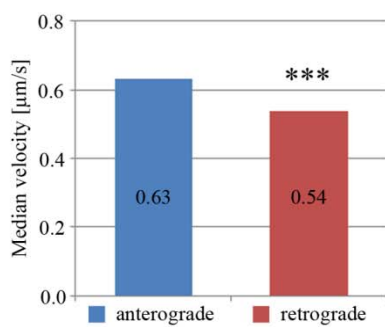
C



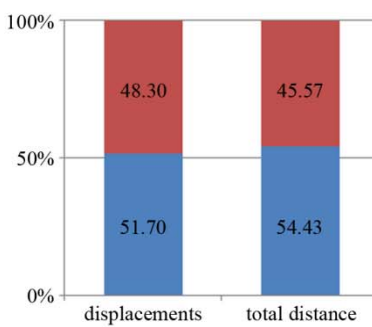
D



E



F



G

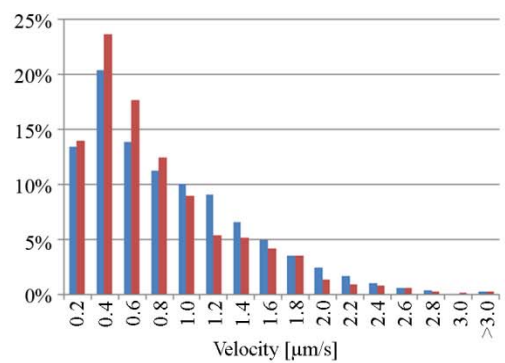


Table1. Numerical values of the particle motility parameters for the RNA reporters for *CaMKII α* , *CaMKII α Δ 1-225* and *β -actin*.

	<i>CaMKIIα</i>			<i>CaMKIIα Δ1-225</i>			<i>β-actin</i>		
Movies [n]	60			49			30		
Particles [n]	181			219			74		
Particle displacements [n]	5097			6601			2474		
Movement categories									
Motile [%]	18,33			13,99			13,71		
Oscillatory [%]	29,19			32,34			34,41		
Stationary [%]	52,47			53,66			51,88		
Particle displacements	ant	ret	total	ant	ret	total	ant	ret	total
Median velocity [μ m/s]	0,63	0,54		0,67	0,64		0,51	0,52	
Interquartile range [μ m/s]	0,81	0,66		0,76	0,74		0,68	0,79	
Displacements [n]	2635	2462	5097	3653	2948	6601	1204	1270	2474
Displacements [%]	51,69	48,3	100	55,34	44,66	100	48,66	53,27	100
Total distance [μ m]	2053,6	1719,1	3772,7	2954,7	2295	5249,7	821,1	936,2	1757,3
Total distance [%]	54,43	45,57	100	56,28	43,72	100	46,72	46,72	100
Directionality value			0,75			0,8			0,83
Net movement (particles) [%]	50	50		51,8	48,2		51,7	48,3	

Interestingly, what is true for the population is not necessarily true for individual particles. In fact, when one takes a closer look at the trajectories of single particles it becomes obvious that most of them show a net movement in either one or the other direction. Exactly half of the particles covered a larger distance in the anterograde, the other half in the retrograde direction, respectively (**Table 1**). Moreover, reversals in direction during the observed timeframe occurred very infrequently (**Fig. 4D**). To be able to express this observation in numerical terms a directionality value was introduced (Kao et al., 2010). This value was calculated by dividing the net distance by the cumulative (total) distance that a particle traveled and is thus a measure for the directedness of the movement. The average directionality value of *CaMKII α* particles was 0.75. This means that, on average, 75% of the total distance that a particle traveled accounted for its net displacement. It is important to keep in mind that the directionality value strictly depends on the timeframe during which the particles were observed. The value reported here can therefore not be compared with those that were previously published (Kao et al., 2010). To conclude, the motile subpopulation of *CaMKII α* particles traveled with similar probabilities in both directions – with a small asymmetry in favor of anterograde movements – whereas the movement of individual particles was rather directed.

3.3 The ‘Mori’ dendritic targeting element of *CaMKII α* is not required for dendritic transport

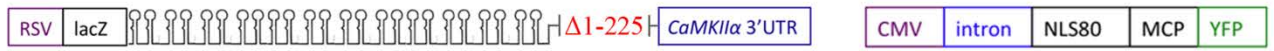
As shown above, *CaMKII α* mRNA localizes to distal dendritic sites by a mechanism that is very likely to employ active transport. More than a decade ago, a dendritic targeting element that is located within the first 94 nucleotides of the *CaMKII α* 3'-UTR (from here on referred to as the ‘Mori’ element) was reported to be both necessary and sufficient for the dendritic localization of this mRNA (Mori et al., 2000). These results were obtained by performing ISH against reporter constructs that contained either the full or truncated versions of the 3'-UTR. It was therefore interesting to investigate whether the function of this localization element could be confirmed using the MS2 system. To test this, I deleted a 225nt long fragment of the *CaMKII α* 3'-UTR that contained the ‘Mori’ element (**Fig. 5A**). Surprisingly, neurons that were transfected with this construct together with NLS-MCP-YFP and subsequently fixed still showed particles in very distal regions of the dendrites (data not shown). It is possible that the difference between my observations and the original results from Mori et al. is due to differences in the used constructs. It is for example conceivable that the MS2-tagged construct is more stable and thus allows localization of the reporter to distal dendrites by diffusion

rather than active transport. To rule out this possibility I performed live imaging experiments. The obvious prediction would be that a *CaMKII α* reporter lacking this element is either completely immobile or displays just oscillatory, diffusive movements. Unexpectedly, long distance runs with high speed were still observable (**Fig. 5B,D; Suppl. Movie 2**). Consequently, I tracked the motile particles and analyzed the same parameters as for the construct containing the full length *CaMKII α* 3'-UTR (**Table 1**). Calculations of the parameters derived from the data of 219 particles yielded interesting results. The fraction of particles falling into the different categories of motility was comparable with the construct that contained the Mori element (**Fig. 5C**). In contrast to the full length construct the average velocities of movements in the anterograde and retrograde direction were not significantly different from each other (**Fig. 5E,G**). The particles, however, spent more time moving anterogradely than retrogradely. Therefore, the particle population covered a slightly larger distance and thus showed a net displacement in the anterograde direction - as was the case for the construct containing the full *CaMKII α* 3'-UTR (**Fig. 5F**). Taken together, the absence of the 'Mori' element did not significantly interfere with dendritic targeting and active transport of the reporter RNA. The element published by Mori et al. could therefore not be confirmed to be necessary for the localization and transport of *CaMKII α* mRNA in dendrites.

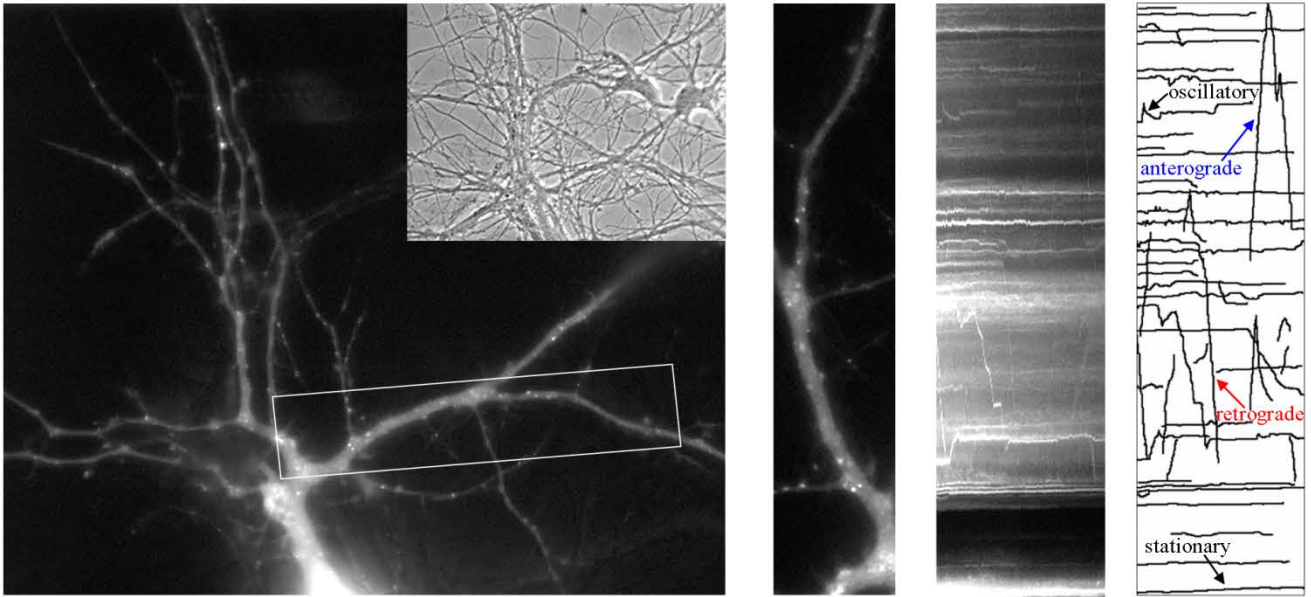
Figure 5 (right side). Kinetics of *CaMKII α* Δ 1-225 mRNA transport

(A) Constructs used for live imaging of *CaMKII α* Δ 1-225 in primary neurons. The 3'-UTR of *CaMKII α* , lacking nucleotides 1-225, was fused to 24xMS2 sites (left). The NLS-MCP-YFP construct contains a NLS to reduce the amount of free cytoplasmic protein. (B) Left panel: Fluorescence and phase contrast images of a living hippocampal neuron transfected with the two MS2 constructs depicted in (A). Middle panels: Zoom-in (left) and kymograph (right) generated from the boxed region in the left panel. Right panel: Traces of individual particles generated from the kymograph. Examples of stationary, oscillatory, anterograde and retrograde particles are highlighted (**Suppl. Movie 2**) (C) Percentage of *CaMKII α* Δ 1-225 particles that fall into the different categories of motility. (D) Diagram depicting traces of all tracked particles. Time is plotted on the x-axis while the y-axis represents the additive distance relative to the first tracking point. (E) Median velocity of particle displacements in the anterograde and retrograde direction, respectively. (F) Percentage of the number of displacements and total distance that all particles traveled in anterograde or retrograde direction. (G) Velocity histogram of anterograde and retrograde particle displacements. Interquartile ranges were 0.76 μ m/s for anterograde and 0.74 μ m/s for retrograde displacements. Statistical significance was assessed with a two-tailed Mann-Whitney test.

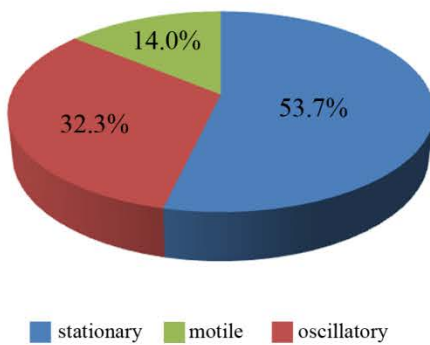
A



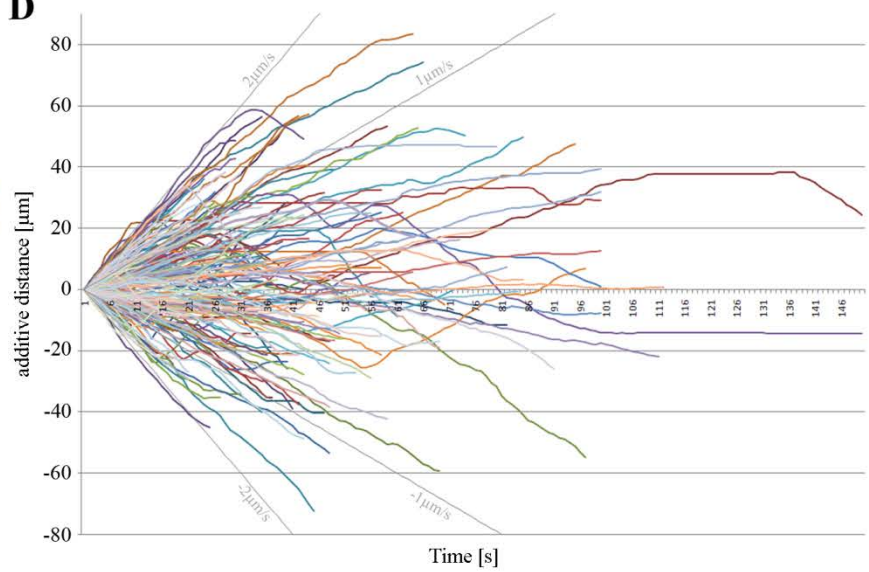
B



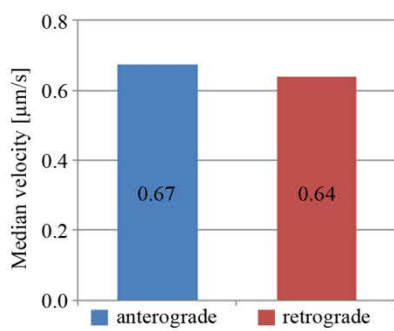
C



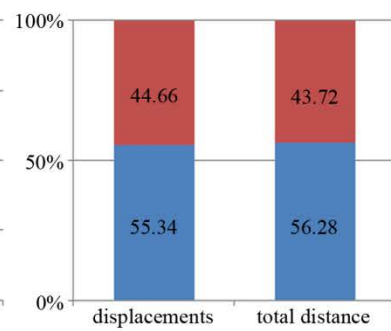
D



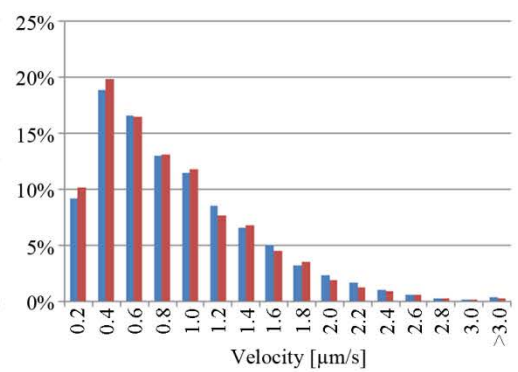
E



F



G



3.4 Visualizing transport and localization of *CaMKII α* mRNA to synapses

An aspect of mRNA localization that has not been addressed in living cells so far is the localization of mRNAs with respect to synaptic sites. The observation that more than half of the RNA particles are stationary led to the assumption that this subpopulation might represent mRNAs that have already reached their destination, which is presumably the synapse (Steward and Levy, 1982; Rao and Steward, 1991). Moreover, I wanted to examine whether the sudden pausing of motile particles occurs close to synapses and might thus indicate anchoring or trapping of the RNPs. To address this, I performed simultaneous live imaging of *CaMKII α* mRNA and a fluorescently tagged form of the postsynaptic density protein 95 (PSD95). Neurons were triple transfected with 24xMS2-*CaMKII α* 3'-UTR, NLS-MCP-YFP and RFP-PSD95. Live imaging experiments were performed with both a conventional widefield microscope and a confocal spinning disc microscope. Similarly to fixed cells, stationary YFP-particles were frequently observed near synapses (**Fig. 6A**, **Suppl. Movie 3**). The similar subcellular localization pattern of the MS2-tagged *CaMKII α* 3'-UTR reporter and the endogenous mRNA relative to postsynaptic sites (Kao et al, 2010) is evidence that the localization pattern of the reporter reflects that of the endogenous counterpart. Interestingly, several cases were recorded where a fast directional RNA particle stopped close to a postsynaptic site and remained stationary for an extended period or the rest of the imaging time (**Fig. 6B**). Although this is no direct evidence, it is tempting to speculate that this represents a recruitment of the RNP to the postsynaptic scaffold, maybe involving a trapping or anchoring event. A further interesting observation was that several of the RFP-PSD95 puncta showed slow dynamic movements (**Fig. 6C**). This is probably caused by the motility of dendritic spines. On rare occasions, small individual PSD95 particles were transported along the dendritic shaft with high speeds. These observations underline the necessity for investigating the interactions between RNPs and PSD95 in the temporal dimension. However, the limited number of cells that were analyzed does not allow a definite conclusion about the relation between the motility of *CaMKII α* mRNA and its localization to postsynaptic sites in living neurons.

3.5 Transport kinetics of *β -actin* mRNA

For a long time it has been assumed that neuronal transport RNPs are 'large' complexes containing a high number of RNA molecules (Krichevsky and Kosik 2001; Kanai et al, 2004). Research performed in the lab challenges this hypothesis by showing that *CaMKII α* , *β -actin*

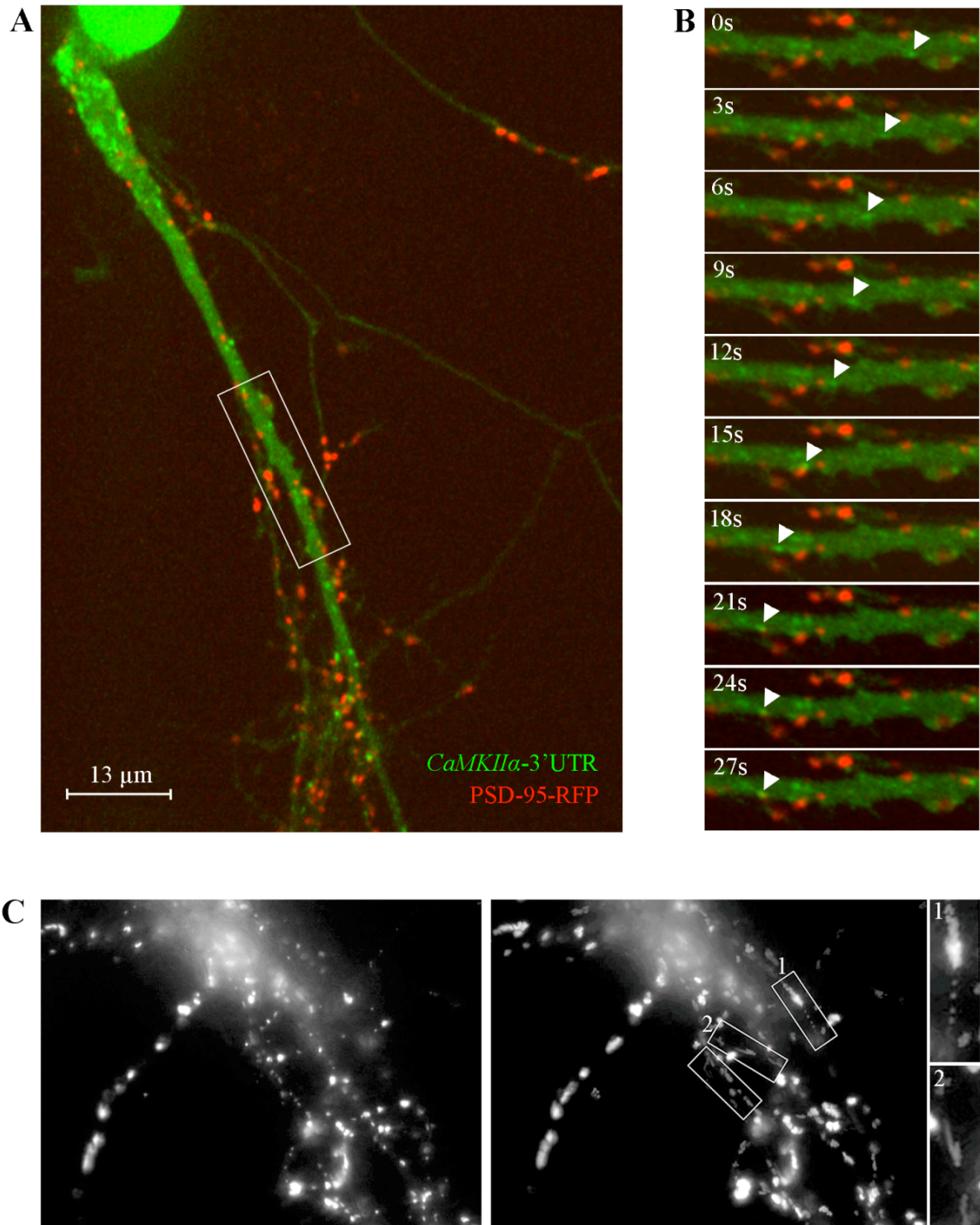


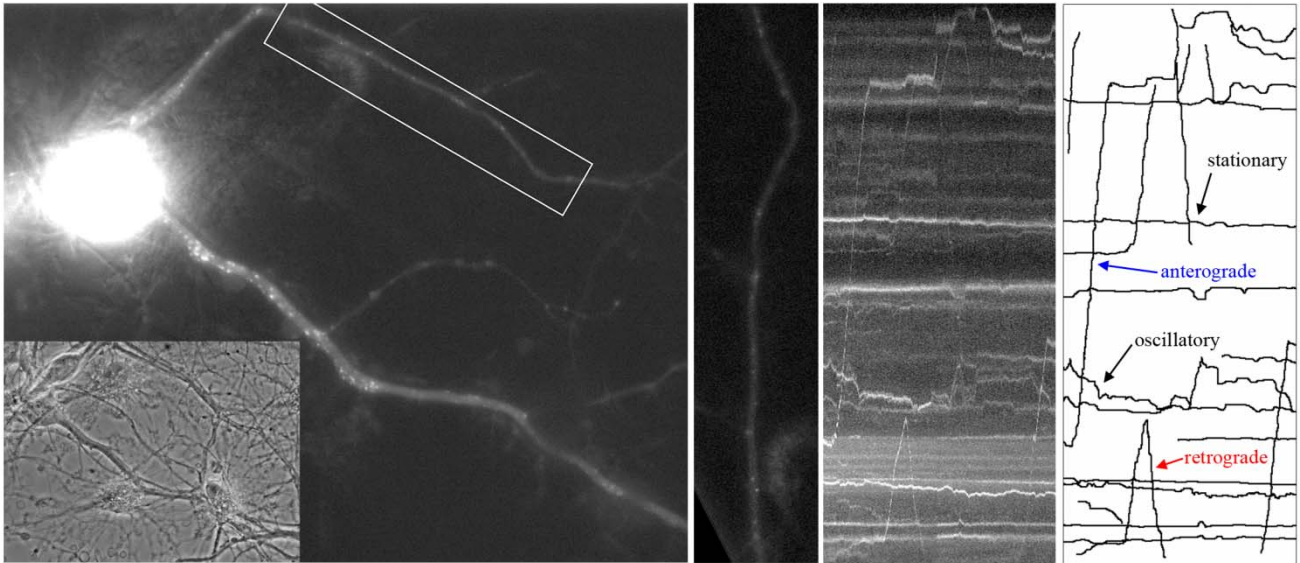
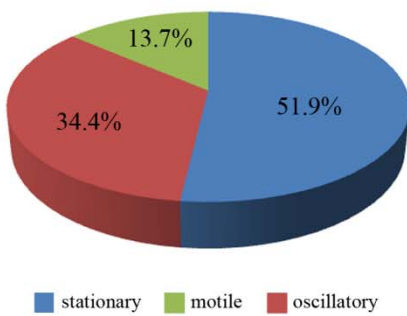
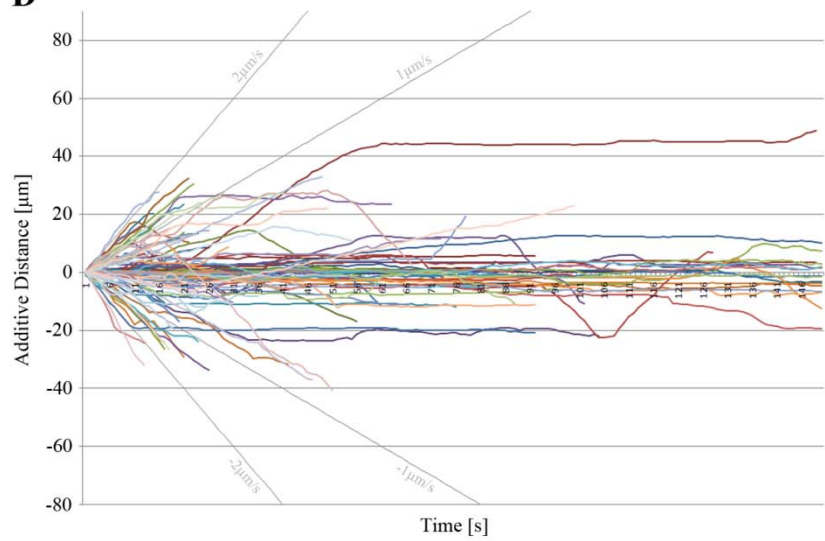
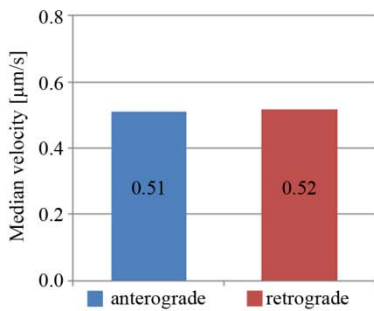
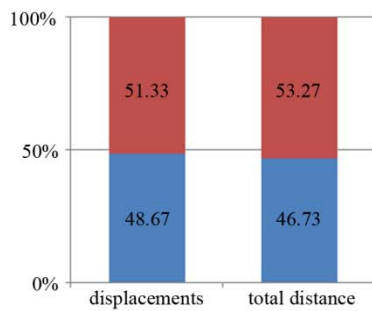
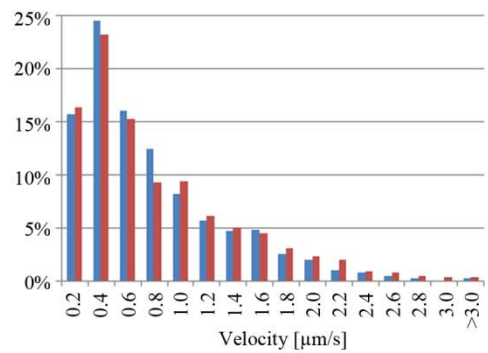
Figure 6. *CaMKII α* mRNA localizes close to PSD-95 in living neurons

(A) Hippocampal neuron transfected with 24xMS2-*CaMKII α* 3'-UTR, MCP-YFP and PSD-95-RFP. (B) Time series of a live cell imaging experiment observing a dendrite (see boxed region) of the triple-transfected hippocampal neuron in (A). A single RNA particle (arrowhead) moved anterogradely with high speed, then stopped close to a postsynaptic site and remained there for the rest of the movie. (Suppl. Movie 3) (C) Single image (left) and maximum intensity projection (right) of a movie taken of a neuron transfected with PSD95-RFP. Boxed regions in the right panel indicate examples of motile PSD95-RFP puncta.

and *MAP2* mRNAs localize to dendrites independently and in low copy numbers (Tübing et al, 2010; Mikl et al, 2011). The independent localization would allow different transport mechanisms to be at play for these transcripts. In fact, different transport mechanisms could be one explanation for the different localization patterns that have been observed for different mRNAs (Paradise and Steward, 1997; Mikl et al., 2011). And different transport mechanisms might be revealed by different transport kinetics. To address this question, I tagged another dendritic mRNA with 24xMS2 sites and studied its transport dynamics (**Fig. 7A,B; Suppl. Movie 4**). *β -actin* is a well characterized mRNA that colocalizes with *CaMKII α* only to a negligible extent (Mikl et al, 2011), arguing that these two RNAs segregate to distinct RNPs. Therefore, I replaced the *CaMKII α* 3'-UTR of the 24xMS2-*CaMKII α* 3'-UTR construct with most of the full length sequence of *β -actin*. As in the case of *CaMKII α* , only a fraction of *β -actin* particles displayed fast movements. Percentages of motile, oscillatory and stationary particles were similar to the other two RNA constructs (**Fig. 7C**). For motile particles the direction of transport was almost equally probable in both directions (**Fig. 7D,F**). Furthermore, the directionality of individual particles was comparable to that of the *CaMKII α* reporters (**Table 1**). Values for the average velocities were slightly lower than for *CaMKII α* (**Fig. 7E,G**), which is probably due to differences in tracking by the experimenter (see Discussion). Interestingly, in contrast to *CaMKII α* , no small bias to the anterograde direction could be observed for *β -actin*. Instead, *β -actin* RNA particles even covered a slightly higher, though not significantly different, distance in the retrograde direction (**Fig. 7F**). However, whether these small differences indeed reflect different transport pathways is questionable and clearly needs further investigation.

Figure 7 (right side). Kinetics of *β -actin* mRNA transport

(A) Constructs used for live imaging of *β -actin* mRNA in primary neurons. The sequence of *β -actin* mRNA was fused to 24xMS2 sites (left). The NLS-MCP-YFP construct contains a NLS to reduce the amount of free cytoplasmic protein. (B) Left panel: Fluorescence and phase contrast images of a living hippocampal neuron transfected with the two MS2 constructs depicted in (A). Middle panels: Zoom-in (left) and kymograph (right) generated from the boxed region in the left panel. Right panel: Traces of individual particles generated from the kymograph. Examples of stationary, oscillatory, anterograde and retrograde particles are highlighted. (**Suppl. Movie 4**) (C) Percentage of *CaMKII α* particles that fall into the different categories of motility. (D) Diagram depicting traces of all tracked particles. Time is plotted on the x-axis while the y-axis represents the additive distance relative to the first tracking point. (E) Median velocity of particle displacements in anterograde and retrograde direction, respectively. (F) Percentage of the number of displacements and total distance that all particles travelled in anterograde or retrograde direction. (G) Velocity histogram of anterograde and retrograde particle displacements. Interquartile ranges were 0.68 μ m/s for anterograde and 0.79 μ m/s for retrograde displacements. Statistical significance was assessed with a two-tailed Mann-Whitney test.

A**B****C****D****E****F****G**

3.6 Dendritic localization of *CaMKII α* and *β -actin* mRNAs is not affected by overexpression of dynamitin/p50

The results obtained so far, together with previous studies, strongly indicate that the fast directed movements observed in a subset of RNA particles are dependent on the activity of microtubule-based molecular motors. As microtubules in proximal dendrites have mixed polarity (Baas et al, 1988) both plus-end and minus-end directed motors are candidates for driving dendritic targeting and transport. In an interesting study Kapitein et al. developed a so called “particles induced by multimerization” (PIM) trafficking assay to study the role of dynein and kinesin in the transport of dendritic cargos. This assay allows the inducible coupling of any protein of choice to a molecular motor. By using this approach they could show that recruitment of dynein targets exogenous as well as axonal cargo to dendrites. Furthermore, inhibition of dynein reduced the amounts of GluR2 in dendrites by a factor of two and led to axonal targeting of this dendritic protein (Kapitein et al, 2010). These findings prompted us to test whether dynein could also be responsible for the dendritic localization of RNPs. Dynamitin/p50 is a component of the dynactin complex, a multisubunit protein complex that enhances the processivity of dynein (King and Schroer, 2000). Artificial overexpression of dynamitin/p50 disrupts the dynactin complex and thereby impairs dynein-driven transport (Burkhardt et al, 1997). As a first pilot experiment I therefore impaired dynein-mediated transport by overexpressing dynamitin/p50 and performed FISH against endogenous *CaMKII α* and *β -actin* mRNAs. Overexpression of dynamitin/p50 was detected by immunostaining for the dynamitin/p50 construct. The overall morphology of neurons transfected with dynamitin was not obviously different from untransfected cells.

For both of the mRNAs, the numbers of particles in dendrites were similar to those detected in untransfected cells (**Fig. 8**). Thus, it seems that the sorting of *CaMKII α* and *β -actin* mRNAs to dendrites is not affected by the overexpression of dynamitin. Nonetheless, this observation does not rule out that dynein is involved in the transport of RNPs. It is conceivable that several motor proteins of different types bind to one cargo complex, as has been reported for vesicular transport in axons (Encalada et al, 2011). It could for example be that dynein mediates retrograde transport in distal dendrites, where microtubule polarity is rather uniform with plus ends pointing towards the tip (Baas et al, 1989), without being necessary for initial sorting to dendrites.

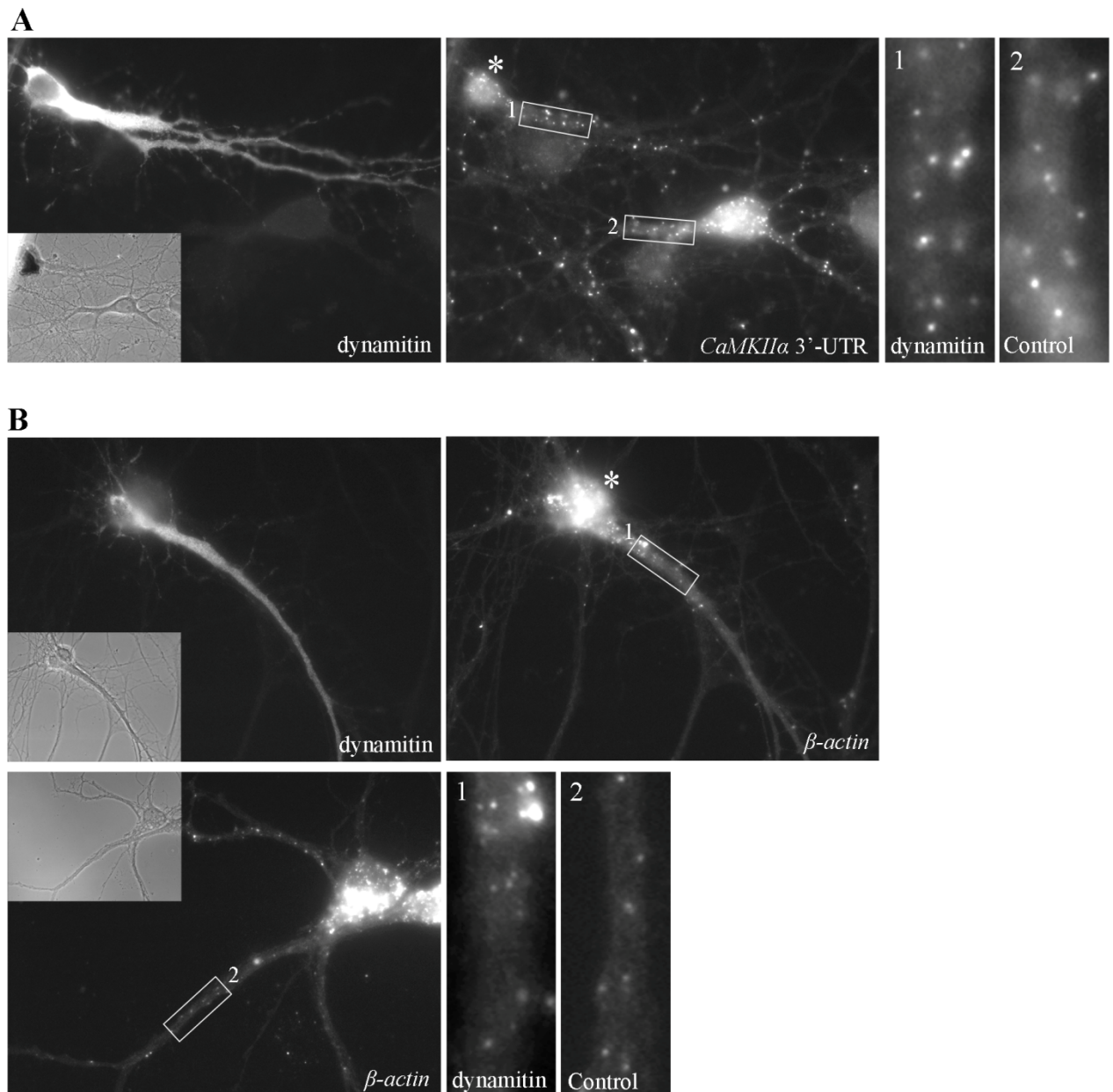


Figure 8. Overexpression of dynamitin/p50 does not affect the amounts of *CaMKIIα* and β -actin RNA particles in dendrites

Endogenous *CaMKIIα* (A) and β -actin mRNAs (B) were detected by FISH in wildtype neurons and neurons transfected with a dynamitin-myc construct. Neurons overexpressing dynamitin-myc were stained with an anti-myc antibody (left panels) and are marked by an asterisk in the middle panels. Total numbers of dendritic *CaMKIIα* and β -actin RNA particles are similar in transfected and untransfected neurons (see magnifications of the boxed regions).

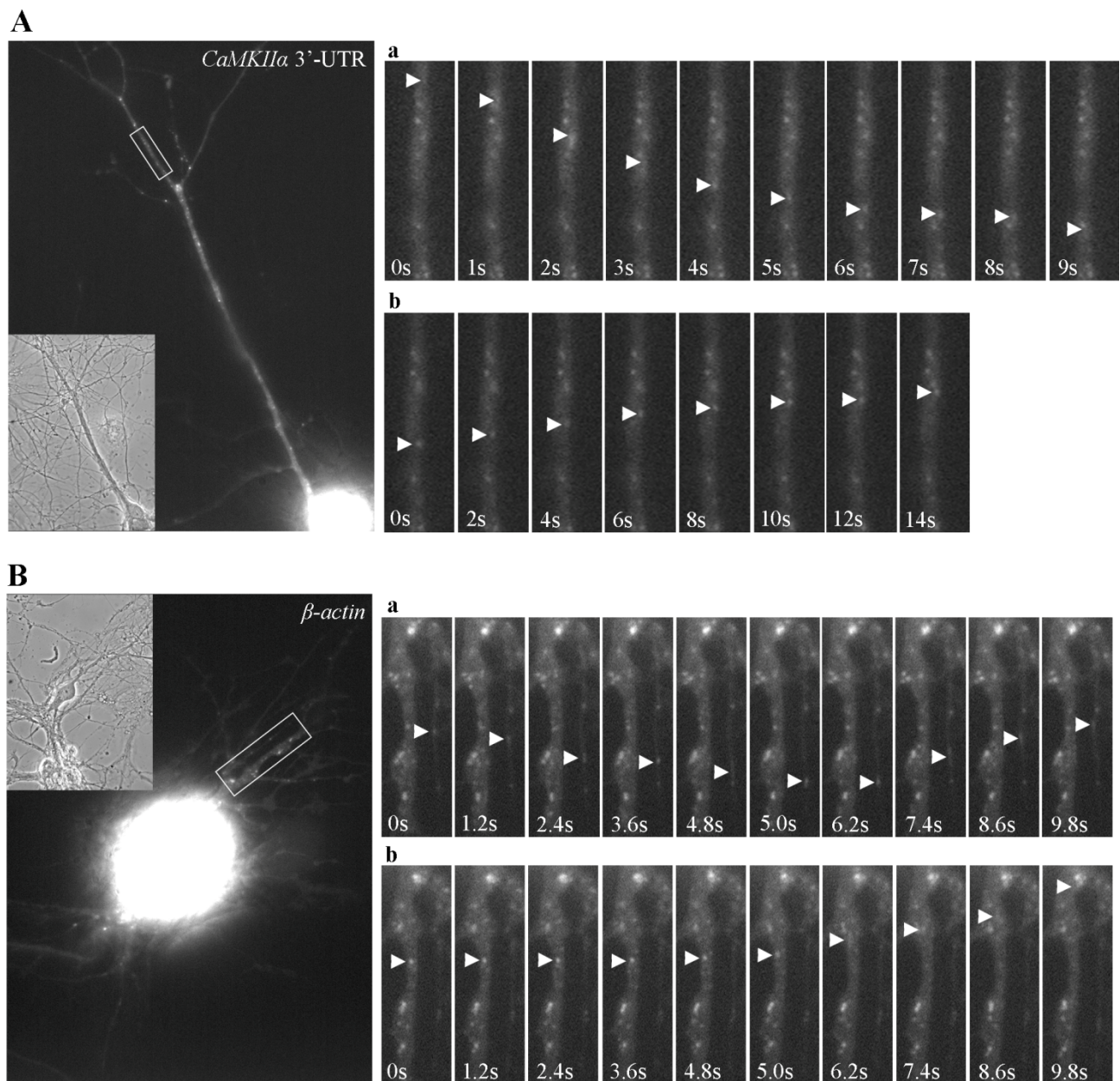


Figure 9. *CaMKII α* and β -actin RNA particles in cells overexpressing dynamin/p50 still display **bidirectional movements**

Living hippocampal neurons transfected with dynamin/p50, MCP-YFP and either 24xMS2-*CaMKII α* 3'-UTR (A) or 24xMS2- β -actin (B). Panels on the right show time series of selected dendrites of living hippocampal neurons corresponding to the boxed regions in the left panels. Both *CaMKII α* and β -actin RNA particles display anterograde (Aa, Ba) and retrograde (Ab, Bb) movements. One example (Aa) of a β -actin RNA particle is shown that reversed direction (Ba) (Suppl. Movies 5 and 6).

To gain further insight into motor-based motility of mRNAs, time lapse imaging was performed in neurons where dynein-mediated transport was impaired. Again, the MS2-tagged *CaMKII α* and *β -actin* mRNA reporters were used for this experiment. Neurons were triple transfected with the MS2 constructs and dynamin/p50 and allowed to express the transgenes overnight. For both RNA constructs, anterograde and retrograde motility could still be detected (**Fig. 9**). For *CaMKII α* , movements in both directions could be observed in distal dendritic sites (**Fig. 9A**; **Suppl. Movie 5**). In the case of *β -actin*, one motile particle was observed in proximal dendrites to reverse direction (**Fig. 9B**; **Suppl. Movie 6**). These examples indicate that bidirectional motility of these two mRNAs can occur in neurons that overexpress dynamin. However, clearly more experiments and most importantly good controls are necessary to be able to conclude that dynein is not involved in the dendritic transport of RNPs.

4. DISCUSSION

The localization of mRNAs to dendrites of hippocampal neurons plays a major role in neurite development, dendritic spine remodeling, and the way neurons process information. Historically, several seminal studies have brought interesting insights into the dynamics of neuronal mRNA transport (Knowles et al, 1996; Rook et al, 2000; Dichtenberg et al, 2008; Kao et al, 2010). In summary, these studies showed that a small subset of RNA particles is transported in a fast, microtubule-dependent manner towards and away from the soma. Both the fraction and the directionality of motile particles were shown to depend on neuronal age and activity. Furthermore, synaptic stimulation can redistribute mRNAs from the dendritic shaft to dendritic spines (Tiruchinapalli et al, 2003; Kao et al, 2010). Different synaptic stimulation protocols exert different effects demonstrating that this process is highly regulated.

The MS2 system is currently the most successful system for imaging RNA transport in dendrites of living neurons. There are several reasons for that. One factor is the good signal to noise ratio that can be achieved. Another important reason is that the reporter undergoes nuclear processing and can be delivered into neurons by transfection. In this work we have made use of the MS2 system to characterize the dynamics of several RNA reporters in detail. Compared to previous publications we increased the numbers of MS2 sites as well as the

temporal resolution of imaging. Furthermore we used a new NLS-MCP-YFP constructs with an improved nuclear localization signal. This allowed us to detect small motile RNA particles that have probably escaped previous investigations. These improvements of the MS2 system, together with the detailed kinetic analysis of the motile fraction of RNA particles described in this chapter, leads to a revised view on the logistics of dendritic mRNA transport.

Several studies in the past have found that the majority of RNA particles are not motile (Knowles et al, 1996; Rook et al, 2000; Dynes and Steward, 2007). This was confirmed by our results where more than fifty percent of the particles did not move at all. The experiments where the RNA reporter was covisualized with a postsynaptic marker revealed that many of these immobile particles reside close to synapses. Another third of the particles displayed short-range oscillatory movements. This pattern of motility resembles diffusive movements and could therefore be representative of RNPs that are floating freely in the cytoplasm. Alternatively, the motility of oscillatory particles might be caused by unstable, transient interactions with molecular motors. The remaining particle fraction (ca. 14-18%) showed long-range movements with high velocity. The values measured for the average velocities of these movements clearly point to a molecular motor based transport mechanism (King and Schroer, 2000; Verhey et al, 2011). Interestingly, the size of this fraction is similar to the motile subpopulation of β -actin mRNA in fibroblasts (Fusco, 2003), which might point to a commonality in the underlying transport mechanisms. One question that was not addressed in this work is how the relative proportions of the mRNAs falling into the different motility categories change with the physiological status of the cell. For β -actin mRNA, for example, there is evidence that the number of motile particles decreases with the age of cultured neurons (Rob Singer, pers. communication).

The velocities measured in this thesis were approximately ten times higher than the values that were published for *CaMKII α* before (Rook et al, 2000). In contrast, a recent publication where endogenously tagged β -actin mRNA was imaged reported values that were even higher than our measurements (Lionnet et al, 2010). Importantly, the first study used frame rates that were approximately 20 times slower than ours, whereas the authors of the second study could acquire images at a 20 times faster rate. Thus, the velocity measures clearly correlate with the number of frames taken per second. This is very likely caused by two factors. First, movements occurring in the interval between two successive frames cannot be detected. Second, fast particles change position very quickly. Therefore, with slow frame rates, it is

often not possible to assign subsequent positions in sequential frames to the same particle, thereby missing the very fast ones. This in turn leads to an underestimation of the average particle velocity.

A major focus of this work was the study of the directionality of mRNA transport. Most importantly, fast movements of RNA particles occurred with almost equal probability in both directions. This is insofar interesting as retrograde movements would theoretically not be necessary at all to target RNPs to dendrites. In contrast to the bidirectional motility of the RNA population, single mRNA particles displayed rather directed movements and rarely reversed direction during the imaging period. This probably facilitates the fast transport of newly synthesized transcripts to distal dendritic sites, thereby keeping the amounts of RNA along the dendrite in balance. This might be important for all synapses to have the same availability of RNPs that can be recruited when needed. Taken together, these observations suggests a model in which mRNA molecules are not directly targeted from the soma towards individual synapses, but reside in dendrites - along which they travel bidirectionally - until they get selectively recruited to postsynaptic sites upon demand. The dendritic mRNA population thus constitutes a readily available pool that can serve the demands of specific synapses without a significant temporal delay. This is in agreement with the recently published “sushi belt model” of RNA localization (Doyle and Kiebler, 2011).

An important question that arises is whether these motility characteristics are common to all dendritically localized mRNAs and whether they are regulated by synaptic activity. It would certainly be very interesting to compare the transport of immediate early gene (IEG) products (for example *Arc*) to that of “housekeeping mRNAs”. It is conceivable that mRNAs coding for IEGs exhibit different transport characteristics, as they need to be targeted to distal dendritic sites quickly after being synthesized, from housekeeping mRNAs that are present in dendrites even without a signaling event.

Although the kinetic analysis of the three different RNA reporters yielded qualitatively similar results, some slight differences were revealed. For *CaMKII α* , the median velocity of particle displacements was significantly higher in the anterograde than in the retrograde direction. *CaMKII α* Δ 1-225 showed the same trend but here no level of significance was reached. A higher velocity towards the anterograde direction was also reported for FMRP, which is an RBP involved in dendritic transport of *CaMKII α* (Dietenberg et al, 2008). This small bias to

the anterograde direction might lead to a faster and more efficient dendritic targeting of this mRNA. Interestingly, it was shown that *oskar* mRNA exhibits a small bias towards the posterior pole of the oocyte during *Drosophila* embryogenesis. This bias is caused by a weakly polarized microtubule cytoskeleton and is sufficient for the posterior localization of *oskar* (Zimyanin et al, 2008). However, there are important differences between that study and the results presented here. First of all, the net posterior displacement of *oskar* was due to a larger percentage of particle displacements in the posterior (57%) versus the anterior (43%) direction. In the case of *CaMKII α* the net displacement was caused by different velocities in the two directions. As this was not the case for *β -actin*, it cannot depend on the polarity of the microtubule cytoskeleton. Even more importantly, the localization patterns of *oskar* and *CaMKII α* mRNAs are completely different. Whereas *oskar* needs to localize to the posterior pole of the oocyte to define the anterior-posterior axis (Ephrussi and Lehman, 1992), *CaMKII α* shows a uniform distribution along the dendrite (Mikl et al, 2011). It should be kept in mind that also without this slight velocity difference between the two directions a dendritic localization of *CaMKII α* would still occur, but probably take significantly longer. Thus it is hardly conceivable that these two transport processes are homologous and governed by an evolutionary conserved transport mechanism.

A comparison of the transport characteristics of *β -actin* and *CaMKII α* mRNAs shows that they are, on the whole, very similar. Particles of these two mRNAs traveled in both directions with almost equal frequency while individual particles showed very directed motility. Interestingly, in contrast to *CaMKII α* , a trend towards net anterograde movement could not be observed for *β -actin* mRNA. It is possible that this small difference in kinetics between the *β -actin* and *CaMKII α* particle populations explains their different localization patterns between. Whereas endogenous *CaMKII α* is distributed more or less uniformly along the dendrite, *β -actin* shows a gradient with more particles at proximal than at distal dendritic sites (Mikl et al, 2011). However, in contrast to the endogenous transcripts, the localization patterns of the MS2-tagged *CaMKII α* and *β -actin* mRNAs were not different to an obvious extent. This discrepancy might be explained by differences in the stability of the endogenous mRNAs and the MS2-reporters. The addition of 24xMS2 sites might increase the stability, for example, and could thereby allow 24xMS2- *β -actin* particles to spread evenly throughout the dendrite over time, while the endogenous counterpart would be degraded before reaching distal dendritic sites. These thoughts, however, are highly speculative and further experiments are

needed to show that the different transport kinetics of *CaMKII α* and *β -actin* do indeed account for their distinct localization patterns.

Unfortunately, the exact values of the kinetic parameters of the three RNA constructs cannot be directly compared with each other. This is due to differences in the way the movies were tracked. While for the first movies for *CaMKII α* and *β -actin*, every particle that displayed a movement was tracked for the entire imaging period, i.e. also during oscillatory and stationary phases, for the later movies particles were only tracked during their motile phases. This probably explains the higher values in velocity for the *CaMKII α* constructs when compared with *β -actin*.

Surprisingly, the results obtained with the *CaMKII α* Δ 1-225 construct clearly show – in conflict with the original study (Mori et al, 2000) – that this element is not necessary for either dendritic localization or transport of *CaMKII α* mRNA. Furthermore the transport characteristics of the two constructs seemed to be largely identical. A closer look at the paper from Mori et al reveals that the reporter lacking the Mori element still localized to dendrites in 5-10% of the cells. This indicates that the Mori element is not entirely indispensable for the localization of *CaMKII α* but that it might have a facilitative effect. However, also this hypothesis could not be corroborated with our approach as the number of cells with RNA particles in dendrites was not obviously different between the deletion and the full length 3'-UTR construct (data not shown). Besides our results, another strong argument against the necessity of the Mori element was brought up by the generation of a mutant mouse that lacks most of the 3'UTR of *CaMKII α* but still contains the Mori element. In hippocampal slices of this mutant mouse, the mRNA does not localize to dendrites anymore despite the presence of the Mori element (Miller et al, 2002). The whole story gets even more complicated by the identification of other localization elements in the 3'-UTR that were argued to mediate dendritic targeting of *CaMKII α* (Blichenberg et al, 2001; Huang et al, 2003; Subramanian et al, 2011). Thus, it seems that multiple elements exist in the 3'-UTR of *CaMKII α* that might regulate its dendritic transport. What the function of these distinct elements is and how they interact is currently unclear and needs further research. Clearly one important step would be the identification of RBPs that bind to these elements.

Both *CaMKII α* and *β -actin* mRNAs were shown to localize to the head of dendritic spines (Tiruchinapalli et al, 2003; Kao et al, 2010). However, how the RNA molecules get there has not been studied in a living cell up to now. I showed here that a large fraction of the stationary

CaMKII α transcripts localize close to postsynaptic sites. Furthermore motile particles sometimes interrupted their movements when passing a synapse. Whether these observations reflect a meaningful cellular process – like trapping or anchoring of the RNP at the postsynaptic density - or are just stochastic events remains to be shown. Importantly, Kao et al. could show that the amounts of *CaMKII α* mRNA particles in dendritic spines increases after application of DHPG (Kao et al., 2010). This result obviously asks for experiments where RNA and synapses are co-imaged while manipulating synaptic activity at the same time.

It is generally accepted that RNPs get transported along the microtubule cytoskeleton by means of molecular motors (Knowles et al 1996; Kanai et al, 2004). As microtubules in proximal dendrites have mixed polarity, both plus-end and minus-end directed motors are candidates for mediating bidirectional transport. There is experimental evidence both in favor of kinesin and dynein for being involved in dendritic RNA transport. Biochemical isolation of presumptive transport RNPs showed that RNP components copurify with conventional kinesin (Kif5) (Kanai et al, 2004). Kapitein et al. argue that dynein is responsible for steering cargo into dendrites while kinesin mediates transport in distal microtubules (Kapitein et al, 2010). Whereas the bidirectional transport of dendritic cargo by a single class of motors is possible, a more likely scenario is the attachment of multiple motors to a RNP, as was reported for axonal vesicles (Encalada et al, 2011).

The preliminary results of our experiments indicate that bidirectional transport of mRNAs is still possible in neurons where dynein-mediated motility is impaired. Importantly however, it must be noted that we cannot be sure whether the overexpression of our dynamitin-construct indeed disrupted the dynactin complex. To show this, proper controls need to be carried out in the future. Furthermore, also if the function of the dynactin complex were severely impaired, dynein motors might still have residual activity that could account for the observed movements. Control experiments and a more detailed analysis of transport kinetics are necessary to conclude that dynein is not involved in the dendritic transport of these mRNAs. Anticipated that our experimental procedure indeed disrupted dynein function, and having in mind that dynein mediates most of the transport directed towards microtubule minus ends (Karki and Holzbaur, 1999; Kardon and Vale, 2009), the results would indicate that the observed movements have been driven solely by plus-end directed motor activity. Therefore, the observations reported here allow the speculation that the mixed polarity of microtubules in

dendrites is sufficient to allow transport of RNPs in both directions and question the necessity of multiple molecular motors for conferring bidirectionality.

III. DYNAMICS AND SYNAPTIC REGULATION OF DENDRITIC PROCESSING BODIES

1. BACKGROUND

Processing bodies are cytoplasmic granules that have been implicated in the degradation and transient storage of translationally repressed mRNAs (Sheth and Parker, 2007). Previous work in the lab has detected P-bodies in dendrites of hippocampal neurons (Vessey et al, 2006). Furthermore, it was shown that they contain dendritic mRNAs as well as miRNAs (Cougot et al, 2008), which suggests that they might be involved in the regulation of local translation and thus in synaptic plasticity. This hypothesis is supported by the finding that P-bodies respond to neuronal activity (Cougot et al 2008; Zeitelhofer et al, 2008). More specifically, Zeitelhofer et al. reported that neuronal activity causes a reduction in the number of dendritic P-bodies. Further evidence comes from the observations that P-bodies show directed movements along dendrites and localize to some extent at the base of dendritic spines (Cougot et al, 2008; Zeitelhofer et al, 2008). In addition, it was reported that synaptic stimulation leads to an increased exchange rate of some P-body components, for example Dcp1a (Cougot et al, 2008). Taken together, these findings suggest a working model in which P-bodies regulate synaptic plasticity by storing translationally inactive mRNAs which can be released for translation at sites and times of demand (**Fig. 10**).

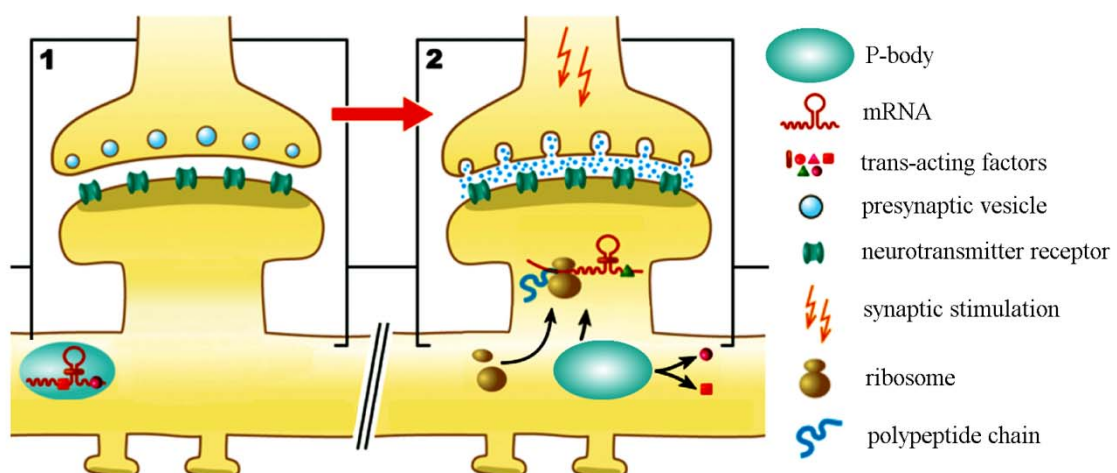


Figure 10. Working model for the role of P-bodies in dendrites

Dendritic P-bodies contain translationally repressed mRNAs. A subset of them resides close to postsynaptic sites (1). Upon synaptic stimulation they are thought to release the stored mRNAs, which then associate with ribosomes to be locally translated (2).

2. AIMS

The implication of P-bodies in the regulation of dendritic protein synthesis and synaptic plasticity raises several interesting questions that have not been addressed so far. I aimed to answer some of these questions in the work presented here. The discovery of P-bodies at the base of dendritic spines, for example, asks for the dynamics of the interaction between P-bodies and postsynaptic sites. Are P-bodies stably or transiently associated with synapses and can they shuttle between nearby dendritic spines? Furthermore, there is little known about the receptors that mediate the effect of synaptic stimulation on the size and distribution of P-bodies. It is tempting to speculate that these effects are induced by signaling pathways that also affect mRNA transport and translation. Previous work in the lab has shown that P-bodies contain dendritic mRNAs. The data stated above suggest that these mRNAs are stored in P-bodies at low levels of neuronal activity and released upon stimulation, but this has not been shown directly. In addition, I was interested in studying the association of mRNAs and P-bodies in living cells. How stable are these interactions and do P-bodies play a role in the active transport of mRNAs?

3. RESULTS

3.1 Dynamics of dendritic P-bodies with respect to postsynaptic sites

To study the dynamics of the spatial relation between P-bodies and synapses, hippocampal neurons were simultaneously transfected with the P-body marker Dcp1a-EGFP (Stöhr et al, 2006) and PSD95-RFP (Marrs et al, 2001), and then subjected to live imaging. The great majority of P-bodies remained stationary during the whole imaging period. Dcp1a particles frequently localized to synapses marked by PSD95, confirming the results obtained in fixed cells (Cougot et al, 2008; Zeitelhofer et al, 2008). Most of the P-bodies that were found close to PSD95 did not show any motility. A small fraction, however, displayed oscillatory movements while staying associated with the postsynaptic compartment indicative of restricted diffusion (**Fig. 11, Suppl. Movie 7**). Some P-bodies showed directed movements over tens of micrometers. On several occasions, fast moving Dcp1a granules could be observed that interrupted their movements when passing a synapse (**Fig. 11B**). Sometimes, these P-bodies stayed associated with PSD95 for the rest of the movie or paused for different periods of time and then moved on. Thus, dendritic P-bodies are not passive, cytoplasmic

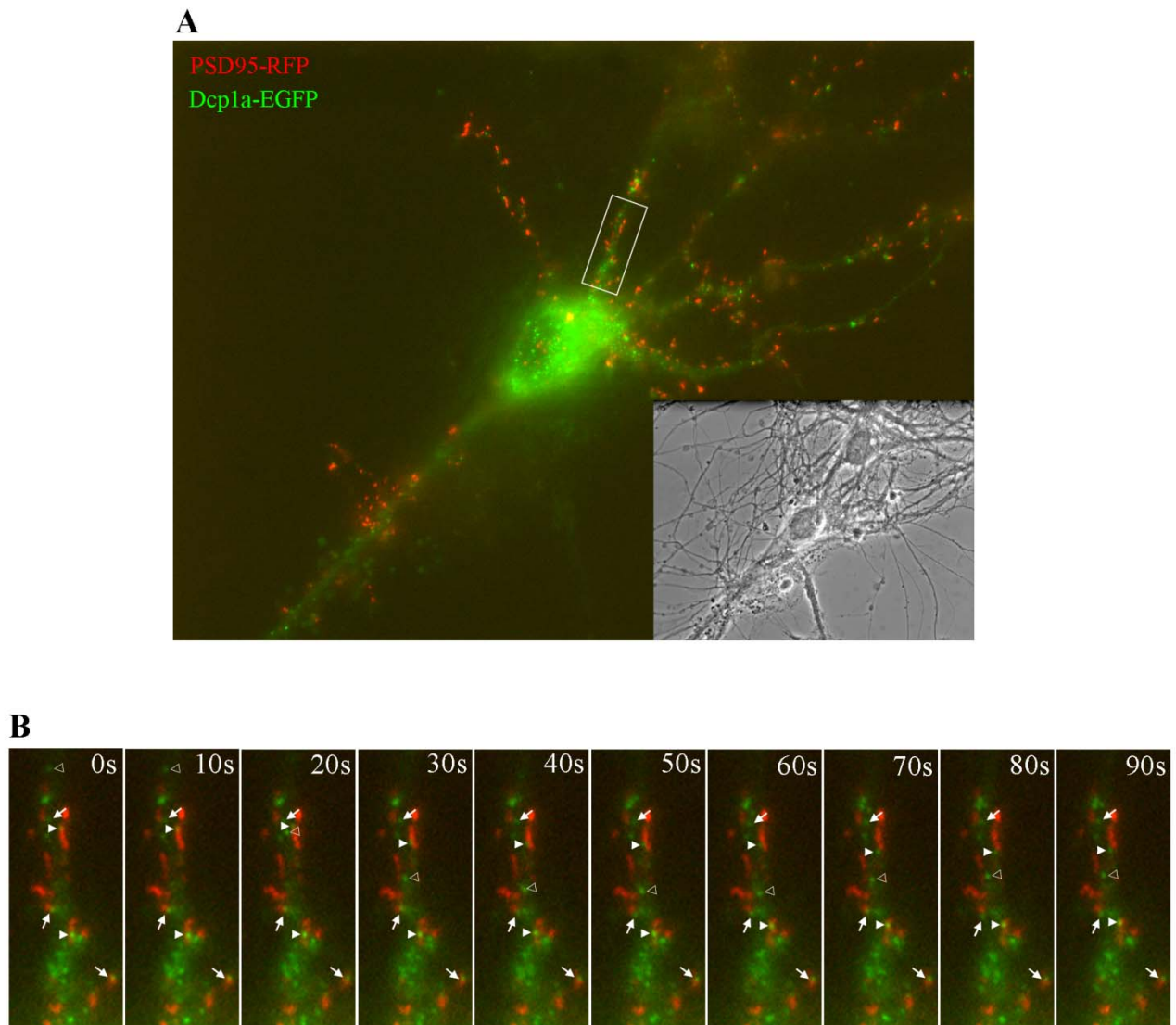


Figure 11. Live-imaging of P-bodies with respect to postsynaptic sites

(A) A living hippocampal neuron cotransfected with the P-body marker Dcp1a-EGFP and PSD95-RFP, a postsynaptic marker. (B) Enlargements of the boxed region in (A) showing images taken at different timepoints (Suppl. Movie 7). Most P-bodies did not move during the timecourse of the movie. A fraction of these stationary granules localized to postsynaptic densities (arrows). Some P-bodies showed short-range movements while staying in close proximity to PSD-95 (arrowheads). One Dcp1a granule displayed fast retrograde transport before stopping at a postsynaptic site to stay associated with it for the rest of the movie (open arrowhead).

granules but can move along dendrites in a manner indicative of active transport and occasionally show dynamic interactions with postsynaptic sites.

3.2 Synaptic activity regulates the assembly of P-body components in dendrites

It has been previously observed in the lab that overnight treatment of neurons with a selection of drugs that silences neuronal activity leads to an increased size of P-bodies. This effect was shown to be reversible as P-body size went down to baseline levels two hours after the neurons were transferred back to normal culture medium (Vendra and Kiebler, unpublished observations). However, these effects had not yet been quantified. To investigate this interesting effect in more detail, I tested different pharmacological treatments (**Fig. 12A,B**) and quantified the size of dendritic P-bodies. For this purpose, cells were fixed after the respective treatments and immunostained for the well-established P-body marker Rck (Parker and Sheth, 2007) (**Fig. 12C-E**). I then determined the average pixel area of Rck spots in the proximal 25µm of dendrites. When neuronal activity was inhibited ('silenced'), the average P-body size increased more than twofold. After recovery from silencing for 70 min, this value returned to levels that were not significantly different from control conditions (**Fig. 12F**).

Hippocampal neurons in culture show spontaneous oscillations of the membrane potential that are accompanied by changes in intracellular calcium concentration and rely entirely on glutamatergic neurotransmission (Bacci et al, 1999). Moreover, glutamate is the main excitatory neurotransmitter of pyramidal cells. Thus, the hypothesis was raised that signaling mechanisms downstream of glutamate receptors might be responsible for the observed reduction in P-body size after recovery from silencing. I therefore stimulated neurons with glutamate followed by immunostaining for Rck. Interestingly, glutamate even had an effect on P-body size when applied in the presence of the silencing mix and without allowing the neurons to recover from silencing (**Fig. 12F**). This observation asked for a more detailed investigation. In addition to tetrodotoxin (TTX), which blocks Na_v-channels and thus the spiking activity of neurons, the silencing mix contained (2*R*)-amino-5-phosphonovaleric acid (APV) and 6-cyano-7-nitroquinoxaline-2,3-dione (CNQX), which are antagonists of the NMDA and AMPA/kainate ionotropic glutamate receptors, respectively (Bacci et al, 1999). Thus the observed effect must be mediated by metabotropic glutamate receptors which are not blocked by the silencing mix (**Fig. 12A**). Group I metabotropic glutamate receptors (mGluRI) have previously been implicated in the regulation of dendritic RNA transport (Antar et al, 2004; Kao et al, 2010) and local translation (Weiler et al, 1997) as well as in LTP (Morris et

al, 1999) and LTD (Huber et al, 2000). Therefore I specifically stimulated mGluRI receptors with the drug (*S*)-3,5-dihydroxyphenylglycine (DHPG) while blocking AMPA and NMDA receptors as well as action potentials with the silencing mix. This treatment led to a reduction in P-body size that was not significantly different from the values obtained after glutamate stimulation (**Fig. 12F**). To summarize, silencing of neuronal activity caused a twofold increase in P-body size in proximal dendrites that could be reversed by restoration of synaptic input. Furthermore, stimulation of mGluRI receptors alone was sufficient to induce a decrease in the size of dendritic P-bodies after silencing neuronal activity.

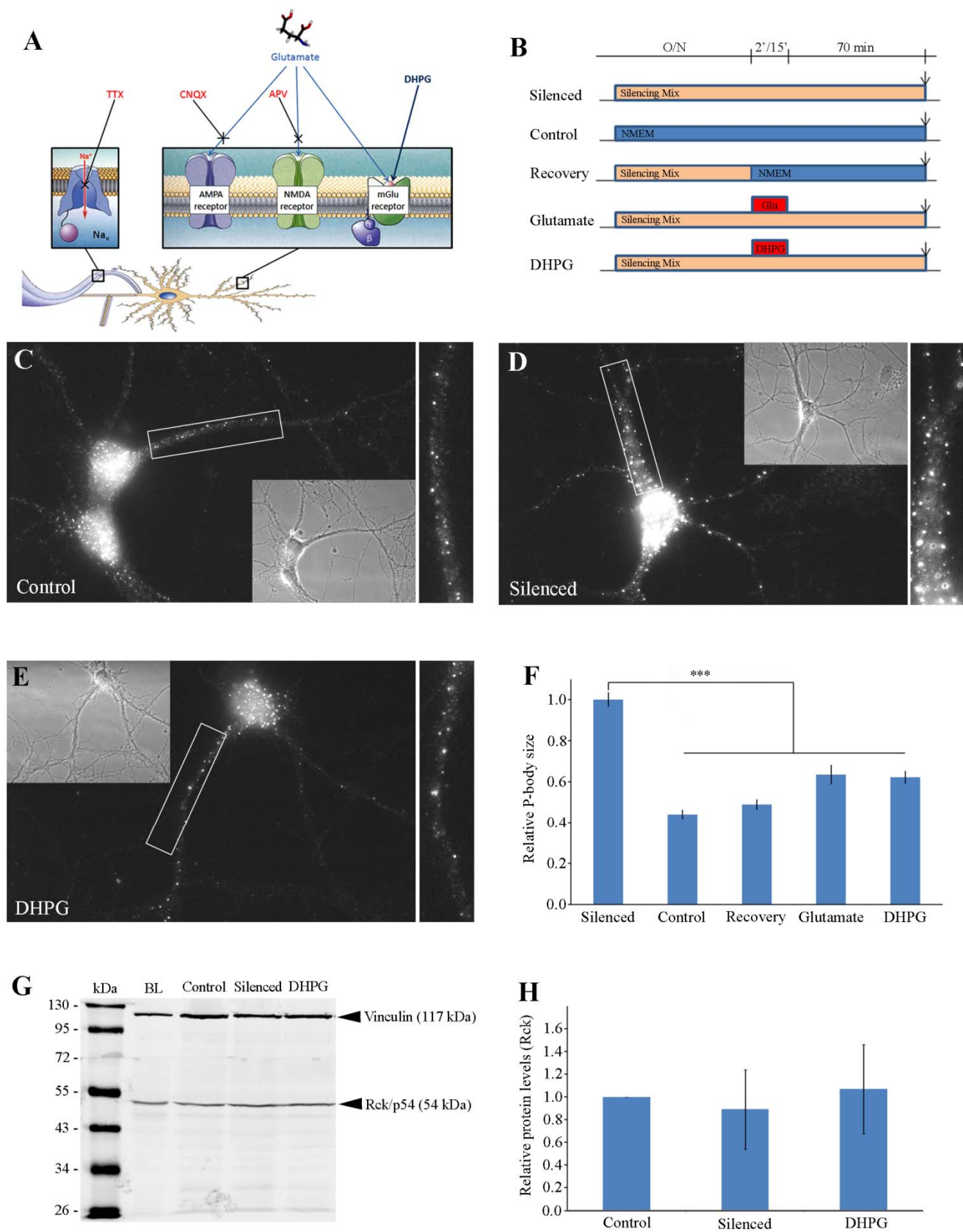
The observed changes in P-body size under different conditions of activity could either be explained by rapid synthesis and degradation of P-body components or by a change in their intracellular distribution. To be able to differentiate between these two possibilities, I determined the protein levels of Rck upon silencing and DHPG stimulation. This was achieved by applying the pharmacological treatments to cultured cortical neurons followed by cell lysis and Western blotting for Rck. The protein concentration of Rck remained constant, irrespective of the treatments applied before (**Fig. 12G,H**). This strongly argues for a rapid assembly and disassembly of Rck that is regulated by synaptic activity.

3.3 Dendritic mRNAs can be detected in P-bodies but do not accumulate there upon silencing of neuronal activity

It was shown previously in the lab that dendritic P-bodies contain *β -actin*, *CaMKII α* and *MAP2* mRNAs (M. Mikl, Diploma thesis, Univ. Vienna 2009). Preliminary experiments failed to detect any significant differences in the amounts of these mRNAs that were localized to P-bodies upon different conditions of neuronal activity, but no detailed quantifications had been carried out yet. Importantly, even small differences might be relevant for a biological function. Therefore, I repeated the experiments followed by quantitative analysis.

Figure 12 (right side). Silencing of neuronal activity leads to a reversible assembly of P-bodies

(A) Receptor specificity of the used drugs and (B) experimental outline for the silencing and stimulation experiments Hippocampal neurons were either not treated (C), silenced overnight with TTX, CNQX and APV (D), stimulated with DHPG (E) or glutamate in presence of the silencing mix (not shown), or allowed to recover from silencing (not shown). Then, neurons were stained for the P-body marker Rck and the pixel area of Rck-puncta was quantified (F). Silencing of neuronal activity led to a significant increase in P-body size. This effect was reversible as stimulation with glutamate or DHPG or a recovery from silencing led to a reduction in P-body size that was close to control conditions. Protein levels of Rck were not affected by silencing or DHPG treatment (F,G). Error bars indicate SEM. Statistical significance was determined using a one-way ANOVA with a Tukey's multiple comparison post-test (***) $p < 0.001$.

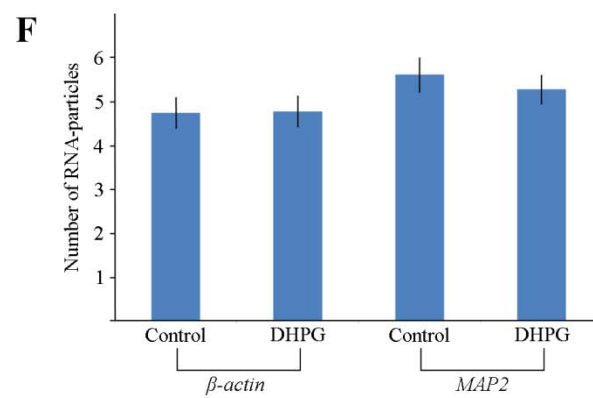
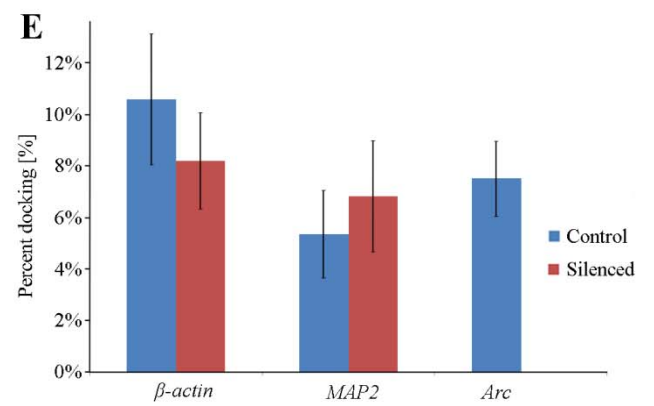
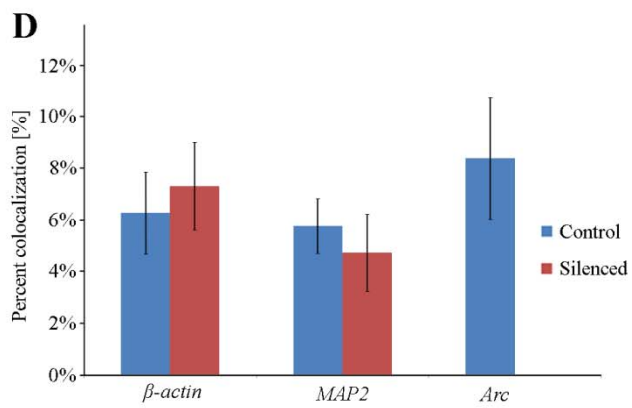
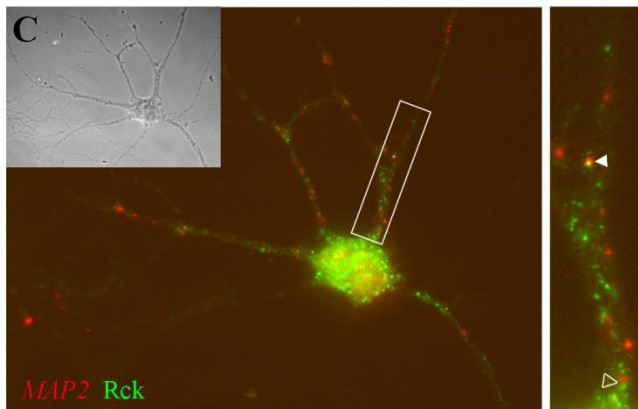
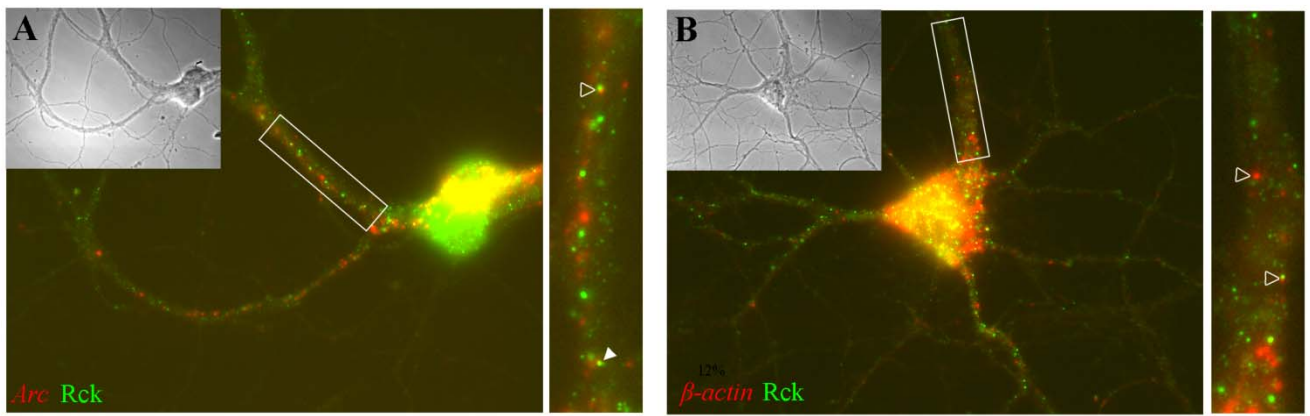


I performed fluorescent *in situ* hybridization (FISH) against the well-described dendritic mRNAs *Arc*, *MAP2* and β -*actin* concomitantly with immunostaining for Rck (**Fig. 13A-C**). In unstimulated neurons, the immediate early gene product *Arc* mRNA is expressed at very low levels and thus difficult to detect (Lyford et al, 1995). Therefore, to increase the amounts of *Arc* in dendrites by artificial overexpression and thereby facilitate its detection, neurons were transfected with a plasmid encoding a reporter construct that contained the 3'-UTR of *Arc*. In contrast, *MAP2* and β -*actin* are expressed at sufficiently high levels to obtain good signals for the endogenous mRNAs. For all of the investigated mRNAs a low degree of colocalization with P-bodies, ranging from 5.8% to 8.4%, was observed (**Fig. 13D**). In addition to the rate of colocalization, the percentage of RNA particles that were in very close proximity or partially overlapping with Rck puncta was determined. The rationale for this experiment was based on previous work in the lab, which showed by live protein-imaging that transport RNPs and P-bodies can interact in a dynamic way by a process termed docking (Zeitelhofer et al, 2008). The percentage of RNA particles docked to P-bodies was in the same range as the observed colocalization rates, ranging from 5.4% for *MAP2* to 10.6% for β -*actin* (**Fig. 13E**). Thus, a fraction of *Arc*, β -*actin* and *MAP2* mRNAs was detected in or in close proximity to P-bodies. This subset probably represents translationally inactive mRNAs. Nevertheless, the great majority of RNA puncta were not found in dendritic P-bodies.

The size and number of P-bodies are thought to be proportional to the number of translationally repressed mRNAs that are associated with P-body components (Parker and Sheth, 2007). Based on the finding that P-body size is regulated by neuronal activity, I tested whether an alteration of activity also affects the localization of mRNAs to P-bodies. Therefore, I repeated the FISH experiments for β -*actin* and *MAP2* after having silenced the neurons overnight. Both the percentages of RNA particles that colocalized and docked with P-bodies were not significantly different from control conditions (**Fig. 13 D,E**). This suggests that there is no enhanced recruitment of β -*actin* and *MAP2* mRNAs to P-bodies upon silencing of neuronal activity.

Figure 13 (right side). A minor fraction of *Arc*, β -*actin* and *MAP2* mRNAs localizes to P-bodies, but silencing of neuronal activity does not lead to an enhanced recruitment

Overexpressed *Arc* (**A**) or endogenous β -*actin* (**B**) and *MAP2* (**C**) mRNAs were detected by FISH concomitantly with immunostaining for Rck. A low percentage of the respective mRNAs colocalized (arrowheads) (**D**) or docked (open arrowheads) (**E**) with P-bodies. Silencing of neuronal activity did not alter the recruitment of these mRNAs to P-bodies to a significant extent (**D,E**). Stimulation of hippocampal neurons with DHPG did not increase the total amounts of β -*actin* and *MAP2* particles in dendrites (**F**). No statistical differences were found by using two-tailed t-tests.

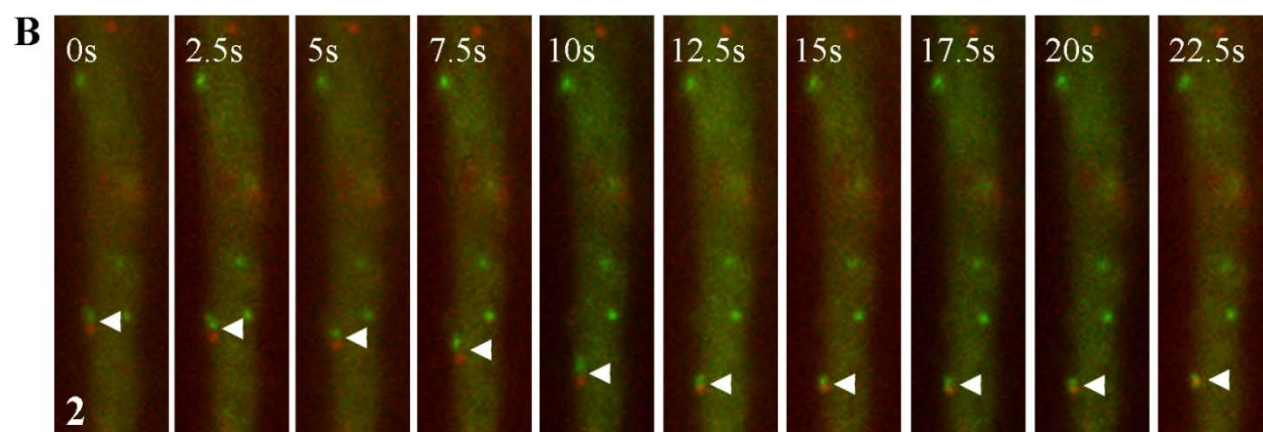
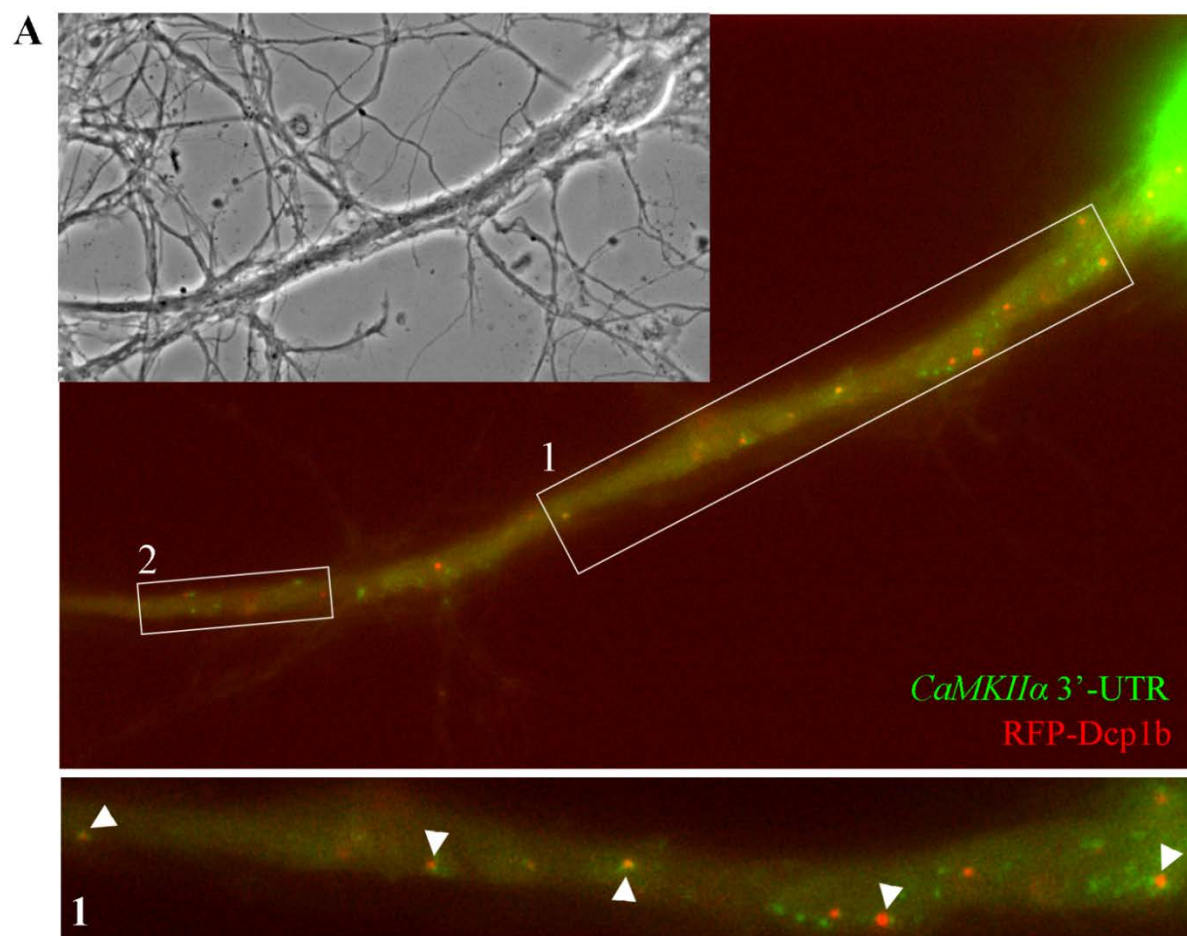


Another mechanism of how synaptic input might affect mRNA localization is not by changing their translational status but by increasing the amounts of specific mRNAs in dendrites. This had been reported for several mRNAs before (Steward et al, 1998; Dictenberg et al, 2008). I tested this possibility for the two mRNAs mentioned above, *β-actin* and *MAP2*. Neurons were stimulated with DHPG followed by FISH for the respective mRNAs. Levels of *β-actin* mRNA in dendrites was not affected by DHPG treatment, which is consistent with observations published before (Dictenberg et al, 2008). Also the number of *MAP2* particles in DHPG-treated dendrites was not significantly different from control conditions (**Fig. 13F**). To conclude, I was neither able to detect an effect of synaptic activity on the localization of *β-actin* and *MAP2* mRNAs to P-bodies nor on the total amounts of these mRNAs in dendrites. Nonetheless, the detection of mRNAs in dendritic P-bodies is an indication that these cytoplasmic granules influence the fate of dendritic mRNAs. At which levels of regulation this occurs will have to be tested in the future.

3.4 Co-transport of *CaMKIIα* mRNA and P-bodies in dendrites of living neurons

The experiments described above show that a fraction of certain mRNAs localize to dendritic P-bodies. This interesting finding was further explored by studying the interaction of RNA particles and P-bodies in living neurons. The interaction between transport RNPs and P-bodies has been studied in the lab before in great detail (Zeitelhofer et al, 2008). In that study, RNAs were visualized indirectly by using the RBP Staufen2 as a marker for transport RNPs (Goetze et al, 2006). A caveat of this method is that the identity of the RNAs bound by Staufen2 is not being revealed. The MS2 system (Bertrand et al, 1998) offers the unique possibility to study interactions between specific RNAs and proteins in the living cell. To do this, hippocampal neurons were transfected with constructs allowing visualization of the *CaMKIIα* reporter RNA mentioned before, together with Dcp1b-RFP, a marker for P-bodies. As the most suitable emission filter available was a CFP/YFP/mCherry triple bandpass filter, Dcp1A-RFP had to be imaged with excitation and emission filters designed for mCherry. This reduced the signal in the Dcp1A channel dramatically.

Figure 14 (right side). Colocalization and co-transport of *CaMKIIα* mRNA and P-bodies in living neurons (A) Living hippocampal neuron transfected with 24xMS2-*CaMKIIα*-3'-UTR, MCP-YFP and RFP-Dcp1b (top). Arrowheads indicate examples of colocalization between the *CaMKIIα* 3'-UTR reporter construct and RFP-Dcp1b (bottom) (**Suppl. Movie 8**). (B) Images from a time-lapse movie corresponding to the boxed region (2) in (A). An RNA particle was co-transported together with RFP-Dcp1b for a short distance (arrowhead). Note that the signals from the red and green channel do not overlap perfectly as the images were acquired sequentially with a short delay.



Live imaging of the transfected cells revealed that *CaMKII α* particles frequently colocalized and docked with P-bodies in living neurons (**Fig. 14A, Suppl. Movie 8**). The extent of colocalization seemed to be higher than in fixed cells, which might be explained by the overexpression of both RNA and Dcp1b (Parker and Sheth, 2007). Most of the interacting particles remained stationary for the time course of the movie. Interestingly however, I could occasionally observe that RNA and Dcp1b were transported together for short distances (**Fig. 14B**) and even stayed associated while reversing direction (**Suppl. Movie 8**). This is a strong argument that the colocalization events observed between RNAs and P-bodies are not merely stochastic events but rather reflect a snapshot of a cellular process which is likely to have some functional significance. In contrast to that, co-transport of RNA and P-bodies over large distances was never observed, indicating that P-bodies are not involved in long-range transport of dendritic mRNAs.

4. DISCUSSION

Although P-bodies have been studied for almost a decade (Sheth and Parker, 2003), their precise function as well as their molecular composition still remain elusive. This is partly due to the diverse cellular processes, e.g. degradation, storage or transport of mRNAs, in which P-bodies seem to play a role. Moreover, the function and composition of P-bodies seems to depend on the cellular context and thus differs between different cell types and organisms (Anderson and Kedersha, 2006; Barbee et al, 2006; Cougot et al, 2008). Even in a single cell different subclasses of P-bodies probably exist and the transitions between them and other RNPs might be continuous. All these points make the study of P-bodies a difficult, but interesting task.

The data presented in this thesis underline the dynamic nature of P-bodies in mammalian neurons. I showed that P-bodies can be actively transported in dendrites and that they often reside close to synaptic sites (Cougot et al, 2008; Zeitelhofer et al, 2008). In addition, they occasionally interact with the postsynaptic compartment in a dynamic manner. Although only a small fraction of them displays this behavior, it might be functionally relevant. Another important finding is that the size of dendritic P-bodies is regulated by synaptic activity. Interestingly, the activation of group I metabotropic glutamate receptors with the drug DHPG seems to be sufficient to induce this effect. It was shown before, that stimulation of this

receptor subgroup leads to an enhanced transport of the RBP ‘translocated in liposarcoma’ (TLS) into dendritic spines (Fujii et al, 2005). As TLS was found to be a component of transport RNPs (Kanai et al, 2004), the authors of that study argued that the translocation of TLS into dendritic spines represents a recruitment of mRNAs to synapses. Furthermore, DHPG affects the transport of FMRP-interacting mRNAs as well as their translational status (Antar et al, 2004; Ferrari et al, 2007; Kao et al, 2010). In addition to its effect on mRNA transport, DHPG was implicated in the initiation of LTD (Huber et al, 2000) and less prominently also in the formation of LTP (Morris et al, 1999). Interestingly, DHPG-induced LTD depends on the RBP Staufen2, which mediates the localization of *Map1b* mRNA to dendrites (Lebeau et al, 2011). All these studies suggest a direct link between the effect of DHPG on dendritic mRNAs and synaptic plasticity. Taken together, activation of mGluRI seems to be a major signal in regulating multiple steps of dendritic protein synthesis. How the stimulation of this glutamate receptor subgroup can exert such diverse effects and how its effect on P-bodies fits into the picture is currently unclear. A probable scenario is that the differential effects of mGluRI stimulation are regulated by the simultaneous activation of other signaling cascades.

Dendritic P-bodies contain mRNAs and respond to neuronal activity. The disassembly of P-bodies upon synaptic stimulation might be concomitant with the release of stored mRNAs. This is supported by the fact that P-bodies need RNA for their assembly (Teixeira et al, 2004) and that the number and size of P-bodies correlates with the amount of translationally silent mRNA (Teixeira et al, 2005; Parker and Sheth, 2007). Thus, it is interesting to argue that P-bodies localize to dendrites close to synapses where they represent storage units for translationally inactive mRNAs. Upon stimulation from the presynaptic site, P-bodies would be recruited to dendritic spines where they disassemble and release the mRNAs for local translation. If these speculations hold true, one would expect that the changes in P-body size are accompanied by a coincidental release or recruitment of mRNA molecules from/to P-bodies. However, such an effect could not be demonstrated in the experiments described above. One possible explanation for this is that mRNAs might be difficult to detect, especially in large P-bodies, due to a limited accessibility of the FISH probe. Alternatively, the increase in the size of P-bodies might go hand in hand with a shift from storage to degradation of mRNAs. Partial degradation and destabilization of mRNAs would hinder binding of the probe. Both of these hypotheses remain speculative and a direct link between the effect of synaptic activity on P-bodies and the fate of dendritic mRNAs still needs to be shown.

Another unsolved question regards the interplay between P-bodies and dendritic mRNA transport. I showed that P-body components and RNAs can occasionally be co-transported in the same RNP. It must be noted however, that this co-transport was only observed in rare cases and thus seems not to be the general rule. In *Drosophila* peripheral neurons evidence was presented that transport RNPs and P-bodies share a large number of components (Barbee et al, 2006). However, this is not the case in mammalian neurons (Zeitelhofer et al, 2008). Our data indicate that mammalian neurons possess at least two molecularly different subsets of motile, RNA-containing, particles. First, transport RNPs that mediate long-range transport of dendritic mRNAs. Second, motile P-bodies that move predominantly over short distances. It is tempting to speculate that the short-range motility of dynamic P-bodies represents a patrolling of neighbouring synapses. Thus, not only the temporal aspects of translational repression by P-bodies might be actively regulated, but also the spatial locations where stored mRNAs are released.

Taken together, dendritic P-bodies can be envisaged as highly regulated dynamic structures that can be remodeled to fulfil different functions based on the demands of the cell.

IV. OUTLOOK

In the last few years, insights into the mechanisms of dendritic mRNA transport and local translation have increased a lot, but several fundamental questions still remain.

The work presented in this thesis points towards a probabilistic behavior of single dendritic RNA particles with respect to their transport. This means that particles are not transported directly to their destination, but frequently switch between different categories of motility and direction of transport. The subcellular distribution of the whole population of a given mRNA thus depends on the probabilities by which these switches occur. The experiments, however, which this model is based on, only capture the dynamics over the timescale of minutes. It would certainly be interesting to investigate mRNA transport for longer periods of time. One possible experiment to do this would be to use photoactivatable or photoconvertible reporters in order to be able to study the distribution of a small population of photoactivated RNPs over hours. Furthermore, to arrive at a full model of the logistics of dendritic RNA transport also other parameters, like the dynamics of degradation and transcription, have to be taken into consideration in the future.

Signals transduced by synaptic receptors can influence both the transport and translation of dendritic mRNAs. It is unclear, however, whether some of the effects that signaling cascades triggered by neurotransmitter receptor signaling can remain confined to single synapses, or whether these signals may alternatively spread throughout the entire dendritic branch or even the whole neuron. To study this, local uncaging of neurotransmitters at single dendritic spines together with imaging of RNA transport or local translation could be used.

Another open question regards the identity of the localization elements that target mRNAs to dendrites. Several elements have been identified, but it is still unclear whether they share a common structural motif and, in most cases, which RNA-binding proteins (RBPs) recognize them. Furthermore the molecular composition of transport RNPs on the protein level is still elusive. It is unclear how many different components constitute a neuronal RNP, not to speak of the function of every single component. Identification of the localization elements (LEs) and their RBPs followed by biochemical and ultrastructural characterization of the RNA-protein complexes will hopefully help to decipher the code that determines whether an mRNA

localizes to dendrites and or not. Once these elements and proteins are identified, their function can be studied by knocking out or genetically manipulating both LEs and RBPs. This would be an important step in order to understand how different dendritic RNPs undergo different fates. In addition to the RBPs it is still not known which types of molecular motors mediate mRNA transport and how they are recruited to RNPs. Interference with the activity of molecular motors together with live RNA imaging and kinetic analysis is one possibility to test this question. Alternative approaches are biochemical interaction studies and electron microscopy.

Furthermore, not much is known about the interplay between transport RNPs and other neuronal RNA granules like P-bodies. It is known that P-bodies respond to neuronal activity and that they store dendritic mRNAs. Additionally, P-bodies localize close to postsynaptic sites in a dynamic manner. A connection however, between these two observations has not yet been made. Surely, imaging RNA, P-body components and synapses at the same time under different physiological conditions is one appealing approach. A very challenging experiment would be to do this not in fixed, but in living cells. The function of P-bodies in regulating neuronal mRNAs could be studied by interfering with P-body assembly by knock-down of critical P-body components and then assessing the effects of this manipulation on RNA localization and synaptic plasticity.

In the long run it will surely be a combination of microscopy, genetics, structural biology, and biochemical approaches that will help to unravel the unsolved mysteries underlying the transport and translation of dendritic mRNAs.

V. MATERIALS

1. Buffers and solutions

SDS-PAGE running buffer (1x)

25 mM Tris
192 mM glycine
0.1% SDS
ddH₂O

Transfer buffer for Western blotting (1x)

25 mM Tris
192 mM glycine
0.1% SDS
20% methanol
ddH₂O

SDS-polyacrylamide gel

Stacking gel 5% (4ml)

2.7 ml ddH₂O
0.67 ml 30% acrylamide mix
0.5 ml 1.5M Tris (pH 8.8)
0.04 ml 10% SDS
0.04 ml 10% APS
4 µl TEMED

Resolving gel 10% (10ml)

4 ml ddH₂O
3.3 ml 30% acrylamide mix
2.5 ml 1.5M Tris (pH 8.8)
0.1 ml 10% SDS
0.1 ml 10% APS
4 µl TEMED

Laemmli buffer (6x)

350 mM Tris-HCl pH (6.8)
10% SDS
30% glycerol
0.1% bromphenol blue
ddH₂O

Ponceau-S solution

0.2% Ponceau-S
3% trichloroacetic acid (TCA)
ddH₂O

Tris-acetate-EDTA buffer (TAE) (50x)

242 g/l Tris base

57.1 ml acetic acid
50 mM EDTA
ddH₂O
pH 7.5 – 7.8

Phosphate buffered saline (PBS)

8,0 g NaCl
0,2 g KCl
1,44 g Na₂HPO₄
ddH₂O to 1 L
pH 7.4

PBS-T

PBS + 0,1% Tween

HBSS (Hank's balanced salt solution)

20 mM HEPES
2 mM CaCl₂
5.4 mM KCl
1 mM MgCl₂
135 mM NaCl
1 mM Na₂HPO₄
5.6 mM glucose
in ddH₂O
pH 7.3

SSC (20x)

3 M NaCl
0,3 M Na-citrate
pH 7,0

NMEM + B27

1x MEM (modified Eagle's medium)
26 mM NaHCO₃
1 mM sodium pyruvate
200 mM L-glutamine
33 mM D-glucose
2% B27 supplement
ddH₂O
pH 7.4

DMEM+HS

DMEM (Dulbecco's modified Eagle's medium)
10% Horse Serum (HS)
1 mM sodium pyruvate
200 mM L-glutamine

Transfection medium

1x MEM (modified Eagle's medium)
15 mM HEPES
1mM sodium pyruvate

2mM L-glutamine
33 mM D-glucose
1x B27 supplement
ddH₂O
pH 7.45

Transfection HBSS (Trans-HBSS)

20 mM HEPES
135 mM NaCl
1 mM Na₂HPO₄
4 mM KCl
2 mM CaCl₂
1mM MgCl₂
10 mM D-glucose
ddH₂O
pH 7.3

Hybridization buffer (Hybe)

50% formamide
5x SSC
0,1% Tween
100 µg/ml tRNA
50 µg/ml Heparin
pH 6.5
(For the washing steps: Hybe buffer without tRNA and Heparin)

2x BBS (BES-buffered saline)

50 mM BES
1,5 mM Na₂HPO₄
280 mM NaCl
ddH₂O
pH 6.90 – 7.30

Blocking solution for immuostainings

2% BSA
2% fetal calf serum
0.2% fish skin gelatine
PBS

Blocking solution for FISH

Roche blocking solution

Tyramide amplification solution

Cyanine3 Tyramide Reagent (Perkin Elmer)
Amplification Diluent (Perkin Elmer)

Silencing mix

1µM TTX (Sigma)
50µM APV (Sigma)
100µM CNQX (Sigma)
NMEM+B27

PCR reagents

Taq Polymerase 5u/μl (Fermentas)
10x Taq buffer (Fermentas)
dNTPs 100mM (Fermentas)
MgCl₂ 25mM (Fermentas)

2. DNA-constructs

FISH

The following sequences were used as templates for FISH probe transcription (see Tuebing et al, 2010):

#F6: *MAP2* (U30938, nucleotides 2532-3738) in pBS II SK
#F9: *CaMKIIα* (NM_177407, 3156-4756) in pBS II KS+
#F38: *Arc* (1.5kb 3'-UTR) in pGEMTeasy
#F66, 67: *β-actin* (NM_031144, 221-740 and 723-1240) in pBS II KS+

Transfections

The following constructs were used for transfections of hippocampal neurons:

#183: DCP1A-EGFP in pCDNA (provided by Jens Lykke Andersen, UCSD)
#216: RFP-DCP1B (provided by Stefan Hüttelmaier, Halle)
#425: pmyrd1EGFP *Arc* 3'UTR FL in pmyrd1EGFP-C2 (provided by L. Schoderböck)
#434: pmax-NLS80-MCP-YFP (provided by K. Czaplinski, Stony Brook).
#462: RSV-lacZ-24xMS2- *CaMKIIα* 3'-UTR (provided by G. Vendra and M. Mrakovcic)
#536: RSV-lacZ-24xMS2-*β-actin*
#549: c-myc-dynamin (provided by Richard Vallee, Columbia U)
#553: PSD-95-RFP in GW1 (provided by David Bredt)
#585: RSV-lacZ-24xMS2-*CaMKIIα* 3'-UTR Δ1-225

Cloning of the MS2 RNA reporter plasmids

#462: RSV-lacZ-24xMS2-*CaMKIIα* 3'-UTR was generated by Georgia Vendra as previously described (Mikl et al, 2011). In short, the 8xMS2 repeats within plasmid RSV-lacZMS2bs-*CaMKIIα* 3'-UTR (Rook et al, 2000) were replaced by 24xMS2 repeats derived from plasmid pSL-MS2-24x (Fusco et al, 2003; provided by Rob Singer, Albert Einstein College of Medicine). Briefly, RSV-lacZMS2bs-*CaMKIIα* 3'-UTR was digested with BamHI/BglII to remove the 8xMS2 sites. The 24xMS2 sites from pSL-MS2-24x were excised by BamHI/BglII digestion and cloned into the BamHI/BglII sites of the RSV-lacZMS2bs-*CaMKIIα* 3'-UTR vector backbone.

#536: RSV-lacZ-24xMS2-*β-actin* was generated by Georgia Vendra and myself. In order to replace the *CaMKIIα* 3'-UTR of plasmid #462 with rat *β-actin* (NM_031144, nucleotides 4-1267), plasmid #462 was cut with BglII/NotI. The vector backbone was then separated from the insert by gel electrophoresis and extraction. The *β-actin* (sequence was amplified from

plasmid #519 by PCR using the primers #12/76 and #14/53 that contained NotI and BglII restriction sites, respectively. The PCR fragment was digested with BglII/NotI and cloned into the BglII/NotI site of the vector backbone of plasmid #462.

#585: RSV-lacZ-24xMS2-*CaMKIIα* 3'-UTR Δ1-225 was generated by myself by deleting nucleotides 1-225 of the *CaMKIIα* 3'-UTR of plasmid #462. To do this, plasmid #462 was cut with PpuMI and re-ligated by blunt-end ligation.

Verification of the MS2 plasmid sequences

All plasmids were sequenced with the forward primer #14/77 that binds upstream of the MS2 sites and by reverse primers that were located inside the RNA reporter sequences specific for each plasmid. These reverse primers were #12/50 for RSV-lacZ-24xMS2-*CaMKIIα* 3'-UTR, primer #14/73 for RSV-lacZ-24xMS2-*β-actin* and primer #13/1 for RSV-lacZ-24xMS2-*CaMKIIα* 3'-UTR Δ1-225. By doing this, the sequence of all MS2 sites could be checked. This was possible as the two sequences could be aligned by help of two point mutations that were located in a linker region approximately in the middle of the 24xMS2 sites. Additionally, the number of the MS2 sites was verified for all plasmids by BamHI/BglII digestion followed by electrophoretic separation of the fragments. The presence and correct length of the RNA reporter inserts were verified by digesting the plasmid with BglII/NotI and by PCR amplification with the primers that were used for cloning.

3. Primers

#12/50 - *CaMKII*3'UTRrev2: agaaccagcagccacattcca
#12/76 - rno-b-act-3UTRshortrev_NotI: aaGCGGCCGCTgcgcaagttaggtttgtca
#13/1 - *CaMKIIα*_rev1940-1921_deletion: cctgccaatgacagctga
#14/53 - rn-b-actin-5UTRfor_BglII: aaAGATCTcactgtcgagtccgcgtc
#14/73 - Rno_bAct_5'UTRrev: gcggccgcggcgaaactggtggcgggt
#14/77 - seqprimer_kosik_MS2for: taataaccgggcaggccat

4. Antibodies

For immunostainings and FISH

Primary antibodies

#120: rabbit α-Rck/p54 (MBL) 1:300 for FISH 1:500 for immunostaining
#176: mouse α-cmyc (Sigma) 1:1000
α-digoxigenin – peroxidase (POD) Fab fragments (Roche) 1:1000

Secondary antibodies

#3: goat α -mouse – Cy2 (Dianova) 1:1000

#5: goat α -rabbit IgG (H+L) - Alexa 488 (Molecular Probes) 1:1000

For Western Blots

Primary antibodies

#119: goat α -Rck/DDX6 (Abnova) 1:400

#209: goat α -Vinculin (Santa Cruz) 1:500

Secondary antibodies

Donkey α -goat – IRDye680 (LiCor) 1:10000

5. Enzymes

T3 RNA Polymerase (Promega)

T7 RNA Polymerase (purified by Lucia Schoderböck)

SP6 RNA Polymerase (Roche/Böhringer Mannheim)

DNase I (Fermentas)

Restriction Enzymes

HindII (Fermentas)

NcoI (Fermentas)

NotI (Fermentas)

NotI-HF (NEB)

SpeI (NEB)

6. Kits

NucAway Spin Columns (Ambion)

EndoFree Plasmid Maxi Kit (Qiagen)

GenElute Plasmid Miniprep Kit (Sigma)

7. Animals

Rats (*Rattus norvegicus*, Sprague Dawley CD-SIFA) were obtained from Charles River Laboratories (Königshofen, Germany).

8. Software

MetaMorph 7.0 and 7.5 (Molecular Devices)

Photoshop CS3 (Adobe)

AnalySIS^B (Olympus Biosystems)

ImageJ 1.43s (NIH, <http://rsb.info.nih.gov/ij>)

Excel (Microsoft)

Odyssey 2.1 (LiCor Biosciences)

Volocity (Perkin Elmer)

Imaris (Bitplane)

Prism 5 (GraphPad)

9. Equipment

Odyssey Infrared Imager (LiCor Biosciences)
Varifuge 3.0R (Heraeus)
Centrifuge 5418 (Eppendorf)
Centrifuge 5417R (Eppendorf)
Thermomixer comfort (Eppendorf)
Photometer GeneQuant 100 (Healthcare Biosciences)
Power supply Power Pac HC (Bio-Rad)
Power supply Power Pac 300 (Bio-Rad)
PAGE chamber Mini-Protean 3 Cell (Bio-Rad)
Gel chamber 40-0911 (Peqlab Biotechnologie)
Gel documentation system E Box 300 SD (Peqlab Biotechnologie)
Hybridization oven 7601 (GFL)
Balance MK Hei-Standard (Heidolph)
pH meter Mp 225 (Mettler Toledo)

10. Microscope setups

For fixed cells

Microscope Axioplan (Zeiss)
Objective 63x/1.40NA oil plan-apochromat (Zeiss)
Light Source X-Cite 120 mercury lamp (EXFO)
Camera F-view II CCD (Soft Imaging Systems)

Filters (all AHF)
Excitation
FITC 475/35
Cy3 543/22
Beam Splitter
FITC 499
Cy3 562
Emission
FITC 530/43
Cy3 593/40

For live imaging

Widefield Setup

Microscope Axiovert 100TV (Zeiss)
Objective 63x/1.40NA oil plan-apochromat (Zeiss)
Objective 100x/1.30NA oil fluar (Zeiss)
Camera CoolSnap HQ2 (Visitron Systems)
Light Source X-Cite 120 mercury lamp (EXFO)
Filter Wheel Controller Ludl MAC 5000 (Visitron Systems)
XY-Stage Corvus high resolution positioning controller (MV)
Piezo stepper E-662 LVPZT-Amplifier Servo (PI Physik Instrumente)
Master Shutter Controller (to synchronize shutters with camera)
Heating chamber (custom built by B. Goetze and M. Kiebler)

Excitation Filters (all BrightLine)

YFP 427/10

mCherry 589/15

GFP 470/22

RFP 556/20

Emission Filters (all AHF)

CFP/YFP/mCherry: 464/547/633

GFP/RFP: 512/630

Beam splitters (all AHF)

CFP/YFP: mCherry 444/521/608

GFP/RFP: 592/574

Confocal spinning disc setup

Microscope Zeiss Observer

Spinning disc unit UltraView VoX (Perkin Elmer)

Lasers 488nm (100W), 561nm (100W)

Emission Filters

GFP/RFP: 552/50 640/120

Camera Hamamatsu EMCCD 9100-13

Objective 63x/1.40NA oil plan-apochromat (Zeiss)

Stage motorized XY ASI stage with piezo Z

VI. METHODS

1. Cell biology

Hippocampal neurons in culture

Cultures of hippocampal neurons were prepared from embryonic day 17 rats as described previously (Goetze et al, 2004). Age of neurons when used for experiments ranged from 14 to 16 days in vitro (DIV). Cultured hippocampal neurons of this age form functional synapses (Mikl et al, 2011). Hippocampal neurons were cultured by Sabine Thomas, Alexandra Hörmann, Jacki Heraud, Kristina Kosenburger and Samantha Herbert.

Cortical neurons in culture

Cortices lacking hippocampi of E17 rats were collected in 37°C HBSS, cut into small pieces and transferred to a 15 ml Falcon tube. Cortical pieces were spinned down for 5 min at 1000g, HBSS was removed and 5ml Trypsin solution (37°C) was added. After incubation for 10 min at 37°C, 5ml DMEM+HS were added to stop trypsinization. Cells were spinned down for 5 min at 1000g and the medium was replaced with 5 ml fresh DMEM+HS. Cells were then dissociated by triturating ten times with a blue tip followed by trituration with a fire-polished Pasteur pipette for 1 min. Afterwards 20 ml DMEM+HS were added and the solution was filtered twice with a 100µm and another two times with a 70µm cell strainer filter (BD). Cells were then counted and plated onto coated culture dishes. Cortical cultures used in this thesis were prepared by Alexandra Hörmann. Age of cortical cultures ranged between 13-16 DIV.

Immunostaining

Neurons grown on glass coverslips (in short referred to as coverslips) were washed briefly with 37°C HBSS and then fixed in 4 % prewarmed PFA (in HBSS) for 15 min. Afterwards, coverslips were washed 3 times in HBSS at RT, permeabilized with 0,1 % Triton in HBSS for 3-5 min, and washed again 3 times. Coverslips were blocked by incubating them in 100 % blocking solution for 30 min. Cells were then incubated with the respective primary antibody diluted in 10 % blocking solution (in HBSS) for 2 hrs. After washing coverslips for 3 x 5 minutes, they were incubated with the secondary antibody coupled to a fluorescent dye for 45 min. Cells were again washed 3 x 5 min in HBSS. Coverslips were then mounted onto microscope slides with 5µl MOWIOL.

***In vitro* transcription of RNA-probes**

Transcription mix

DNA template (linearized plasmid)	0.5-1 µg
rNTP labeling mix (Digoxigenin)	2 µl
10x Transcription buffer	2 µl
RNA Polymerase (T3, T7 or SP6)	2 µl
RNase inhibitor	1 µl
DEPC H ₂ O	x µl
Total volume	20 µl

The transcription mix was incubated at 37°C for 2 hours. Afterwards the template was removed by adding 2µl of RNase-free DNase I for 7 min at 37°C. Unincorporated nucleotides were removed using NucAway Spin columns (Ambion) according to the manufacturer's protocol. To assess the success of the transcription, 1-2µl of the samples were run on a 1% agarose gel at 75 mV and checked for the correct length. The concentration of the probe was measured photometrically.

Fluorescent *in situ* hybridization (FISH)

First, coverslips were washed with HBSS (37°C) and then fixed in prewarmed 4% PFA (in HBSS) for 15 min. Cells were washed in PBT for 2 x 15 min, and then in PBT/Hybe (1:1) for 15 min at RT. Samples were then prehybridized at 65°C in 400 µl Hybe for 2 hours. During this step the probes were prepared. For each sample 400 ng of the riboprobe were diluted in 50µl Hybe, denatured at 97°C for 7 min, put on ice for 2 min and then another 350 µl Hybe (65°C) were added. Coverslips were then incubated in this hybridization mix over night at 65°C. The next day the following washing steps were done: 2 x 30 min in hybe (65°C), 2 x 30 min in Hybe/PBT (1:1; 65°C), 4 x 30 min in PBT (65°C). Then, coverslips were blocked for 2 hours at RT in the ISH blocking solution. After blocking, samples were incubated with the respective primary antibody against the labelled riboprobes (antiDIG-POD diluted 1:1000 in PBT) at 4°C over night or at RT for 2 hours. For simultaneous detection of RNA and protein the primary antibody against the protein was also added at this step. Coverslips were then washed 2 x 20 min in PBT at RT. For a double detection of RNA and protein, the secondary antibody coupled to a fluorescent dye (diluted 1:1000 in PBT) was added for 1 hour at RT. Samples were then washed again 2 x 20 min in PBT. This was followed by the TSA

amplification: 75 µl tyramide-Cy3 (1:75 in Amplification buffer) were added to the samples (on Parafilm) and incubated for 7 min at RT. Coverslips were then washed 3 x 10min in PBT, rinsed with ddH₂O and mounted with Mowiol for microscopic analysis.

CaPO₄ transfection of cultured hippocampal neurons

Transfection solution

ddH ₂ O	x µl
2,5 M CaCl ₂	6 µl
Plasmid DNA	3 µg
2x BBS (pH 6,90 – 7,30)	60 µl
total volume	120 µl

The transfection solution was prepared by first adding the CaCl₂ and then the correct amount of plasmid DNA to ddH₂O. After having mixed the reagents well, 60µl 2x BBS was added dropwise while tapping the tube gently. The solution was then bubbled for about 10 times. Neurons were prepared for transfection by transferring 3 coverslips to a small dish containing 2 ml of transfection medium or in the case of videodishes by replacing the NMEM with transfection medium. The transfection solution was then added to the neurons, and the cells were put at 37°C in an incubator without CO₂ supply. Formation of the precipitate was observed with a microscope using a 10x objective. Once there was a dense and even spread precipitate, neurons were transferred to prewarmed Trans-HBSS and washed for a maximum of 5 minutes. Neurons on coverslips (or in videodishes) were then transferred to NMEM and incubated at least for 8 hours or overnight (36,5 °C / 5% CO₂) to allow for expression of the transfected constructs. Optimal expression times had to be tested empirically for every DNA construct as previously described (Goetze et al, 2004).

2. Pharmacological treatments

Silencing of neuronal activity

5 ml of the silencing mix (1µM TTX, 50µM APV, 100µM CNQX in NMEM) were prepared and equilibrated for at least 1 hour. This mix was then added to the neurons and incubated over night.

Glutamate and DHPG stimulation

Neurons were treated with 10 μ M glutamate for 2 min (Zeitelhofer 2008) or 50 μ M DHPG (Tocris) for 15 min (Dictenberg 2008), either in NMEM or in the silencing mix. After stimulation, cells were transferred back to NMEM or the silencing mix or fixed immediately.

3. Molecular biology

Restriction digestion

10 units of the restriction enzyme (or 5 units per enzyme if two enzymes were used at the same time) and 2,5 μ l of the appropriate 10x buffer were mixed with 20,5 μ l of a DNA-solution. This mix was incubated at 37°C for a minimum of 3 hours and then the enzyme was inactivated by heating the digestion mix to 65°C for 15 min. The success of the digestion was assessed by separating the DNA on an agarose gel.

Polymerase Chain Reaction (PCR)

PCR mix

0.5 μ l DNA
5 μ l Taq buffer (10x)
3 μ l MgCl₂ (25mM)
1 μ l dNTPs (10mM each)
1 μ l Primer forward (10 μ M)
1 μ l Primer reverse (10 μ M)
0.5 μ l Taq polymerase (5u/ μ l)
38 μ l ddH₂O

PCR protocol

- 1.) 94°C – 30sec
- 2.) 94°C – 30sec
- 3.) 56°C – 30sec Steps 2. – 4. → 30 cycles
- 4.) 72°C – 2min
- 5.) 72°C – 5min
- 6.) 4°C – forever

Maxi Prep

Maxi-preps were done by using the EndoFree Plasmid Purification Kit from Qiagen. All steps were done according to the manufacturer's protocol.

Agarose gel electrophoresis

For a 1% agarose gel, 1g of agarose was dissolved in 100ml 1xTAE by heating the solution with a microwave oven. After cooling, 50 μ l of diluted ethidium-bromide was added, and the gel was allowed to solidify at RT. After addition of 6x loading buffer samples were loaded and the gel was run at 75 V for the appropriate time.

4. Biochemistry

Lysis of cortical neurons

Cortical neurons in culture were washed with pre-warmed PBS and then lysed by adding 25 μ l 2x Laemmli buffer (preheated to 95°C) per plate. The cell lysate was then scraped, transferred to Eppendorf-tubes and stored at -20°C.

SDS-PAGE

For the separation of proteins on a polyacrylamide gel a 1,5mm thick 10% separation gel and a 5% stacking gel was used. Cell lysates were heated to 95°C for 5 min and then 50 μ l were loaded per slot. A prestained page ruler (3 μ l) and brain lysate (BL, 9 μ l) were loaded as marker and positive control, respectively. Electrophoresis was performed at 100 Volts for 2 hrs in SDS-PAGE running buffer.

Western blot

Proteins separated by SDS-PAGE were blotted onto a nitrocellulose membrane at 100 Volts for 90 min. Blotting was performed at 4°C in a blot tank filled with transfer buffer. Afterwards the success of blotting was assessed by reversibly staining the membrane with Ponceau-S. The membrane was blocked with a Detector Block Solution (DB) for 1 h and incubated with the primary antibodies (diluted in DB) overnight. The next day, the membrane was washed three times with PBT for 5 min, followed by incubation with the infrared-dye conjugated secondary antibody for 45 min. The membrane was washed again three times in

PBT for 15min and scanned with the Odyssey Scanner (LiCor). Quantification of the membranes (Western blots) was done with ImageJ (NIH).

5. Microscopy

Imaging of fixed samples

Microscope slides were imaged on a Zeiss Axioplan microscope using a Plan apochromat 63x/1.40NA oil immersion objective (Zeiss) and a X-Cite 120 mercury lamp (EXFO). Images were acquired with an F-view II CCD camera (Soft Imaging Systems) controlled by the imaging software AnalySIS^B (Olympus Biosystems). Images were processed with Photoshop CS3 (Adobe) and not modified other than adjustments of brightness, contrast, levels and magnification.

Widefield live cell imaging

For live cell imaging the heating chamber of the microscope was set to 37°C and turned on at least one hour before microscopy to allow equilibration. Shortly before imaging the culture medium was replaced with prewarmed HBSS or PBS (37°C) and videodishes were mounted onto a microscope holder. Live imaging was performed with an Axiovert 100TV microscope equipped with a Plan apochromat 63x/1.40NA oil immersion objective (both Zeiss) and a X-Cite 120 mercury lamp (EXFO). For imaging of *β-actin*-24xMS2 in cells overexpressing dynamitin a FLUAR 100x/1.30NA oil objective (Zeiss) was used. Images were acquired with a CoolSnap HQ2 camera (Visitron Systems) controlled by the imaging software MetaMorph 7.5 (Molecular Devices). For single-color microscopy usually 1 image was acquired per second. Dual-color imaging was performed with inter-image intervals of 1.5 to 2 seconds. Exposure times were in a range between 300 and 800 msec. The CFP/YFP/mCherry filter set was used for RNA live imaging while the GFP/RFP filter set was used for dual color protein imaging.

Confocal spinning disc live cell imaging

Dual-color live imaging of *CaMKIIα*-3'-UTR-24xMS2 and PSD95-RFP was performed on a Zeiss Observer microscope equipped with a UltraView VoX confocal spinning disc unit (Perkin Elmer) and a 63x/1.40NA oil immersion objective (Zeiss). Acquisition of images was done with a Hamamatsu EMCCD 9100-13 camera and the Volocity imaging software (Perkin

Elmer). A 488nm and 561nm laser-line (both 100 Watt) were used for excitation of YFP and RFP, respectively, with the power set to 4%. In the YFP channel images from 5 z-planes were acquired per timepoint with an axis step size of 1 μm by using a piezo Z, while in the RFP channel only one image was recorded. Exposure times were set to 75ms for both channels. In total 211 timepoints were acquired within 5min with an average of 0.7 timepoints per second. Three-dimensional z-stacks were converted into two-dimensional movies and pictures using maximum intensity projections. Images were processed with Volocity (Perkin Elmer) and Photoshop CS3 (Adobe) and not modified other than adjustments of brightness, contrast, levels and magnification. Live imaging with the spinning disc microscope was done with the generous help of Pawel Pasierbek (Bio-optics Facility, IMP-IMBA).

6. Data analysis

ISH-colocalization

Numbers of RNA particles as well as colocalization and docking events with P-bodies were scored manually by switching quickly between the images acquired in the two channels. Colocalization was defined as a significant overlap (>50%) of two signals while docking was defined as an overlap of less than 50%. Colocalization and docking rates were calculated as the number of events divided by the total number of RNA particles. Cell bodies and the most proximal regions of dendrites were excluded from the analysis. Levels of statistical significance were calculated with a two-tailed t-test.

Calculation of P-body size

Average pixel areas of P-bodies were calculated with Metamorph 7.0 (Molecular Devices). First, images were thresholded according to pixel intensities to exclude background signal in dendrites. Regions were defined that included the proximal 25 μm of dendrites and excluded somata. Then the pixel areas of all objects above threshold lying within the defined regions were calculated by performing an “Integrated Morphometry Analysis” with the Metamorph 7.0 software. Data from same conditions derived from at least three independent experiments were pooled. Levels of statistical significance were calculated with a one-way ANOVA followed by Tukey’s multiple comparison test (*** $p < 0.001$, ** $p < 0.01$, * $p < 0.05$).

Live imaging of RNA

Particle tracking

Motile particles were tracked manually with the “Track Points” option of Metamorph 7.0 (Molecular Devices). This gives values for x and y coordinates as well as distance and angle with respect to the previous track point. These data can then be transferred to an Excel file (Microsoft). Additionally the angle of the dendrite was measured for every tracked particle to calculate the direction of a given particle displacement. This was done by using the following formula: $\text{sgn} \{ \cos (\varphi - \psi) \}$ where φ = angle of dendrite and ψ = angle of particle displacement. A value of +1 obtained by this formula indicates an anterograde displacement while -1 indicates a retrograde displacement.

Particle tracking parameters

-Velocity of particle displacements: The velocity of a particle displacement was calculated by dividing the distance that a given particle travelled between two consecutive frames by the average interframe interval for that movie.

-Definition of active versus oscillatory movements: To distinguish active transport from oscillatory movements and stationary particles a cutoff was introduced. First, to compensate for tracking errors and variation in interframe intervals caused by the camera, the particle trajectories were smoothened by applying a sliding window with a width of 5 frames to the velocity values for the particle displacements. Displacements where the smoothened value was above 0.145 μm were defined as resulting from active transport. The value of 0.145 μm is identical with the diagonal between two pixels and corresponds to the mean tracking error. For the calculation of the average particle velocities the non-smoothened values of those frames where the sliding frame value was above cutoff were taken into consideration. Values for anterograde and retrograde displacements were calculated independently.

-Statistical tests to compare velocities of particle displacements: To test whether datasets are derived from a Gaussian distribution a D’Agostino and Pearson omnibus normality test was performed. As this test was not passed, levels of statistical significance were determined with a Mann-Whitney U-test (***p<0.001, **p<0.01, *p<0.05).

-Total distance: The fraction of the distance that the whole particle population travelled in a given direction was calculated by summing the velocity values of all particle displacements and calculating the percentage that was anterograde and retrograde, respectively.

-Total time: The fraction of time that the particle population spent in anterograde or retrograde direction was calculated as the percentage of frames of all particle displacements spent in that direction. Due to the large number of displacements the variation in interframe intervals was not corrected for.

-Directionality value: This value was defined as the fraction of the total distance that a given particle covered that accounted for its net displacement. It was calculated by dividing the net distance by the total distance or, in mathematical terms:

$$Directionality\ value = \frac{|\sum_{i=1}^n x_i|}{\sum_{i=1}^n |x_i|}$$

where x_i denotes single particle displacements.

Types of motility

Three different types of particle motility were defined:

-Stationary: Particles that did not move at all during the observed time frame.

-Oscillatory: Particles that did not move more than 3 μm and switched direction at least once.

-Motile: Particles that moved more than 3 μm in one direction.

For determining the percentage of particles showing the different types of movement, a time window consisting of 10 consecutive frames taken randomly from the first 100 frames of a movie was taken. Two time windows, separated by at least 10 frames, were analyzed per movie. Only movies with many particles and a good signal to noise ratio were subjected to analysis. At least one movie was analyzed per culture.

REFERENCES

- Ainger, K., Avossa, D., Morgan, F., Hill, S.J., Barry, C., Barbarese, E., and Carson, J.H. (1993). Transport and localization of exogenous myelin basic protein mRNA microinjected into oligodendrocytes. *The Journal of Cell Biology* 123, 431-441.
- Anderson, P., and Kedersha, N. (2006). RNA granules. *The Journal of Cell Biology* 172, 803-808.
- Andreassi, C., and Riccio, A. (2009). To localize or not to localize: mRNA fate is in 3'UTR ends. *Trends in Cell Biology* 19, 465-474.
- Antar, L.N., Afroz, R., Dichtenberg, J.B., Carroll, R.C., and Bassell, G.J. (2004). Metabotropic glutamate receptor activation regulates fragile x mental retardation protein and *Fmr1* mRNA localization differentially in dendrites and at synapses. *The Journal of Neuroscience* 24, 2648-2655.
- Baas, P.W., Deitch, J.S., Black, M.M., and Banker, G.A. (1988). Polarity orientation of microtubules in hippocampal neurons: Uniformity in the axon and nonuniformity in the dendrite. *PNAS* 85, 8335-8339.
- Bacci, A., Verderio, C., Pravettoni, E., and Matteoli, M. (1999). Synaptic and intrinsic mechanisms shape synchronous oscillations in hippocampal neurons in culture. *European Journal of Neuroscience* 11, 389-397.
- Banerjee, S., Neveu, P., and Kosik, K.S. (2009). A coordinated local translational control point at the synapse involving relief from silencing and MOV10 degradation. *Neuron* 64, 871-884.
- Barbee, S.A., Estes, P.S., Cziko, A.M., Hillebrand, J., Luedeman, R.A., Collier, J.M., Johnson, N., Howlett, I.C., Geng, C., Ueda, R., *et al.* (2006). Staufen- and FMRP-containing neuronal RNPs are structurally and functionally related to somatic P bodies. *Neuron* 52, 997-1009.
- Bear, M.F., Huber, K.M., and Warren, S.T. (2004). The mGluR theory of fragile X mental retardation. *Trends in Neurosciences* 27, 370-377.
- Bertrand, E., Chartrand, P., Schaefer, M., Shenoy, S.M., Singer, R.H., and Long, R.M. (1998). Localization of *ASH1* mRNA particles in living yeast. *Molecular Cell* 2, 437-445.
- Blichenberg, A., Rehbein, M., Mueller, R., Garner, C.C., Richter, D., and Kindler, S. (2001). Identification of a cis-acting dendritic targeting element in the mRNA encoding the alpha subunit of Calcium/calmodulin-dependent protein kinase II. *European Journal of Neuroscience* 13, 1881-1888.
- Bramham, C.R., and Wells, D.G. (2007). Dendritic mRNA: transport, translation and function. *Nature Reviews Neuroscience* 8, 776-789.
- Bratu, D.P., Cha, B.J., Mhlanga, M.M., Kramer, F.R., and Tyagi, S. (2003). Visualizing the distribution and transport of mRNAs in living cells. *PNAS* 100, 13308-13313.

- Brechbiel, J.L., and Gavis, E.R. (2008). Spatial regulation of nanos is required for its function in dendrite morphogenesis. *Current Biology* 18, 745-750.
- Brengues, M., Teixeira, D., and Parker, R. (2005). Movement of eukaryotic mRNAs between polysomes and cytoplasmic processing bodies. *Science* 310, 486-489.
- Bullock, S.L., Ringel, I., Ish-Horowicz, D., and Lukavsky, P.J. (2010). A'-form RNA helices are required for cytoplasmic mRNA transport in *Drosophila*. *Nature Structural and Molecular Biology* 17, 703-709.
- Burkhardt, J.K., Echeverri, C.J., Nilsson, T., and Vallee, R.B. (1997). Overexpression of the dynamitin (p50) subunit of the dynactin complex disrupts dynein-dependent maintenance of membrane organelle distribution. *The Journal of Cell Biology* 139, 469-484.
- Cajigas, I.J., Will, T., and Schuman, E.M. (2010). Protein homeostasis and synaptic plasticity. *EMBO Journal* 29, 2746-2752.
- Cougot, N., Bhattacharyya, S.N., Tapia-Arancibia, L., Bordonne, R., Filipowicz, W., Bertrand, E., and Rage, F. (2008). Dendrites of mammalian neurons contain specialized P-body-like structures that respond to neuronal activation. *The Journal of Neuroscience* 28, 13793-13804.
- Dahm, R., and Kiebler, M. (2005). Silenced RNA on the move. *Nature* 438, 432-435.
- Dahm, R., Kiebler, M., and Macchi, P. (2007). RNA localisation in the nervous system. *Seminars in Cell & Developmental Biology* 18, 216-223.
- Davis, H.P., and Squire, L.R. (1984). Protein synthesis and memory: A review. *Psychological Bulletin* 96, 518-559.
- Delanoue, R., Herpers, B., Soetaert, J., Davis, I., and Rabouille, C. (2007). *Drosophila* squid/hnRNP helps dynein switch from a *gurken* mRNA transport motor to an ultrastructural static anchor in sponge bodies. *Developmental Cell* 13, 523-538.
- Dictenberg, J.B., Swanger, S.A., Antar, L.N., Singer, R.H., and Bassell, G.J. (2008). A direct role for FMRP in activity-dependent dendritic mRNA transport links filopodial-spine morphogenesis to fragile X syndrome. *Developmental Cell* 14, 926-939.
- Doe, C.D., Chu-LaGraff, Q., Wright, D.M., and Scott, M.P. (1991). The prospero gene specifies cell fates in the *Drosophila* central nervous system. *Cell* 65, 451-464.
- Doyle, M., and Kiebler, M.A. (2011). Mechanisms of dendritic mRNA transport and its role in synaptic tagging. *EMBO Journal* 30, 3540-3552.
- Driever, W., and Nüsslein-Volhard, C. (1988). The bicoid protein determines position in the *Drosophila* embryo in a concentration-dependent manner. *Cell* 54, 95-104.
- Dynes, J.L., and Steward, O. (2007). Dynamics of bidirectional transport of *Arc* mRNA in neuronal dendrites. *The Journal of Comparative Neurology* 500, 433-447.
- Eberwine, J., Miyashiro, K., Kacharina, J.E., and Job, C. (2001). Local translation of classes of mRNAs that are targeted to neuronal dendrites. *PNAS* 98, 7080-7085.

- Encalada, S.E., Szpankowski, L., Xia, C.H., and Goldstein, L.S. (2011). Stable kinesin and dynein assemblies drive the axonal transport of mammalian prion protein vesicles. *Cell* *144*, 551-565.
- Ephrussi, A., and Lehmann, R. (1992). Induction of germ cell formation by *oskar*. *Nature* *358*, 387-392.
- Eulalio, A., Behm-Ansmant, I., and Izaurralde, E. (2007). P bodies: at the crossroads of post-transcriptional pathways. *Nature Reviews Molecular Cell Biology* *8*, 9-22.
- Engert, F., and Bonhöffer, T. (1999). Dendritic spine changes associated with hippocampal long-term synaptic plasticity. *Science* *399*, 66-70.
- Farina, K.L., and Singer, R.H. (2002). The nuclear connection in RNA transport and localization. *Trends in Cell Biology* *12*, 466-472.
- Ferrari, F., Mercaldo, V., Piccoli, G., Sala, C., Cannata, S., Achsel, T., and Bagni, C. (2007). The fragile X mental retardation protein-RNP granules show an mGluR-dependent localization in the post-synaptic spines. *Molecular and Cellular Neurosciences* *34*, 343-354.
- Forrest, K.M., and Gavis, E.R. (2003). Live imaging of endogenous RNA reveals a diffusion and entrapment mechanism for *nanos* mRNA localization in *Drosophila*. *Current Biology* *13*, 1159-1168.
- Frey, U., Krug, M., Reymann, K.G., and Matthies, H. (1988). Anisomycin, an inhibitor of protein synthesis, blocks late phases of LTP phenomena in the hippocampal CA1 region in vitro. *Brain Research* *452*, 57-65.
- Frey, J. U. (2001). Long-lasting hippocampal plasticity: a cellular model for memory consolidation. *Results and Problems in Cell Differentiation* *34*, D. Richter (Ed.): Cell polarity and subcellular RNA localization. Springer-Verlag, Berlin-Heidelberg
- Fujii, R., Okabe, S., Urushido, T., Inoue, K., Yoshimura, A., Tachibana, T., Nishikawa, T., Hicks, G.G., and Takumi, T. (2005). The RNA binding protein TLS is translocated to dendritic spines by mGluR5 activation and regulates spine morphology. *Current Biology* *15*, 587-593.
- Fusco, D., Accornero, N., Lavoie, B., Shenoy, S.M., Blanchard, J., Singer, R.H., and Bertrand, E. (2003). Single mRNA molecules demonstrate probabilistic movement in living mammalian cells. *Current Biology* *13*, 161-167.
- Gao, Y., Tatavarty, V., Korza, G., Levin, M.K., and Carson, J.H. (2008). Multiplexed dendritic targeting of alpha calcium calmodulin-dependent protein kinase II, neurogranin, and activity-regulated cytoskeleton-associated protein RNAs by the A2 pathway. *Molecular Biology of the Cell* *19*, 2311-2327.
- Giorgi, C., and Moore, M.J. (2007). The nuclear nurture and cytoplasmic nature of localized mRNPs. *Seminars in Cell and Developmental Biology* *18*, 186-193.
- Giorgi, C., Yeo, G.W., Stone, M.E., Katz, D.B., Burge, C., Turrigiano, G., and Moore, M.J. (2007). The EJC factor eIF4AIII modulates synaptic strength and neuronal protein expression.

Cell 130, 179-191.

Goetze, B., Grunewald, B., Baldassa, S., and Kiebler, M. (2004). Chemically controlled formation of a DNA/calcium phosphate coprecipitate: application for transfection of mature hippocampal neurons. *Journal of Neurobiology* 60, 517-525.

Goetze, B., Tuebing, F., Xie, Y., Dorostkar, M.M., Thomas, S., Pehl, U., Boehm, S., Macchi, P., and Kiebler, M.A. (2006). The brain-specific double-stranded RNA-binding protein Staufen2 is required for dendritic spine morphogenesis. *The Journal of Cell Biology* 172, 221-231.

Govindarajan, A., Israely, I., Huang, S.Y., and Tonegawa, S. (2011). The dendritic branch is the preferred integrative unit for protein synthesis-dependent LTP. *Neuron* 69, 132-146.

Govindarajan, A., Kelleher, R.J., and Tonegawa, S. (2006). A clustered plasticity model of long-term memory engrams. *Nature Reviews Neuroscience* 7, 575-583.

Grossman, A.W., Elisseou, N.M., McKinney, B.C., and Greenough, W.T. (2006). Hippocampal pyramidal cells in adult *Fmr1* knockout mice exhibit an immature-appearing profile of dendritic spines. *Brain Research* 1084, 158-164.

Grünwald, D., and Singer, R.H. (2010). In vivo imaging of labelled endogenous β -actin mRNA during nucleocytoplasmic transport. *Nature* 467, 604-607.

Hachet, O., and Ephrussi, A. (2004). Splicing of *oskar* RNA in the nucleus is coupled to its cytoplasmic localization. *Nature* 428, 959-963.

Hinton, V.J., Brown, W.T., Wisniewski, K., and Rudelli, R.D. (1991). Analysis of neocortex in three males with fragile X syndrome. *American Journal of Medical Genetics* 41, 289-294.

Hirokawa, N., Niwa, S., and Tanaka, Y. (2010). Molecular motors in neurons: transport mechanisms and roles in brain function, development, and disease. *Neuron* 68, 610-638.

Ho, V.M., Lee, J.A., and Martin, K.C. (2011). The cell biology of synaptic plasticity. *Science* 334, 623-628.

Holt, C.E., and Bullock, S.L. (2009). Subcellular mRNA localization in animal cells and why it matters. *Science* 326, 1212-1216.

Huang, Y.S., Carson, J.H., Barbarese, E., and Richter, J.D. (2003). Facilitation of dendritic mRNA transport by CPEB. *Genes and development* 17, 638-653.

Huber, K.M., Kayser, M.S., and Bear, M.F. (2000). Role for Rapid Dendritic Protein Synthesis in Hippocampal mGluR-Dependent Long-Term Depression. *Science* 288, 1254-1256.

Hüttelmaier, S., Zenklusen, D., Lederer, M., Dichtenberg, J., Lorenz, M., Meng, X., Bassell, G.J., Condeelis, J., and Singer, R.H. (2005). Spatial regulation of β -actin translation by Src-dependent phosphorylation of ZBP1. *Nature* 438, 512-515.

Jenny, A., Hachet, O., Zavorszky, P., Cyrklaff, A., Weston, M.D., Johnston, D.S., Erdelyi, M., and Ephrussi, A. (2006). A translation-independent role of *oskar* RNA in early *Drosophila*

oogenesis. *Development* 133, 2827-2833.

Kanai, Y., Dohmae, N., and Hirokawa, N. (2004). Kinesin transports RNA: isolation and characterization of an RNA-transporting granule. *Neuron* 43, 513-525.

Kandel, E.R. (2001). The molecular biology of memory storage: a dialogue between genes and synapses. *Science* 294, 1030-1038.

Kang, H., and Schuman, E.M. (1996). A requirement for local protein synthesis in neurotrophin-induced hippocampal synaptic plasticity. *Science* 273, 1402-1406.

Kao, D.I., Aldridge, G.M., Weiler, I.J., and Greenough, W.T. (2010). Altered mRNA transport, docking, and protein translation in neurons lacking fragile X mental retardation protein. *PNAS* 107, 15601-15606.

Kapitein, L.C., Schlager, M.A., Kuijpers, M., Wulf, P.S., van Spronsen, M., MacKintosh, F.C., and Hoogenraad, C.C. (2010). Mixed microtubules steer dynein-driven cargo transport into dendrites. *Current Biology* 20, 290-299.

Kapitein, L.C., Schlager, M.A., van der Zwan, W.A., Wulf, P.S., Keijzer, N., and Hoogenraad, C.C. (2010). Probing intracellular motor protein activity using an inducible cargo trafficking assay. *Biophysical Journal* 99, 2143-2152.

Kardon, J.R., and Vale, R.D. (2009). Regulators of the cytoplasmic dynein motor. *Nature Reviews Molecular Cell Biology* 10, 854-865.

Karki, S., and Holzbaur, E.L.F. (1999). Cytoplasmic dynein and dynactin in cell division and intracellular transport. *Current Opinion in Cell Biology* 11, 45-53.

King, S.J., and Schroer, T.A. (2000). Dynactin increases the processivity of the cytoplasmic dynein motor. *Nature Cell Biology* 2, 20-24.

Kloc, M., Zearfoss, N.R., and Etkin, L.D. (2002). Mechanisms of subcellular mRNA localization. *Cell* 108, 533-544.

Knowles, R.B., Sabry, J.H., Martone, M.E., Deerinck, T.J., Ellisman, M.H., Bassell, G.J., and Kosik, K.S. (1996). Translocation of RNA granules in living neurons. *The Journal of Neuroscience* 16, 7812-7820.

Köhrmann, M., Luo, M., Kaether, C., DesGroseillers, L., Dotti, C.G., and Kiebler, M.A. (1999). Microtubule-dependent recruitment of Staufen-green fluorescent protein into large RNA-containing granules and subsequent dendritic transport in living hippocampal neurons. *Molecular Biology of the Cell* 10, 2945-2953.

Krichevsky, A.M., and Kosik, K.S. (2001). Neuronal RNA granules: A link between RNA localization and stimulation-dependent translation. *Neuron* 32, 683-696.

Lebeau, G., Miller, L.C., Tartas, M., McAdam, R., Laplante, I., Badeaux, F., DesGroseillers, L., Sossin, W.S., and Lacaille, J.C. (2011). Staufen2 regulates mGluR long-term depression and *Map1b* mRNA distribution in hippocampal neurons. *Learning and Memory* 18, 314-326.

- Leung, K.M., van Horck, F.P., Lin, A.C., Allison, R., Standart, N., and Holt, C.E. (2006). Asymmetrical β -actin mRNA translation in growth cones mediates attractive turning to netrin-1. *Nature Neuroscience* 9, 1247-1256.
- Lionnet, T., Czaplinski, K., Darzacq, X., Shav-Tal, Y., Wells, A.L., Chao, J.A., Park, H.Y., de Turris, V., Lopez-Jones, M., and Singer, R.H. (2011). A transgenic mouse for in vivo detection of endogenous labeled mRNA. *Nature Methods* 8, 165-170.
- Liu, G., Grant, W.M., Persky, D., Latham, V.M., Jr., Singer, R.H., and Condeelis, J. (2002). Interactions of elongation factor 1 alpha with F-actin and β -actin mRNA: implications for anchoring mRNA in cell protrusions. *Molecular Biology of the Cell* 13, 579-592.
- Long, R.M., Singer, R.H., Meng, X., Gonzalez, I., Nasmyth, K., and Jansen, R. (1997). Mating type switching in yeast controlled by asymmetric localization of *ASH1* mRNA. *Science* 277, 383-387.
- Lopez de Heredia, M., and Jansen, R.P. (2004). mRNA localization and the cytoskeleton. *Current Opinion in Cell Biology* 16, 80-85.
- Lyford, G.L., Yamagata, K., Kaufmann, W.E., Barnes, C.A., Sanders, L.K., Copeland, N.G., Gilbert, D.J., Jenkins, N.A., Lanahan, A.A., and Worley, P.F. (1995). *Arc*, a growth factor and activity-regulated gene, encodes a novel cytoskeleton-associated protein that is enriched in neuronal dendrites. *Neuron* 14, 433-445.
- Maher-Laporte, M., Berthiaume, F., Moreau, M., Julien, L., Lapointe, G., Mourez, M., and DesGroseillers, L. (2010). Molecular composition of Staufen2-containing ribonucleoproteins in embryonic rat brain. *PLoS One* 5, 1-10.
- Marrs, G.S., Green, S.H., and Dailey, M.E. (2001). Rapid formation and remodeling of postsynaptic densities in developing dendrites. *Nature Neuroscience* 4, 1006-1013.
- Matsuzaki, M., Honkura, N., Ellis-Davies, G.C.R., and Kasai, H. (2004). Structural basis of long-term potentiation in single dendritic spines. *Nature* 429, 761-766.
- Megias, M., Emri, Z.S., Freund, T.F., and Gulyas, A.I. (2001). Total number and distribution of inhibitory and excitatory synapses on hippocampal CA1 pyramidal cells. *Neuroscience* 102, 527-540.
- Meister, G., and Tuschl, T. (2004). Mechanisms of gene silencing by double-stranded RNA. *Nature* 431, 343-349.
- Mikl, M. (2009). Analysis of RNA localization to dendrites of hippocampal neurons. Diploma thesis, University of Vienna
- Mikl, M., Vendra, G., Doyle, M., and Kiebler, M.A. (2010). RNA localization in neurite morphogenesis and synaptic regulation: current evidence and novel approaches. *Journal of Comparative Physiology A* 196, 321-334.
- Mikl, M., Vendra, G., and Kiebler, M.A. (2011). Independent localization of *MAP2*, *CaMKII α* and β -actin RNAs in low copy numbers. *EMBO Reports* 12, 1077-1084.

- Miller, S., Yasuda, M., Coats, J.K., Jones, Y., Martone, M.E., and Mayford, M. (2002). Disruption of dendritic translation of *CaMKII α* impairs stabilization of synaptic plasticity and memory consolidation. *Neuron* 36, 507-519.
- Morris, S.H., Knevet, S., Lerner, E.G., and Bindman, L.J. (1999). Group I mGluR agonist DHPG facilitates the induction of LTP in rat prelimbic cortex in vitro. *Journal of Neurophysiology* 82, 1927-1933.
- Muslimov, I.A., Santi, E., Homel, P., Perini, S., Higgins, D., and Tiedge, H. (1997). RNA Transport in Dendrites: A cis-Acting targeting element is contained within Neuronal *BCI* RNA. *The Journal of Neuroscience* 17, 4722-4733.
- Nevo-Dinur, K., Nussbaum-Shochat, A., Ben-Yehuda, S., and Amster-Choder, O. (2011). Translation-independent localization of mRNA in E. coli. *Science* 331, 1081-1084.
- Okada, D., Ozawa, F., and Inokuchi, K. (2009). Input-specific spine entry of soma-derived Vesl-1S protein conforms to synaptic tagging. *Science* 324, 904-909.
- Oleynikov, Y., and Singer, R.H. (1998). RNA localization: different zipcodes, same postman? *Trends in Cell Biology* 8, 381-383.
- Pak, D.T., and Sheng, M. (2003). Targeted protein degradation and synapse remodeling by an inducible protein kinase. *Science* 302, 1368-1373.
- Paradies, M.A., and Steward, O. (1997). Multiple subcellular mRNA distribution patterns in neurons: a nonisotopic *in situ hybridization* Analysis. *Journal of Neurobiology* 33, 473-493.
- Parker, R., and Sheth, U. (2007). P-bodies and the control of mRNA translation and degradation. *Molecular Cell* 25, 635-646.
- Pfeiffer, B.E., and Huber, K.M. (2006). Current advances in local protein synthesis and synaptic plasticity. *The Journal of Neuroscience* 26, 7147-7150.
- Rao, A., and Steward, O. (1991). Evidence that protein constituents of postsynaptic membrane specialization are locally synthesized: analysis of proteins synthesized within synaptosomes. *The Journal of Neuroscience* 11, 2881-2895.
- Reiss, A.L., and Freund, L. (1990). Fragile X Syndrome. *Biological Psychiatry* 27, 223-240.
- Riechmann, V., and Ephrussi, A. (2001). Axis formation during *Drosophila* oogenesis. *Current Opinion in Genetics and Development* 11, 374-383.
- Rook, M.S., Lu, M., and Kosik, K.S. (2000). *CaMKII α* 3'-untranslated region-directed mRNA translocation in living neurons: visualization by GFP linkage. *The Journal of Neuroscience* 20, 6385-6393.
- Schifferer, M., and Griesbeck, O. (2009). Application of aptamers and autofluorescent proteins for RNA visualization. *Integrative Biology* 1, 499-505.
- Schnapp, B.J. (1999). RNA localization: A glimpse of the machinery. *Current Biology* 9, 725-727.

- Schratt, G.M., Tuebing, F., Nigh, E.A., Kane, C.G., Sabatini, M.E., Kiebler, M., and Greenberg, M.E. (2006). A brain-specific microRNA regulates dendritic spine development. *Nature* *439*, 283-289.
- Schuman, E.M., Dynes, J.L., and Steward, O. (2006). Synaptic regulation of translation of dendritic mRNAs. *The Journal of Neuroscience* *26*, 7143-7146.
- Shestakova, E.A., Singer, R.H., and Condeelis, J. (2001). The physiological significance of β -actin mRNA localization in determining cell polarity and directional motility. *PNAS* *98*, 7045-7050.
- Sheth, U., and Parker, R. (2003). Decapping and decay of messenger RNA occur in cytoplasmic processing bodies. *Science* *300*, 805-808.
- Siegel, G., Obernosterer, G., Fiore, R., Oehmen, M., Bicker, S., Christensen, M., Khudayberdiev, S., Leuschner, P.F., Busch, C.J., Kane, C., *et al.* (2009). A functional screen implicates microRNA-138-dependent regulation of the depalmitoylation enzyme APT1 in dendritic spine morphogenesis. *Nature Cell Biology* *11*, 705-716.
- St Johnston, D. (2005). Moving messages: the intracellular localization of mRNAs. *Nature Reviews Molecular Cell Biology* *6*, 363-375.
- St Johnston, D., and Nüsslein-Volhard, C. (1992). The origin of pattern and polarity in the *Drosophila* embryo. *Cell* *68*, 201-219.
- Steward, O., and Banker, G.A. (1992). Getting the message from the gene to the synapse: sorting and intracellular transport of RNA in neurons. *Trends in Neurosciences* *15*, 180-186.
- Steward, O., and Levy, W.B. (1982). Preferential localization of polyribosomes under the base of dendritic spines in granule cells of the dentate gyrus. *The Journal of Neuroscience* *2*, 284-291.
- Steward, O., Wallace, C.S., Lyford, G.L., and Worley, P.F. (1998). Synaptic activation causes the mRNA for the IEG *Arc* to localize selectively near activated postsynaptic sites on dendrites. *Neuron* *21*, 741-751.
- Subramanian, M., Rage, F., Tabet, R., Flatter, E., Mandel, J.L., and Moine, H. (2011). G-quadruplex RNA structure as a signal for neurite mRNA targeting. *EMBO Reports* *12*, 697-704.
- Teixeira, D., Sheth, U., Valencia-Sanchez, M.A., Brengues, M., and Parker, R. (2005). Processing bodies require RNA for assembly and contain nontranslating mRNAs. *RNA* *11*, 371-382.
- Tiruchinapalli, D.M., Oleynikov, Y., Kelic, S., Shenoy, S.M., Hartley, A., Stanton, P.K., Singer, R.H., and Bassell, G.J. (2003). Activity-dependent trafficking and dynamic localization of zipcode binding protein 1 and β -actin mRNA in dendrites and spines of hippocampal neurons. *The Journal of Neuroscience* *23*, 3251-3261.
- Tübing, F., Vendra, G., Mikl, M., Macchi, P., Thomas, S., and Kiebler, M.A. (2010). Dendritically localized transcripts are sorted into distinct ribonucleoprotein particles that

display fast directional motility along dendrites of hippocampal neurons. *The Journal of Neuroscience* 30, 4160-4170.

Verhey, K.J., Kaul, N., and Soppina, V. (2011). Kinesin assembly and movement in cells. *Annual Review of Biophysics* 40, 267-288.

Vessey, J.P., Vaccani, A., Xie, Y., Dahm, R., Karra, D., Kiebler, M.A., and Macchi, P. (2006). Dendritic localization of the translational repressor Pumilio2 and its contribution to dendritic stress granules. *The Journal of Neuroscience* 26, 6496-6508.

Weiler, I.J., Irwin, S.A., Klintsova, A.Y., Spencer, C.M., Brazelton, A.D., Miyashiro, K., Comery, T.A., Patel, B., Eberwine, J., and Greenough, W.T. (1997). Fragile X mental retardation protein is translated near synapses in response to neurotransmitter activation. *PNAS* 94, 5395-5400.

Wilkie, G.S., and Davis, I. (2001). *Drosophila wingless* and pair-rule transcripts localize apically by dynein-mediated transport of RNA particles. *Cell* 105, 209-219.

Zeitelhofer, M., Karra, D., Macchi, P., Tolino, M., Thomas, S., Schwarz, M., Kiebler, M., and Dahm, R. (2008). Dynamic interaction between P-bodies and transport ribonucleoprotein particles in dendrites of mature hippocampal neurons. *The Journal of Neuroscience* 28, 7555-7562.

Zimyanin, V.L., Belaya, K., Pecreaux, J., Gilchrist, M.J., Clark, A., Davis, I., and St Johnston, D. (2008). In vivo imaging of *oskar* mRNA transport reveals the mechanism of posterior localization. *Cell* 134, 843-853.

ACKNOWLEDGEMENTS

In the end, I want to thank everybody who made this thesis possible. Most importantly Michael Kiebler and Georgia Vendra. Georgia, as my direct supervisor, has taught me most of the techniques and always had time for discussions. But more importantly she has introduced me into the, back then to me unknown, world of science and showed me both sides of the coin. Michael has infected me with his enthusiasm and supported me in every possible way. I am especially thankful that I was allowed to attend the 'Neural Circuits' meeting in Heidelberg. In retrospect this turned out to be a crossroad for me.

Furthermore, I want to thank a number of people who helped me during my stay in the lab, be it experimentally or in other ways:

- Martin, Maria and Alex R. helped me to get started
- Our technicians and 'backbones' of the lab Sabine and Alexandra. Sabine provided me with millions of cells and Alex helped me with biochemistry
- Zsafia for sharing cloning problems
- And last but not least all present and past members of the Kieblerlab not mentioned above, who made the months of my diploma work such a pleasant time: Lukas, Sebastian, Jacki, Philipp, Michi, Raimund, Paul, Birgit, David, Matias, Angela.....thanks for the fun beer and cocktail hours - see you at 4 in the kitchen.

Finally, I wish to dedicate this thesis to my grandparents, for whom it was obviously more important than for me that this work comes to an end.

ZUSAMMENFASSUNG

Die dendritische Lokalisierung einiger mRNAs und deren aktivitätsabhängige lokale Translation spielt eine entscheidende Rolle bei der Modifikation einzelner Synapsen. Um ihren Zielort zu erreichen, assoziieren mRNAs mit speziellen RNA-Bindeproteinen und bilden sogenannte Ribonukleoprotein-Partikel (RNPs). Diese werden dann von molekularen Motoren entlang des Zytoskeletts transportiert.

Ziel der vorliegenden Arbeit war es, die Dynamik des RNP-Transports in lebenden hippocampalen Neuronen zu untersuchen. Zur mikroskopischen Visualisierung der mRNAs benutzte ich das MS2 System und analysierte die Kinetik einzelner RNA-Partikel im Detail. Untersuchungen der beiden mRNAs *CaMKII α* und *β -actin* ergaben, dass ein Teil der Partikel mit hoher Geschwindigkeit (bis zu 2 μ m/s) in Dendriten transportiert wird. Diese Bewegungen erfolgten mit gleicher Wahrscheinlichkeit in beide Richtungen des Dendriten. Interessanterweise zeigten *CaMKII α* RNA-Partikel eine leicht höhere Geschwindigkeit in die anterograde Richtung, was die Effizienz der dendritischen Lokalisierung dieser mRNA erhöhen könnte. Für *β -actin* wurde kein signifikanter Geschwindigkeitsunterschied festgestellt. Die Deletion eines Elements in der 3'-UTR von *CaMKII α* , das laut einer vorhergehenden Publikation für die Lokalisation dieser mRNA zuständig ist, hatte keine Auswirkung auf deren dendritischen Transport. Dies zeigt, dass die Lokalisationselemente dendritischer mRNAs womöglich weit komplexer sind als bisher angenommen wurde. Des weiteren wurden RNA-Partikel gleichzeitig mit dem postsynaptischen Marker PSD95 visualisiert. Diese Experimente ergaben, dass sich stationäre RNA-Partikel oft in der räumlichen Nähe von Synapsen befinden.

In einem Nebenprojekt untersuchte ich die dynamischen Eigenschaften und die synaptische Regulation dendritischer P-bodies. P-bodies sind cytoplasmatische RNA/Protein-Komplexe, die eine Funktion in der Degradation und Speicherung von mRNAs besitzen. In dieser Arbeit konnte ich die mRNAs *Arc*, *β -actin* und *MAP2* in dendritischen P-bodies nachweisen. Ausserdem zeigte sich, dass sich P-bodies für längere Zeiträume in der Nähe von Synapsen aufhalten und dass sie auf synaptische Stimulation oder Hemmung mit einer reversiblen Änderung ihrer Größe reagieren. Diese Ergebnisse unterstützen die Hypothese, dass P-bodies dendritische mRNAs speichern, um diese bei synaptischer Stimulation wieder freigegeben und dadurch deren Translation ermöglichen.

CURRICULUM VITAE

Georg Ammer

Address	Hanfpointstraße 29, 4050 Traun, Austria Tumblingerstraße 54/373, 80337 Munich, Germany
E-mail	g.ammer@gmx.at
Birthdate and place	23 July 1986, Linz, Austria
Citizenship	Austrian

Education

November 2010 - present	Master studies: Molecular biology; Behavior, Neurobiology and Cognition, University of Vienna, Austria
February 2009	First Diploma (proved to be equivalent to B.Sc.)
October 2005 – present	Studies: Molecular Biology, University of Vienna, Austria
2004 – 2005	Community Service, General Hospital (AKh) Linz, Austria
1992 - 2004	Primary School and Highschool (BRG), Traun, Austria

Work Experience

Since September 2011	Master thesis (Neurobiology): In vivo electrophysiology to dissect the motion vision circuit of <i>Drosophila</i> , Prof. Alexander Borst, Max Planck Institute of Neurobiology, Martinsried/Munich, Germany
April 2011 – June 2011	Internship: Visual input to the neural circuit for <i>Drosophila</i> courtship behavior, Dr. Barry Dickson, Institute of Molecular Pathology (IMP), Vienna, Austria
November 2009 – January 2010	Internship: Cellular neurophysiology (patch clamp), Prof. Sigismund Huck, Department of Biochemistry and Molecular Biology, Center for Brain Research, Medical University of Vienna, Austria
May 2009 – September 2009 March 2010 – March 2011	Internship and master thesis (Molecular Biology): RNA imaging in living hippocampal neurons, Dr. Georgia Vendra and Prof. Michael Kiebler, Department of Neuronal Cell Biology, Center for Brain Research, Medical University of Vienna, Austria